A COMPREHENSIVE EVALUATION OF THE EFFECTS OF AGGREGATE GRADATIONS ON MECHANISM PERFORMANCE OF WEARING COURSE MIXTURES

Nhat Thanh Tran

A dissertation submitted in partial fulfilment of the requirement for the degree of Doctor of Engineering

Department of Civil and Environmental Engineering

Nagaoka University of Technology

Niigata, Japan

July 2019

ACKNOWLEDGEMENTS

The present study was carried out at the Highway Engineering Laboratory, Department of Civil and Environmental Engineering, Nagaoka University of Technology. I thank the Nagaoka University of Technology for providing the necessary facilities to conduct the study.

I would like to thank my advisor, Professor Osamu Takahashi, for his patients giving me numerous valuable and great pieces of advice, and supporting me in many other ways.

I would like to thank the members of my dissertation committee, Professor Takumi Shimomura, Professor Eiji Iwasaki, Associate Professor Takeshi Miyashita, and Dr Augusto Cannone Falchetto for their valuable comments and suggestions. I also would like to thank Assistant Professor Takeshi Nakamura for his helpful comments during seminars at Highway Engineering Laboratory.

I have a feeling of a friendly atmosphere in our Laboratory. I must thank my tutor, Mr Nhan, who had done many things for me not only in living conditions but also in my study at the beginning of my life in Japan. I would like to thank Miss Kaori Tanaka, Mr Ryuhei Kobayashi, Mr Ryoma Sakai, and other laboratory members for their assistance in my study, living conditions, and the Japanese.

I thank former graduate students at the Nagaoka University of Technology, Japan for sharing me with their data to raise the quality of the present study.

I am grateful for the Ministry of Education, Culture, Sport, Science and Technology of Japan for providing me with the Monbukagakusho Scholarship as well as allow me to take part in the research in Japan.

Finally, I thank my family and Vietnamese friends for supporting and encouraging me to earn this achievement.

A comprehensive evaluation of the effects of aggregate gradations on mechanism performance of wearing course mixtures

By Nhat Thanh Tran

*Doctor dissertation***,** Department of Civil and Environmental Engineering,
Nagaoka University of Technology, Japan, 2019.

ABSTRACT

The wearing course mixture or the surface layer in pavements is directly affected by the traffic loads and the weather conditions, thereby potentially resulting in cracking and rutting on the layer. The common methods for designing asphalt mixtures are the Marshall and Superpave methods, which are mainly based on volumetric evaluations. However, the current standards around the world (Marshall and Superpave) do not provide a clear guideline to comply with the volumetric requirements of hot mix asphalt (HMA) mixtures. In addition, the use of volumetric properties may be not sufficient to evaluate performance of HMA mixtures. Furthermore, the standards in developing countries such as Vietnam and Indonesia exclude rational test to evaluate mechanism performance of HMA mixtures.

In mix design procedure, selecting an adequate aggregate gradation may improve cracking and rutting resistance of HMA mixtures. Based on the continuous maximum density (CMD) theory and the dominant aggregate size range (DASR) model, the present study aimed to apply and develop several gradation parameters to investigate the effect of aggregate gradation on the performance of HMA mixtures in terms of volumetric property (CMD_{area}), workability (*WI* and $CMD_{area\text{-}stone}$), cracking (*GCI* and $CMD_{area\text{-}DASR}$), rutting (*RRI*), and shear strength (P_{rms}, CMD_{area}, and CMD_{sand}). The results indicated that the gradation parameters based on the CMD and the DASR model have potential applications to evaluate the performance of HMA mixtures. Therefore, asphalt designers can apply these gradation parameters for designing a stable a gradation at the early stage of mix design procedures of HMA mixtures.

The present study also investigated three asphalt binder parameters, i.e., the design asphalt content, effective asphalt content, and apparent film thickness (AFT), in order to examine the effects of the asphalt binder composition on the cracking resistance and shear strength of HMA mixtures. The

experiments demonstrated that among three asphalt binder parameters, the *AFT* has the most substantial effects on the cracking resistance and shear strength of asphalt mixtures.

This study also examined if the notched semi-circular bending (SCB) test can replace the three-point bending beam (TPBB) test to assess fracture resistance of asphalt mixtures at intermediate temperature conditions. In addition, the present study also applied the crack tip opening angle (CTOA) to evaluate the cracking propagation of HMA mixtures in the notched SCB test. The TPBB test was performed using the JRA B005 standard, and the notched SCB test was conducted using the following three standards: EN 12697-44, AASHTO TP 105-13, and AASHTO TP 124-16. The results indicated the notched SCB test using the EN 12697-44 standard may present a viable alternative to the TPBB test to characterise fracture resistance of asphalt mixtures. Furthermore, the CTOA is a candidate indicator for assessing the potential for cracking propagation.

The present study also developed two simple protocols using the Marshall specimen to evaluate rutting resistance of HMA mixtures. The first protocol is the combination of the unconfined compression test and the shear circle test, and the second protocol is the indirect tension test using a reasonably low deformation rate and an adjusted testing temperature. The results indicated that both the cohesions estimated from the first protocol and the tension strength obtained from the second protocol have strong relationships with rutting resistance of HMA mixtures. Therefore, the proposed protocols are potential measures for ranking rutting performance of asphalt mixtures.

CONTENTS

LIST OF TABLES

LIST OF FIGURES

Chapter 1. Introduction

1.1. Background

In the last few decades, a hot mix asphalt (HMA) mixture, as a well-known road construction material, has become the leading choice for surface layer materials used in pavements. The surface layer of asphalt pavements or the wearing course mixture directly exposes to traffic loads and weather conditions. Accordingly, the increase in the traffic volume of heavy vehicles in combination with ambient conditions (temperatures or moistures) has increased the incidence of premature failures (rutting or cracking) in wearing course mixtures [1-3]. In fact, HMA design plays a critical role in preventing premature failures for HMA mixtures before the mixtures are applied in construction sites.

In general, asphalt mixtures have two components, i.e., asphalt binder and mineral aggregate [3]. The mineral aggregates constitute the main component (approximately 92-96% of total mass) of HMA mixtures, and their physical properties have significant effects on the performance of mixtures [1-3]. During the HMA mixture design process, aggregates in the asphalt mixture are designed to comply with a permissible distribution of particles sizes. This size distribution (often as a percent of total weight) is known as aggregate gradation. Aggregate gradation may be the most important characteristic of a mineral aggregate within the mixture. It strongly influences almost all the fundamental properties of asphalt mixtures such as volumetric, workability, cracking, rutting, and moisture [1-7]. Therefore, designing an appropriate level of aggregate gradation is one of the primary tasks for mixture designers.

Current asphalt design standards around the world have followed the Marshall and Superpave methods, which apparently focus on the volumetric properties of asphalt mixtures [1-3]. For aggregate gradation design, these standards recommend the upper and lower grading limits, namely permissible ranges of particles sizes. Pavement engineers have to determine a percentage of each classified aggregate so that the gradation curve falls inside of all permissible ranges. In general, each medium of the permissible ranges is taken as only one target gradation value of each sieve. However, selecting this target gradation may not result in the desired mixture that should comply with the specification of volumetric parameters [8]. Asphalt pavements must deal with that through trial and error for different aggregate gradations. As a result, this process is tedious and time-consuming.

A current study tried to apply the Bailey method for gradation design in order to ensure proper volumetric parameters and adequate performance of asphalt mixtures in the Superpave method [8]. However, this study could not find a clear relationship between Bailey parameters and with the voids in mineral aggregate (VMA) of asphalt mixtures, which is the most important parameter in the Superpave

method. In fact, achieving a desired VMA is the most challenging task in the gradation design [9]. A recent study indicated a good relationship of aggregate gradation with the VMA using the continuous maximum density (CMD) theory [10]. However, this study only focused on the mixtures using the Superpave method while numerous countries have continued to use the Marshall method to design HMA mixtures such as Vietnam, Indonesia, Netherland, Japan, and Germany. There is therefore a need to conduct in-depth investigations that clarify the application of CMD theory on volumetric properties of HMA mixtures when using the Marshall design.

After HMA mixture design, pavement engineers also face another challenge in ensuring excellent performance of HMA mixtures. It has been reported that the specification of volumetric parameters alone is insufficient to guarantee high cracking or rutting resistance in asphalt mixtures [1, 2]. Therefore, in the last few decades, extensive studies have been conducted to render a rational approach to evaluate performance of HMA mixtures using aggregate gradation [1-14]. In this direction, several theories of aggregate gradation are developed to comprehensively understand the nature of performance of asphalt mixtures [11]. However, to the best of our knowledge, previous studies applied the theories of aggregate gradation to only investigate one or few behaviours of asphalt mixtures. The search of the literature found no well-established research that evaluates the relationship of aggregate gradation with almost all the important properties of asphalt mixtures. Therefore, a comprehensive evaluation of the effects of aggregate gradations on mechanism performance of asphalt mixtures is needed.

1.2. Objective of research

This study investigated a comprehensive evaluation of the effects of aggregate gradation on the various performance tests of HMA mixtures using the theory of CMD and the dominant aggregate size range (DASR). The primary objective of this study was to develop several gradation parameters that have potential application for ranking performance of HMA mixtures. In addition, the present study aimed to improve the specifications of mechanical tests that access the rutting and cracking potential of HMA mixtures.

1.3. Organization, scopes, and approach of thesis

The thesis is composed of nine chapters and organized as follows.

Chapter 1: Introduction. This chapter explained the background, objectives, thesis organization, and potential benefits of this study.

Chapter 2: Review and discussion on the current aggregate gradation design. This chapter presented a review on the theories and design methods of aggregate gradation. The advantages and limitations for each aggregate gradation theory and design were highlighted.

Chapter 3: Effect of aggregate gradation on asphalt mixture design. A concern in the mix design is how to choose an aggregate gradation which leads to a desired VMA value for the mixture. The objective of the study was to investigate an appropriate aggregate gradation parameter, namely the area of continuous maximum density (CMD_{area}), for achieving desired *VMA* properties of asphalt mixtures. Furthermore, the relationships of the CMD_{area} with the rutting resistance of HMA mixtures were evaluated. Thirty 19.0-mm nominal maximum particle size (NMPS) wearing course mixtures were designed using the Superpave method, and thirteen 12.5-mm NMPS wearing course mixtures were designed using the Marshall method. Three different fine aggregates from two sources (natural sand and manufactured screening) were used to fabricate these HMA specimens. The results indicated that the only principle of gradation designs in the Superpave and Marshall methods is insufficient to comply with the minimum requirement for the *VMA*. In addition, the experiments demonstrated that the CMD_{area} has potential applications to control the value of *VMA*, in spite of aggregates sources, typical aggregate gradation, and mixture designs.

Chapter 4: Effect of aggregate gradation on the workability of asphalt mixtures. Simple indices easily help to evaluate the performance of hot mix asphalt mixtures. The present study aimed to develop a simple workability index and rutting resistance index for wearing course mixtures. Seven Vietnamese blends of different aggregate gradations were developed using the conventional Marshall mix design method. The Superpave gyratory compactor was employed to measure the workability of the seven blends, namely the workability energy parameter of asphalt mixtures. The wheel tracking test was also conducted to evaluate rutting resistance of those mixtures. The results showed a strong relationship between the workability index and the workability energy of hot mix asphalt mixtures. In addition, the workability energy value of an asphalt mixture may be high when the area of continuous maximum density for a proportion of stone is low. Furthermore, the rutting resistance index correlated well with rutting resistance of the hot mix asphalt mixtures. This chapter also applied the proposed workability and rutting resistance indexes to evaluate the workability of six Indonesian wearing course mixtures. The results indicated high relationships of the workability and rutting resistance indexes proposed by this study with the workability of six Indonesian wearing course mixtures.

Chapter 5: Effect of aggregate gradation on the cracking of asphalt mixtures at service temperatures. Cracking is one of the main failure mechanisms of asphalt pavements. This chapter investigated the effects of aggregate gradation on the cracking performance of HMA mixtures at two stages, i.e., the cracking initiation and cracking propagation stages at a high service temperature (30 ^{o}C). Based on the CMD of aggregate gradation and the DASR model, a novel cracking performance index-designated the gradations-based cracking resistance index (*GCI*) was developed to easily evaluate the cracking resistance of wearing course mixtures. This simple index was applied to comparatively

investigate cracking resistance in a variety of dense-, coarse-, and fine-graded mixtures with 12.5-mm NMPS. This study employed the notched semi-circular bending test to evaluate the cracking resistance of the HMA mixtures. The experiments demonstrated a strong relationship between *GCI* and cracking resistance at the cracking initiation stage (J_c). In addition, cracking resistance was observed to increase with increasing *GCI* value. Mixtures with low $CMD_{area-DASR}$ values of aggregate gradation have high cracking resistance at the cracking initiation (J_c) and propagation (K_{Ic}) stages. These findings indicate that the novel indexes have potential applications for evaluating the cracking performance of wearing course mixtures. The chapter also explored the effects of fine aggregate on the resistance of HMA mixtures to cracking resistance. Overall, fine aggregate significantly improved the cracking resistance of mixtures when the aggregate gradations were controlled to achieve the same gradations.

Chapter 6: Effect of aggregate gradation on the cracking of asphalt mixtures design at low service temperatures. This chapter included two objectives. First, this chapter examined the effects of aggregate gradation and asphalt content on the cracking performance of asphalt mixtures at a low service temperature (15 ^{o}C) using the characteristics of continuous maximum density, the dominant aggregate size range model, and apparent film thickness. Second, this chapter investigated if the notched semi-circular bending (SCB) test presents a viable alternative to the three-point bending beam (TPBB) test for assessing fracture properties of asphalt mixtures at intermediate temperature conditions. The TPBB test was conducted using the JRA B005 standard, and the notched SCB test was performed using the following three standards: EN 12697-44, AASHTO TP 105-13, and AASHTO TP 124-16. The experiments showed that the notched SCB test using the EN 12697-44 standard may be able to replace the TPBB test for assessing the cracking resistance of asphalt mixtures.

Chapter 7: Effect of aggregate gradation on the shear strength of asphalt mixtures. HMA mixtures may exhibit premature rutting when the shear strength of the mixtures is insufficient to resist repeated heavy loads in combination with high ambient temperatures. Based on the CMD theory, the present study investigated the effects of aggregate gradation on the shear strength properties of HMA mixtures, i.e., the cohesion (*C*), the internal friction angle (ϕ), and the compaction slope (*K*). In addition, this study aimed to evaluate relationships of the shear strength parameters with the rutting resistance of HMA mixtures. The *C* value and the ϕ value of HMA mixtures were determined using a combination of the unconfined compression (UC) test and the indirect tensile (IDT) test. The *K* value was also obtained from the data of Superpave gyratory compaction. The experiments showed that the CMD theory of aggregate gradation has potential applications for evaluating not only aggregate interlock parameters (ϕ and *K*) but also the *C* property of asphalt mixtures. In addition, the experimental study found that the apparent film thickness is a potential parameter that reflects the effect of asphalt composition on the *C* of

HMA mixtures. The statistical analysis also demonstrated that a rational model using the *C* and the *K* has a strong relationship with the rutting resistance of wearing course mixtures.

Chapter 8: Use of compression test, circle shear test, and indirect tensile test for rutting potential assessment of wearing course mixtures. Rutting resistance of an asphalt mixture is significantly dependent on its shear strength. In order to characterize shear strength properties of asphalt mixtures, this chapter aimed to investigate relationships between two different methods, i.e., the combination of the UC and the IDT tests, and the combination of the UC and the circle shear (CS) tests. In addition, the UC test combined with the CS test was conducted using the Marshall cylindrical specimens to verify whether this protocol could address the shear strength of asphalt mixtures. This chapter also aimed to evaluate the relationship between the IDT strength of conventional Marshall specimens and the rutting resistance of wearing course mixtures using various fine aggregates. The results showed that the cohesion parameters of the two shear methods were correlated well, whereas there was not a strong relationship for the internal friction angle parameters between the two methods. Furthermore, the cohesion obtained from the combination of the UC and the CS tests using the Marshall specimens is a candidate indicator for ranking rutting performance of asphalt mixtures. In addition, the experimental results showed that the IDT test using Marshall cylindrical specimens has potential applications for evaluating rutting resistance, regardless of aggregate source. The study also explored the effects of fine aggregate on the resistance of HMA mixtures to permanent deformation. Overall, fine aggregate significantly influenced the rutting resistance of mixtures when the aggregate gradations were controlled to achieve the same gradations. In contrast, fine aggregates with different gradations were not strongly associated with the rutting resistance of HMA mixtures.

Chapter 9: Conclusion, recommendation, and future research. This chapter summarized the findings and future works of the present study.

1.4. Implementable findings

The present study provided a comprehensive procedure for the design of aggregate gradation to ascertain the volumetric properties (VMA) of HMA mixtures. In addition, this study introduced new practical and cost-effective gradation parameters that help asphalt designers for selecting a proper aggregate gradation at the early stage. Furthermore, the present study developed new procedures that include simple mechanics testing methods for rutting and cracking potential assessments. Therefore, highway agencies, consulting laboratories, and contractors may implement these protocols depending on their experience and equipment.

References

[1] Haryanto, I., and Takahashi, O. Ductile Fracture Assessment of Indonesian Wearing Course Mixtures Using J Integral and Crack Tip Opening Angle, International Journal of Pavement Engineering 9 (3), pp. 165-176, 2008.

[2] Tran, N.T., and Takahashi, O. Improvement on aggregate gradation design and evaluation of rutting performance of Vietnamese wearing course mixtures.The 8th international conference on maintenance and rehabilitation of pavements, Singapore, pp. 212-221, 2016.

[3] Christopher, W.J., *et al*. A manual for design of hot mix asphalt with commentary, Report NCHRP 673, Washington DC, 274p, 2011.

[4] Haryanto, I., and Takahashi, O. Effect of gradation on workability of hot mix asphalt mixtures, Baltic J. Road Bridge Eng. 2 (1) 21-28, 2007.

[5] Haryanto, I., and Takahashi, O. A rutting potential assessment using shear strength properties for Indonesian wearing course asphalt mixtures, International Journal of Pavements, 6 (1-2-3), 27-38, 2007.

[6] Tran, N.T., and Takahashi, O. Effect of aggregate gradation on the cracking performance of wearing course mixtures, Construction and Building Materials, 152, pp. 520-528, 2017.

[7] Tran, N.T, and Takahashi, O. Investigation on indices of workability and rutting resistance for wearing course mixtures, Baltic Journal of Road and Bridge Engineering, 12 (1), 30-37, 2017.

[8] Goh, T.S., and Takahashi, O. Design evaluation of Superpave asphalt mixtures for Tokyo International Airport Pavement, International Journal of Pavement, 10 (1-2-3), pp. 27-38, 2011.

[9] Anderson, R., and Bahia, H. Evaluation and selection of aggregate gradations for asphalt mixtures using Superpave, Transportation Research Record 1583, pp.91-97, 1997.

[10] Nguyen, L.T.N. A Study on aggregate gradation design for Superpave method, Master thesis, Nagaoka University of Technology, Japan, 2015.

[11] Fang, M. et al. Aggregate gradation theory, design and its impact on asphalt pavement performance: a review, International Journal of Pavement Engineering, 2018.

[12] Kim, S., et al. Porosity of the dominant aggregate size range to evaluate coarse aggregate structure of asphalt mixtures, Journal of Materials in Civil Engineering © ASCE, 21(1), 32-39, 2009.

[13] Christopher, W. J., et al. Manual for design of hot mix asphalt with commentary. National Research Council, Washington, D.C, Report NCHRP 673, 2011.

[14] Chun, S., Roque, R., and Zou, J. Effect of gradation characteristics on performance of Superpave mixtures in the field. Journal of the Transportation Research Board, 2294, 43-52, 2012.

Chapter 2. Review and discussion on the current aggregate gradation design

2.1. Aggregate gradation design with permissible ranges

The Marshall method is one of the old methods for designing HMA asphalt mixtures. In general, the Marshall design procedure is regularly divided in the following order: testing material sources, determining aggregate gradation, preparing samples, testing and analysing volumetric properties of mixtures, plotting the test results, and finally selecting a design asphalt content (AC). The manner of Marshall design is almost the same in various countries. However, the requirements of materials, the analysis of test results, and the interpretations of data are different for each country [1-4].

Table 1. Aggregate gradation design in Vietnam, Japan, and Europe for 12.5 NMPS mixtures

Sieve size	Vietnamese standard (2011)		Japanese Standard (1989)		European Standard (2013)	
(mm)	Range	Mean	Range	Mean	Range	Mean
12.5	90 - 100	95	95 - 100	97.5	90 - 100	95
9.5	74 - 89	81.5	***	***	***	***
4.75	48 - 71	59.5	55 - 70	62.5	***	***
2.36	30 - 55	42.5	35 - 50	42.5	10 - 55	32.5
1.18	21 - 40	30.5	***	***	***	***
0.6	15 - 31	23	18 - 30	24	***	***
0.3	11 - 22	16.5	10 - 21	15.5	***	***
0.15	8 - 15	11.5	6 - 16	11	***	***
0.074	6 - 10	8	4 - 8	6	2 - 12	7

In the process of the Marshall method, designing aggregate gradation plays an important role in determining the physical properties and performances of HMA mixtures. Based on the experiments, each country individually issues a standard that introduces acceptable ranges for selecting aggregate gradation. As shown in Table 1, each standard presents the upper and lower grading limits for each sieve size of aggregate particles [5-7]. Designers have to design desired blends of different sizes of aggregates rationally so that the gradation curve falls inside of all acceptable ranges. In general, the conventional aggregate gradation taken from mean values of the permissible ranges is the de facto standard. Figure 1 presents an example for a conventional aggregate gradation for the Vietnamese standard. However, the target gradation based on the medians of the ranges alone does not correctly ensure not only the desired

volumetric properties but also the excellent performance of HMA mixtures [1, 2, 4]. Therefore, with these acceptable ranges, it is complicated to understand and explain the relationship of aggregate gradation with the behaviour of asphalt mixtures.

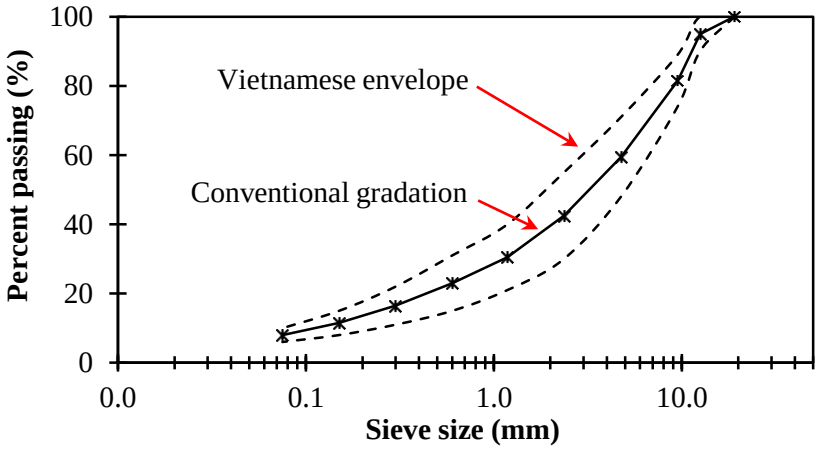

Figure 1. Vietnamese permissible ranges and conventional aggregate gradation

2.2. The theory of maximum density curve (1907)

Theoretically, the best aggregate gradation for asphalt mixtures should have the densest particle packing [3]. The maximum packing density provided by aggregate gradation creates proper contact points among aggregate particles within the mixtures and decreases air voids in the mixtures. As a result, this may increase the stability of the mixtures [8]. However, a packed aggregate should not be excessively tight because air voids of mixtures should be sufficient to prevent bleeding or rutting [8].

In this direction, numerous studies have proposed the simplified ideal curve of parabola maximum density [3, 8, 9]. One of the best known of gradations for maximum density is the Fuller's maximum density curve, and this curve can be presented by following equation [8, 9]:

$$p = 100\left(\frac{d}{D}\right)^n \quad (1)$$

Where, d is the diameter of the sieve size; D is the maximum size of the aggregate; n is grading parameter; and p is the percent passing of aggregates at the sieve d.

A previous study indicated that when the n is equal to 0.5, a maximum packing density provided by aggregate gradation can be obtained [9]. However, numerous studies demonstrated that only the Fuller's maximum density curve is insufficient to control volumetric properties and behaviours of HMA mixtures [9].

2.2.1. Aggregate gradation design in the Superpave method (2015)

At the beginning of the 1960s, based on the Fuller grading theory, the Federal Highway Administration developed an aggregate gradation chart which uses 0.45 as the value of the power *n* [8]. Figure 2 shows a maximum density line (MDL) on the 0.45 power gradation chart in the Superpave method. The maximum density line can be drawn from two points, the original point and the nominal maximum size points. This chart is conveniently adjusted in order to determine the distance of a practical aggregate gradation with the MDL. The Superpave method, which is the current American standard, recommends this aggregate gradation chart to be applied as part of the mix design procedure [10]. As shown in Figure 2, the Superpave method also provides control points for adjusting the aggregate gradation.

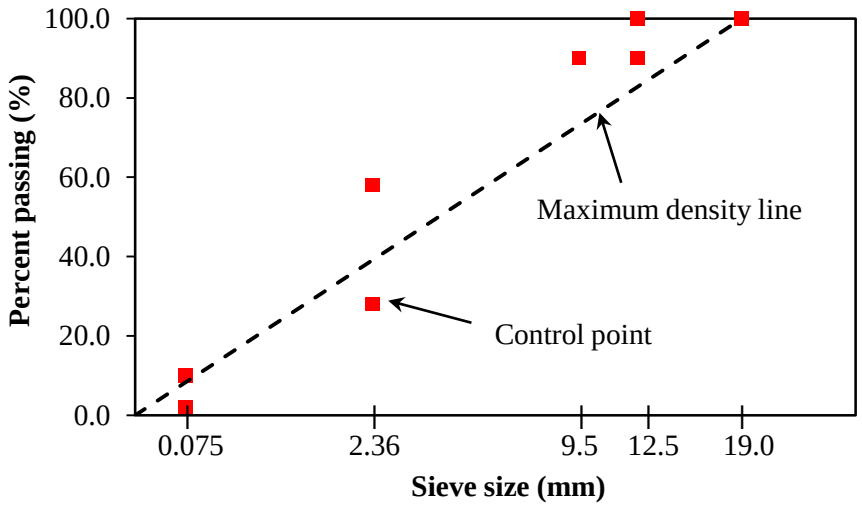

Figure 2. Superpave gradation control points for a 12.5-mm NMPS gradation with the 0.45 power

The current Indonesian standard has proposed the control points and the restricted zone to design an aggregate gradation (Figure 3) [1]. However, the sieve size of this gradation chart is presented on a logarithmic scale instead of the 0.45 power. The restricted zone is initially introduced by the Federal Highway Administration for the Superpave method [8]. This restricted zone aimed to control the effect of fine aggregates on the VMA and void compaction problems during construction [8, 11]. In general, asphalt mixtures having aggregate gradations that fall below the restricted zone show good rutting resistance [8]. However, previous studies indicated that asphalt mixtures having aggregate gradations that fall in the restricted zone are able to meet the minimum VMA requirement and performs well for years in actual field conditions [8, 12]. As a result, the Federal Highway Administration excluded the restricted zone in the current Superpave standard [10].

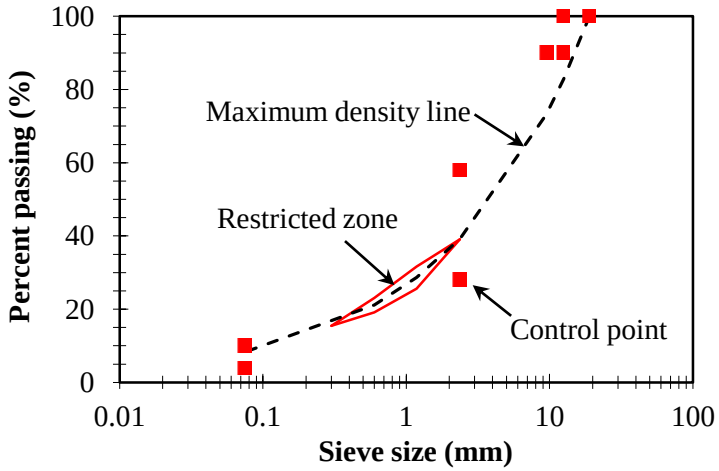

Figure 3. Indonesian aggregate gradation design

Even though the 0.45 power gradation chart in the Superpave method or a logarithmic gradation chart in the Indonesian standard is commonly applied by asphalt engineers, current aggregate design guidelines in these standards are unable to provide a guarantee for selecting a stable aggregate gradation. The previous study indicated that using the 0.45 power gradation chart in the Superpave method is difficult to determine an aggregate gradation that complies with the minimum VMA requirement [4]. In addition, asphalt mixtures having aggregate gradations that enter the control points still have low resistance to rutting [1, 4].

2.2.2. The theory of continuous maximum density (2011)

A concept associated with the maximum density gradation is continuously developed using the theory of CMD line. This theory proposed a method to calculate a value of percent passing on the CMD line for the next sieve size using the following equation [3]:

$$P_{CMD}(d_i) = \left(\frac{d_{i+1}}{d_i}\right)^{0.45} \times P(d_{i+1}) \quad (2)$$

Where, $P_{CMD}(d_i)$ is percent passing for sieve size d_i on the CMD line; d_{i+1} is one sieve lager than d_i; $P(d_{i+1})$ is percent passing for sieve d_{i+1}.

Figure 4 also presents the meaning of parameters in the theory of the CMD line. This figure indicates that if the $P(d_{i+1})$ is the percent passing for sieve d_{i+1}, the $P_{CMD}(d_i)$ calculated using equation (2) is the expected percent passing for the next sieve size d_i that creates the densest particle packing. As a result, a CMD line, which parallels to the Fuller MDL and goes through the $P(d_{i+1})$, can be obtained by

using two points, i.e., the $P(d_{i+1})$ and the $P_{CMD}(d_i)$. Based on this theory, previous studies also proposed a CMD chart to evaluate the effects of aggregate gradation on the air voids and the VMA of asphalt mixtures [3, 13]. One of the components of this chart, a deviation from the CMD line to $P(d_i)$ for sieve d_i, is calculated by the following equation [3]:

$$P_{dev}(d_i) = P_{CMD}(d_i) - P(d_i) \tag{3}$$

Where, $P(d_i)$ is percent passing by weight at sieve d_i.

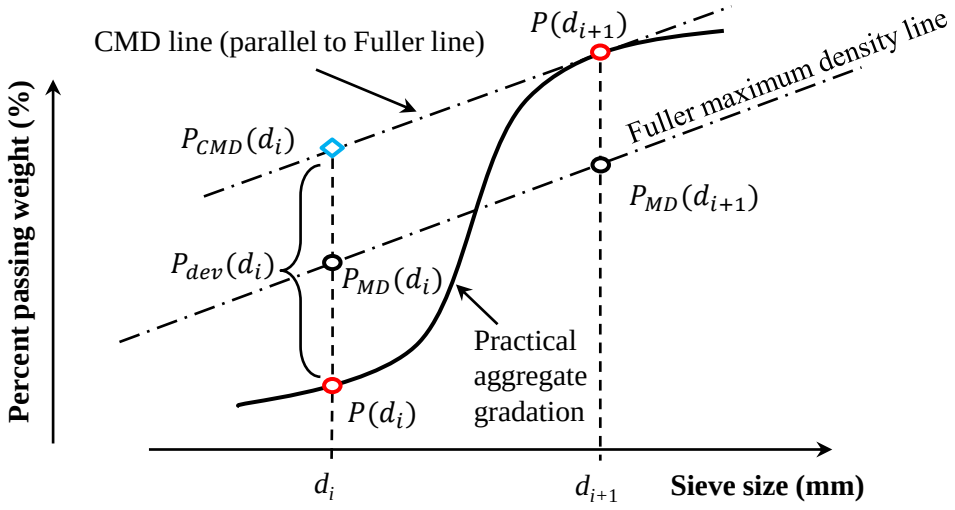

Figure 4. Concept of CMD and meaning of P_{CMD}, P_{dev}

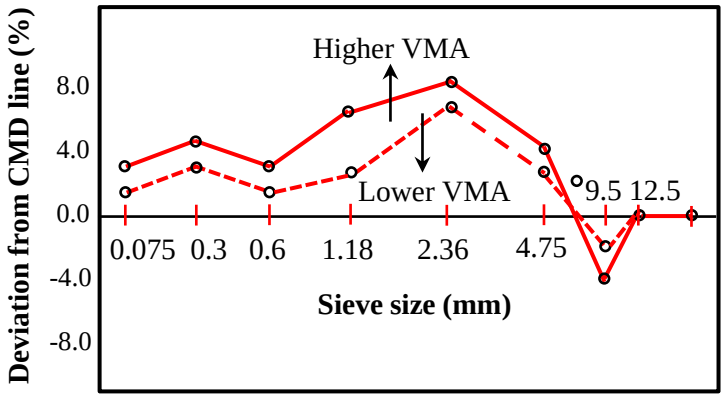

Figure 5. Effect of aggregate gradations on VMA using the CMD chart

The research reported by the American Association of State Highway and Transportation Officials demonstrated that the CMD chart is convenient and helpful to produce the proper air voids

content and VMA [3]. As shown in Figure 5, the CMD pilot illustrates how much the aggregate gradation is far away from the CMD line. Consequently, asphalt mixtures having aggregate gradations that are closer to the horizontal line (through the original) tend to have a lower value of VMA. However, this study did not mention specific guidelines for the application of the CMD chart.

Based on the CMD chart, a recent study conducted by Nguyen also proposed a new parameter, namely CMD_{area}, to evaluate relationships of aggregate gradation with the VMA of HMA mixtures in the Superpave method [13]. The CMD_{area} is defined as the following equation [13]:

$$CMD_{area} = \sum_{0.075}^{NMPS} A_i \tag{4}$$

Where A_i is the area between $P_{dev}(d_i)$ and $P_{dev}(d_{i+1})$ as shown in Figure 6 .

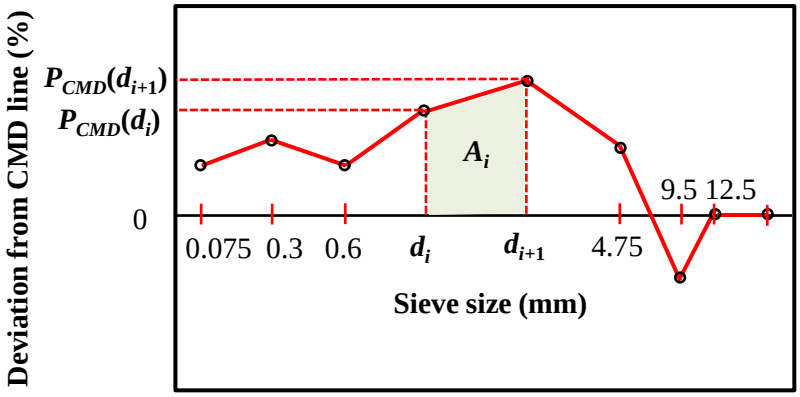

Figure 6. Meaning of A_i

A sieve size of the horizontal axis in Figure 6 is represented on a logarithmic scale, so that the distance of each sieve is almost the same. As the sequence, a value of A_i for two sieves, d_i and d_{i+1}, does not have a large difference between different sieve sizes [13]. The previous study also demonstrated that the CMD_{area} has a strong correlation with the *VMA* of asphalt mixtures [13]. Therefore, this parameter has potential applications for evaluating volumetric properties of asphalt mixtures. However, the past study did not establish the relationships of aggregate gradation parameters using the CMD theory with the performance of asphalt mixtures such as rutting, cracking, and workability. It has been reported that even though asphalt mixtures meet the requirements of volumetric properties, the mixtures still have bad rutting and cracking resistance [1, 2, 4].

2.3. The Bailey method (2002)

The Bailey method was proposed by Mr. Bailey of the Illinois Department of Transportation (DOT) to provide a rational method for selecting an adequate aggregate gradation [14]. The first step in the Bailey method is to decide a chosen the unit weight of coarse aggregate (CA CUW). When the CA CUW of mixtures is smaller than 90% of the loose unit weight of coarse aggregates (CA LUW), between 95% and 100% of the CA LUW, and between 110% and 125% of the CA LUW, the mixtures are classified into fine-graded, coarse-graded, and stone mastic asphalt mixtures, respectively [14]. An aggregate gradation is evaluated using the control sieves. i.e., the half sieve (HS), the primary control sieve (PSC), the secondary control sieve (SCS), and the tertiary control sieve (TCS). The HS determines interceptor particles that are smaller than the HS. Interceptors are too large to fill air voids created by the larger coarse aggregate particles, thereby potentially disrupting the coarse aggregate structure. The PSC determines a sieve where splits particles into coarse and fine aggregates. Next, the SCS is considered as a sieve that breaks fine aggregates into coarse sand and fine sand. Finally, the TCS further divides fine sand into two categories. Based on these control sieves, the Bailey method proposed three ratios, namely CA ratio for coarse aggregate, FA_c ratio for coarse sand, and FA_f ratio for fine sand, to evaluate whether an aggregate gradation is stable. Table 2 presents the values of HS, PCS, SCS, TCS and proper ranges of the CA, FA_c, FA_f ratios for 12.5 mm NMPS mixtures [14].

Table 2. Values of Bailey parameters for 12.5 mm NMPS mixtures

Bailey parameters		Aggregate gradation	
		Coarse-graded	Fine-graded
Control Sieves (mm)	HS	6.25	1.18
	PCS	2.36	0.60
	SCS	0.60	0.15
	TCS	0.15	Not available
Recommended values	CA ratio	0.50 - 0.65	0.60 - 1.00
	FA_c ratio	0.35 - 0.50	0.35 - 0.50
	FA_f ratio	0.35 - 0.50	Not available

The Bailey method aims to introduce a gradation design that results in a proper VMA and better performance mixtures in the Superpave procedure [14]. However, the recent study indicates that the use of the Bailey parameters is difficult for controlling the VMA and rutting resistance of HMA mixtures [4]. Furthermore, the low relationships of Bailey parameters with the VMA and rutting resistance of HMA mixtures were obtained [4].

2.4. The dominant aggregate size range model (2009)

The dominant aggregate size range (DASR) is an interactive range of aggregate particles that create the backbone aggregate of HMA mixtures [15-17]. The DASR model can be divided into three main components as shown in Figure 7. The first component is the coarse aggregates or the DASR aggregates that dominantly form the primary structural network of the aggregate and create the air voids in the mixture. The second components that are smaller than the DASR aggregates are defined as interstitial components (IC) [15]. The IC component includes asphalt binder and fine aggregates which fill voids created by the DASR aggregate. The final components that larger than the DASR aggregates simply float in the DASR matrix. As a result, the final component does not significantly contribute to the friction strength of HMA mixtures [15]. Aggregate interlock occurs within the aggregate structure effectively when relative volume proportions between contiguous size aggregates in the DASR is lower than 70/30 [15].

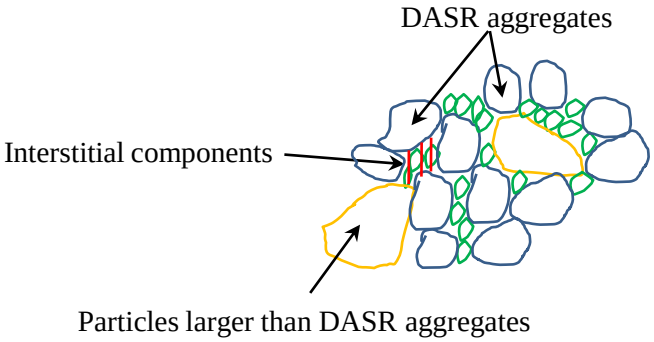

Figure 7. Components of DASR model

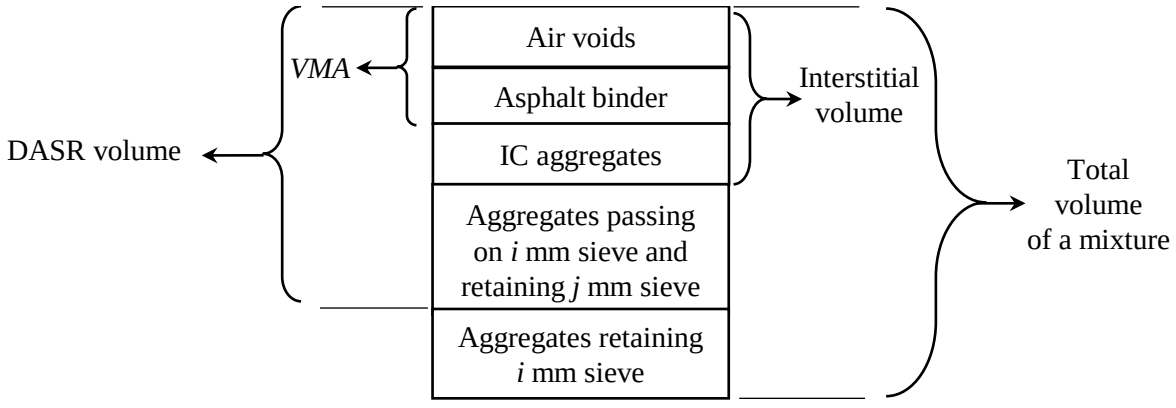

Figure 8. Components of DASR model with a range of *i*-*j* mm

Figure 8 also shows the components of the DARD model with a range of *i-j* mm. The previous studies also demonstrated that the characteristics of IC components have strong influences on the performance of HMA mixtures [16-17]. Based on aggregate gradation, the disruption factor (*DF*) was proposed to check whether the proportion of potential fine aggregate can disrupt the DASR structure. The *DF* value is calculated as the following equation [16]:

$$DF = \frac{\text{Volume of potentially disruptive IC particles}}{\text{Volume of DASR voids}} \quad (5)$$

A high proportion of fine aggregates may destroy the points of interaction among coarse aggregate particles [16]. In contrast, a low proportion of fine aggregates may be insufficient to fill the air voids created by coarse aggregate particles, thereby reducing the dense packing of the backbone aggregate [16]. However, only the *DF* may be insufficient to evaluate the rutting and cracking performance of HMA mixtures [17]. Furthermore, the application of the DASR model for evaluating the workability of HMA mixtures has yet to be established.

2.5. Summary

Based on the search of the literature, the findings are summarized as follows.

- The current standards of most countries used the permissible ranges to design an aggregate gradation. The conventional aggregate gradation obtained from the mean values of the permissible ranges is commonly applied. However, selecting the conventional aggregate gradation does not provide a guarantee for designing a stable aggregate gradation.
- The Fuller's maximum density theory seems to be a useful and practical tool for designing a proper aggregate gradation. Based on this theory, the 0.45 power gradation chart in the Superpave method is proposed to evaluate the effects of aggregate gradation on the air voids and the VMA of asphalt mixtures. Despite that, this chart also has not yet provided clear guidance to determine an adequate gradation that results in a stable asphalt mixture.
- The CMD theory has potential applications for evaluating the effects of aggregate gradations the VMA of asphalt mixtures. However, to the best of our knowledge, no studies have previously conducted an in-depth discussion on the relationships of the CMD theory with performance (rutting, cracking, and workability) of asphalt mixtures.
- The Bailey method proposes a gradation optimization tool to determine appropriate proportions of aggregates in the mixtures. Nonetheless, the gradations obtained from this method may not be insufficient to ensure the minimum VMA requirement and excellent behaviour of asphalt mixtures.
- The DASR model provides a potential concept to evaluate aggregate interlock within asphalt

mixtures. However, there is a need to conduct an in-depth discussion on the application of the *DF* parameter of the DASR model. In addition, the correlation between this model and the workability of HMA mixtures has yet to be discussed.

References

[1] Haryanto, I., and Takahashi, O. Ductile Fracture Assessment of Indonesian Wearing Course Mixtures Using J Integral and Crack Tip Opening Angle, International Journal of Pavement Engineering 9 (3), pp. 165-176, 2008.

[2] Tran, N.T., and Takahashi, O. Improvement on aggregate gradation design and evaluation of rutting performance of Vietnamese wearing course mixtures.The 8th international conference on maintenance and rehabilitation of pavements, Singapore, pp. 212-221, 2016.

[3] Christopher, W.J., *et al*. A manual for design of hot mix asphalt with commentary, Report NCHRP 673, Washington DC, 274p, 2011.

[4] Goh, T.S., and Takahashi, O. Design evaluation of Superpave asphalt mixtures for Tokyo International Airport Pavement, International Journal of Pavement, 10 (1-2-3), pp. 27-38, 2011.

[5] Vietnam Institute of Transport Science and Technology, TCVN 8819. Specification for construction of hot mix asphalt concrete pavement and acceptance, 2011.

[6] Japan Road Association. Manual for asphalt pavement, 1989.

[7] The British Standards Institution, PD 6682-2:2009+A1:2013, Part 2: Aggregates for bituminous mixtures and surface treatments for roads, airfields and other trafficked areas - Guidance on the use of BS EN 13043, 2013.

[8] National Asphalt Pavement Association Research and Education Foundation. Hot mix asphalt materials, mixture design and construction, 1996.

[9] Fang, M. et al. Aggregate gradation theory, design and its impact on asphalt pavement performance: a review, International Journal of Pavement Engineering, 2018.

[10] AASHTO Designation, M 323-13. Standard specification for Superpave volumetric mix design, 2015.

[11] The Asphalt Institute, Superpave mix design: Superpave series No. 2, 3rd ed., 2001.

[12] Watson, D.E., Johnson A., and Jared, D. The Superpave gradation restricted zone and performance testing with Georgia loaded wheel tester, Transportation Research Record 1583, pp. 106-111, 1997.

[13] Nguyen, L.T.N. A Study on aggregate gradation design for Superpave method, Master thesis, Nagaoka University of Technology, Japan, 2015.

[14] Varik W.R et al. Bailey method for gradation selection in HMA mixture design, Transportation Research Circular, Number E-C044, TRB, Wasington D.C, USA, 2002.

[15] Kim, S.,et al. Porosity of the dominant aggregate size range to evaluate coarse aggregate structure of asphalt mixtures, Journal of Materials in Civil Engineering, 21 (1), pp.32-39, 2009.

[16] Al Guarin. Interstitial component characterization to evaluate asphalt mixture performance, PhD thesis, University of Florida, Gainesville, Florida, 2009.

[17] Roque, R. et al. Continuation of Superpave projects monitoring, final report of Florida Department of Transportation, University of Florida, Gainesville, Florida, 2011.

[18] Iman H. Improvement of asphalt mixture design procedure and performance evaluation methods on Indonesian wearing course mixture, PhD dissertation, Nagaoka University of Technology, Japan, 2007.

[19] Denneman, E., Verhaeghe , B.M.J.A., and Sadzik E. S. Aggregate packing characteristics of good and poor performing asphalt mixes, Proceedings of the 26th Southern African Transport Conference, pp. 213-224, 2007.

[20] Chun, S., Roque, R., and Zou, J. Effect of gradation characteristics on performance of Superpave mixtures in the field, Journal of the Transportation Research Board, 2294, pp.43-52, 2012.

Chapter 3. Effect of aggregate gradation on asphalt mixture design

3.1. Introduction

Wearing course mixtures is directly affected by repeated traffic loads and weather conditions. As a result, a combination of a high volume of heavy vehicle and a severe climate potentially causes this layer to failure mechanisms such as rutting or cracking [1, 2]. Therefore, designing a stable asphalt mixture plays an important role in controlling the failure mechanisms of asphalt mixtures. The Vietnamese standard proposed two types of mixtures, i.e., 9.5 mm and 12.5 mm NMPS mixtures to use for wearing course mixtures [3]. These mixtures are designed in accordance with the Marshall method, focuses on the volumetric properties of HMA mixtures to select a design AC [3].

Aggregate skeleton plays a fundamental role in determining the volumetric and physical properties of the HMA mixtures. Properties of the aggregate skeleton are significantly dependent on an aggregate gradation. In the process of gradation design, the current Vietnamese standard proposes the upper and lower grading limits called permissible ranges [3]. Asphalt designers have to choose a percent passing of aggregate at each sieve to achieve an aggregate gradation that enters inside of all permissible ranges. For practicality, the middle aggregate gradation of permissible ranges is commonly applied in Vietnam. The aggregate gradation design aims to obtain an asphalt mixture that satisfies with the volumetric requirements in the Marshall method. The *VMA* is one of the most important parameters in the Marshall method. However, the aggregate gradation procedure in the current Vietnamese standard does not provide a clear guideline to comply with the minimum VMA requirement. In fact, complying with the VMA requirement is the most difficult challenge for designers in the volumetric design process [4].

A previous study proposed the CMD theory to evaluate the effect of aggregate gradation on the VMA of asphalt mixtures [5]. The past results indicated this theory has a strong association with the VMA in the mixtures. However, this study only conducted for the Superpave method and to the best of our knowledge, no studies have previously investigated the relationships of the CMD theory with the VMA in the Marshall method, which is the current mixture design in most countries.

The objective of this chapter was to investigate the relationship of aggregate gradation with the VMA of asphalt mixtures using the CMD theory. First, the present study conducted seven asphalt mixtures (dense-, coarse-, and fine-graded) that represents 12.5-mm NMPS Vietnamese wearing course mixtures. Next, this study evaluated the application of the CMD theory for the data obtained from previous studies. The relationship of the CMD theory with rutting performance of asphalt mixtures was also investigated.

3.2. Literature review

3.2.1. The theory continuous maximum density

The theory of CMD and the CMD_{are} parameter have been described in chapter 2.

3.2.2. The VMA of asphalt mixtures

In the last few decades, using VMA to evaluate and design asphalt mixtures have received a growing interest in asphalt researchers [1-10]. As shown in Figure 9, the *VMA* includes two components, namely, the effective asphalt content (V_{be}) and the air voids in mixture (*VIM*). The VMA is considered to be the most important parameter that strongly influences the performance of HMA mixtures [6, 7]. HMA mixtures having low VMA values generally show a low cracking resistance at low temperatures and low fatigue resistance at normal temperatures [7, 8]. In contrast, HMA mixtures having high VMA values tend to have a low rutting resistance at high temperatures [10]. Therefore, the VMA values should be high enough to ensure good rutting and cracking resistance [6, 7].

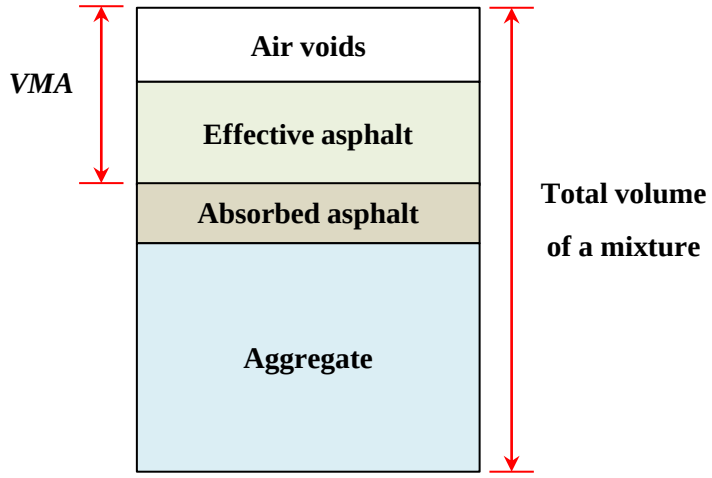

Figure 9. Definition of VMA

In the mixture design procedure, almost asphalt standards have specified the minimum VMA requirement to obtain a stable asphalt mixture [1, 3, 9]. This requirement is also applied for an acceptable aggregate gradation. However, numerous studies have recently reported problems in achieving the minimum VMA requirement [5-7, 10]. The process of trial and error for choosing appropriate gradations is difficult and time-consuming. The current gradation designs such as permissible ranges in Vietnamese and Japanese standards, or the 0.45 power gradation chart in the American standard are not sufficient to ensure the minimum VMA requirement [2, 5, 10]. In recent years, the Bailey method was proposed to

design aggregate gradations for HMA mixtures. However, the current study also indicated that in the Superpave method, relationships of the VMA with the Bailey parameters were not high [10].

Based on the CMD theory, the current study proposed the CMD_{area} to control the gradation design in Superpave mixtures [5]. The past results indicated that the CMD_{area} is strongly associated with the VMA mixtures [5]. The Superpave method controls a constant VIM value of 4% while the Marshall method requires from 3% to 6% for the VIM value. Because the VIM is one of the VMA components, different VIM values can lead to different VMA values of asphalt mixtures. However, the application of the CMD theory for Marshall mixtures has yet to be established. Therefore, the present study aimed to examine whether the CMD theory can be applied to the Marshall method.

3.3. Experimental work

3.3.1. Material sources

The present study used a straight asphalt (virgin asphalt) with a penetration grade of 60/80 to fabricate the HMA specimens for the experiments. The available aggregates were divided into coarse (12.5 - 4.75 mm) and medium (4.75 - 2.36 mm) aggregates, as well as into coarse and fine sands. The aggregate classification helps to design the desired blends of different sizes of aggregates rationally. All materials used in the present study were produced in a specific area of Japan.

3.3.2. Design of aggregate gradation

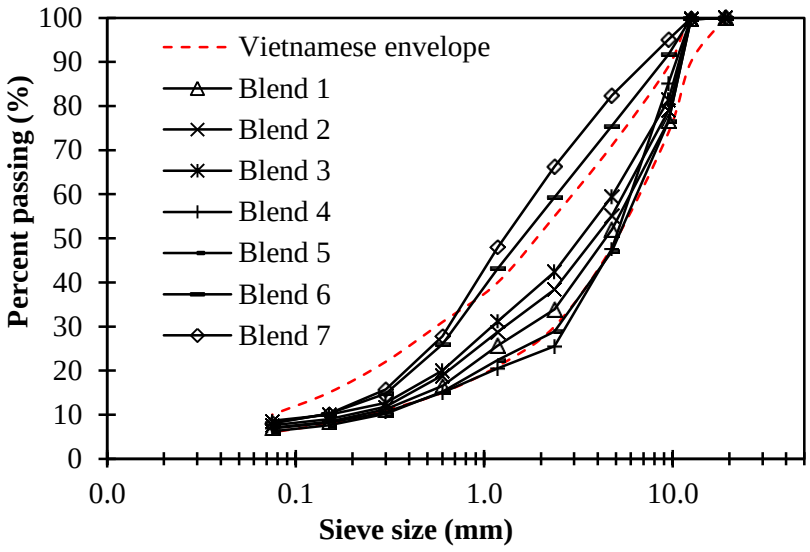

Figure 10. Aggregate gradations for analysing

Seven aggregate gradations were designed to represent dense-, coarse- and fine-graded HMA mixtures. The first group (Blends 1 to 3) comprised dense-graded HMA mixtures, where Blend 3 represented the conventional aggregate gradation that is commonly applied in Vietnam. The second group (Blends 4 and 5) comprised coarse-graded HMA mixtures. The aggregate retention on the 2.36-mm sieve for Blend 4 was selected to be slightly lower than 76%, which is the minimum requirement for this sieve for an aggregate gradation prepared for stone matrix asphalt mixtures [11]. The final group (Blends 6 and 7) comprised fine-graded HMA mixtures. Because the minimum aggregate retention of 30% on a 2.36-mm sieve is recommended for such mixtures [12], the aggregate retention on this sieve for Blend 7 was designed to be slightly over 30%.

3.3.3. Mix design procedure

Figure 11 shows the flow of mix design procedures. All the HMA mixtures were designed in accordance with the Marshall method, which is the current Vietnamese standard [13]. The design procedure was listed as the following steps:

1. Prepare and evaluate aggregates, sands, filler and asphalt binder.
2. Make two samples with a tentative asphalt content (AC) to conduct the rice test, and then calculate the theoretical maximum specific gravity (G_{mm}) of the loose asphalt mixtures and the effective specific gravity of aggregate (G_{se}).
3. Fabricate Marshall briquettes in five asphalt contents. Seventy-five blows are applied on each side for the samples.
4. Measure and determine properties of each sample (volumetric, stability and flow).
5. Evaluate the asphalt mixture properties to determine an acceptable range of AC based on the specified requirements as presented in Table 3**.**
6. Determine a design AC, namely the mean value of the acceptable AC range.
7. Make five samples at the design AC. Compare the properties with the design criteria for three samples, and determine the residual stability index for the two samples.

Table 3. Marshall requirements for 12.5-mm NMPS mixtures

The properties of asphalt mixture	Required values
Voids in mineral aggregates (VMA)	≥ 14 (%)
Voids in mixture after 2×75 blows (VIM)	3 – 6 (%)
Stability	≥ 8.0 (kN)
Flow	2 – 4 (mm)
Residual stability	≥ 75 (%)

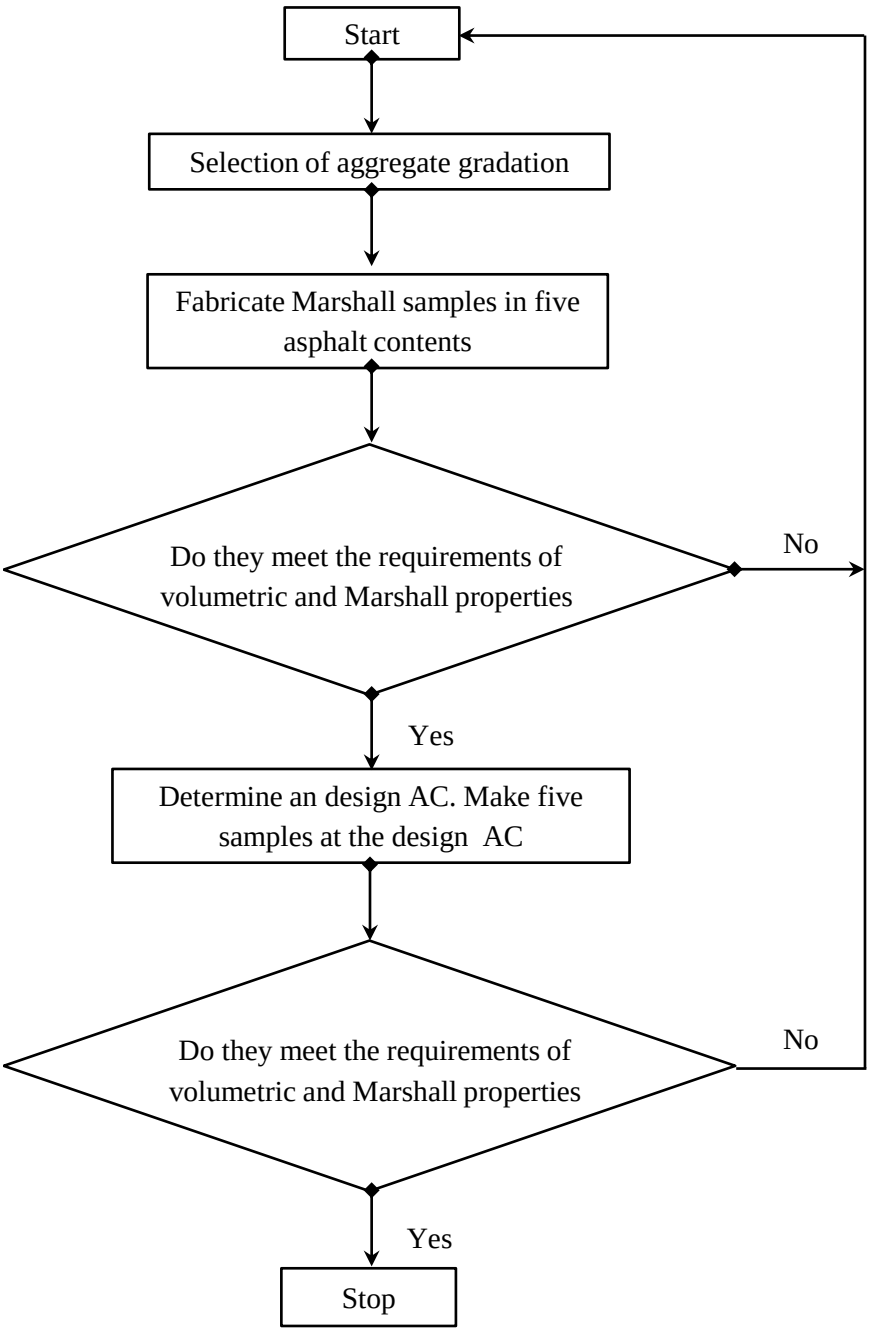

Figure 11. Mix design flow for Vietnamese wearing course mixtures

3.4. Results and discussion

3.4.1. Result of mix design for Vietnamese wearing course mixtures

Figure 12 shows results of mixtures design for the seven mixtures at five asphalt contents. It was found that Blends 2 and 3 could not comply with the minimum requirement of VMA. According to

TCVN 8820, for dense-graded HMA mixtures, the design AC can be established at the air voids of 4% [13]. Because the acceptable AC range did not appear, the design AC for Blends 2 and 3 was determined when air voids content of the mixtures yields 4.0%.

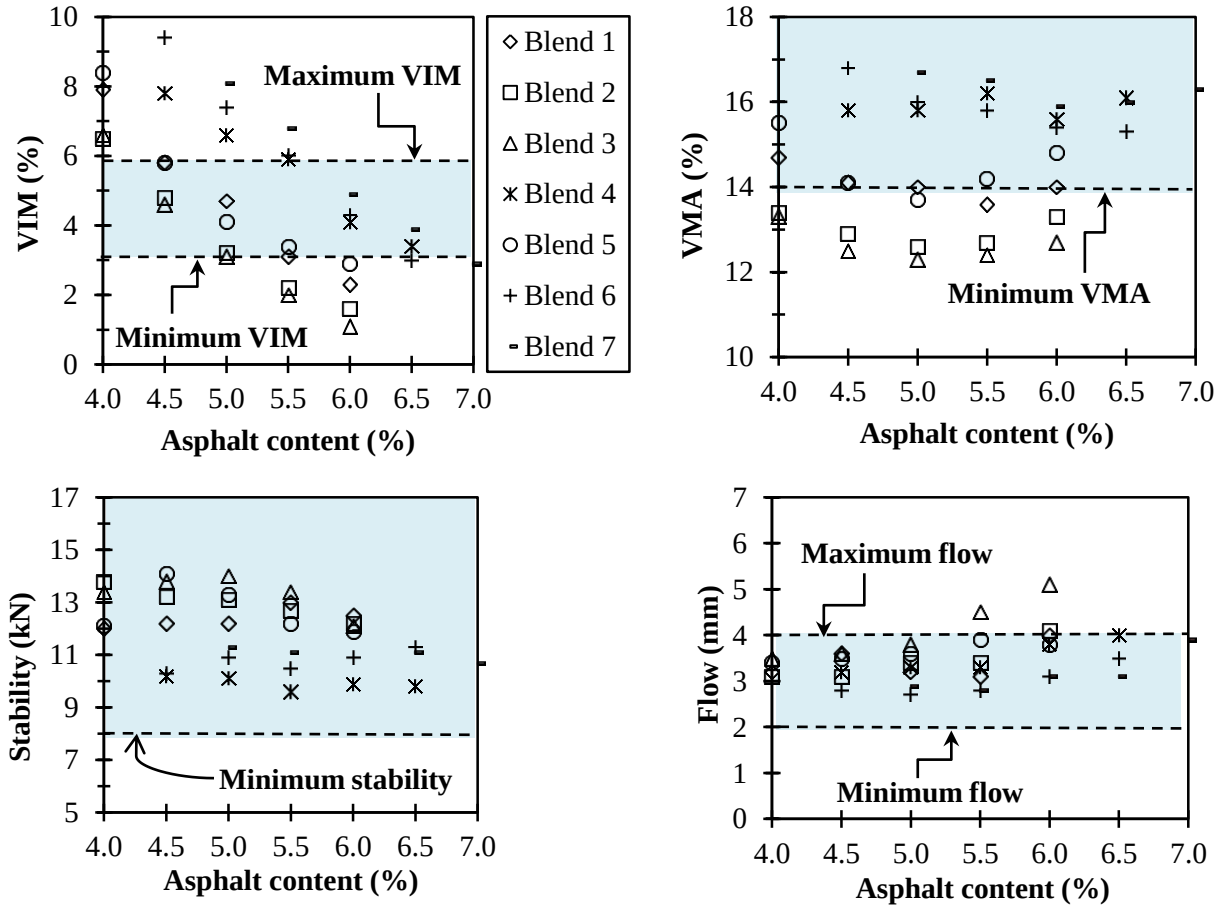

Figure 12. Volumetric and Marshall properties of seven mixtures at five asphalt contents

Table 4 shows the acceptable AC range and the design AC for the seven HMA mixtures. Table 5 also presents results of volumetric properties for the seven blends at the design AC. As mentioned above, the *VMA* is the most important volumetric properties in the mix design procedures. Mixtures 2 and 3 did not meet the minimum VMA requirement even though the aggregate gradations of these mixtures fall inside the recommended ranges specified by the Vietnamese standard. In addition, the results illustrated that dense-graded mixtures were more difficult to satisfy the VMA requirement than coarse and fine-graded mixtures. Among the dense-graded mixtures, only Blend 1 having the gradation curve that enters into all specified ranges meets the minimum VMA requirement. Therefore, it is a tough challenge for mixture designer to select an appropriate aggregate gradation that achieves a sufficient *VMA* for the

mixture even though the gradation complies with the control points. Mixture designers must conduct a trial and error process.

Table 4. Acceptable AC range and design AC

Mixture	Acceptable AC range (%)	Margin of acceptable AC range (%)	Design AC (%)
1	4.5 – 5.0	0.5	4.75
2	–	–	4.70
3	–	–	4.60
4	5.5 – 6.5	1.0	6.00
5	4.5 – 4.9	0.4	4.70
6	5.5 – 6.5	1.0	6.00
7	5.7 – 7.0	1.3	6.35

Note: Design AC values of Blends 2 and 3 were determined for the VIM value of 4.0%

Table 5. Volumetric properties and Marshall-stability results for seven mixtures at the design AC

Mixture		Design AC (%)	VIM (%)	VMA (%)	Stability (kN)	Flow (mm)	Residual stability (%)	Meet all requirements
Dense-graded	1	4.75	5.3	14.0	11.4	3.9	88.5	Yes
	2	4.70	4.1	12.7	12.7	3.2	89.8	No
	3	4.60	4.0	12.2	12.2	3.8	86.4	No
Coarse-graded	4	6.00	4.0	15.6	9.9	3.7	85.1	Yes
	5	4.70	5.5	14.3	12.0	3.0	90.9	Yes
Fine-graded	6	6.00	4.2	15.3	11.0	3.1	92.7	Yes
	7	6.35	4.3	16.1	12.0	3.7	75.6	Yes

3.4.2. Analysis of the effect of CMD on the VMA

Table 6 presents CMD_{area} values for seven aggregate gradations, and Figure 13 shows the effect of the CMD_{area} on the *VMA* of the mixtures. A strong linear correlation ($R^2 = 0.92$) was obtained between the CMD_{area} and the *VMA*. The trend line indicated that the *VMA* of HMA mixtures increases when the CMD_{area} of aggregate gradation increases. These results confirmed that the CMD_{area} of aggregate gradation is a helpful tool for a *VMA* assessment of asphalt mixtures.

Table 6. CMD_{area} values for seven blends

Blend	1	2	3	4	5	6	7
CMD_{area}	5.9	4.6	3.4	8.3	7.4	7.0	9.8

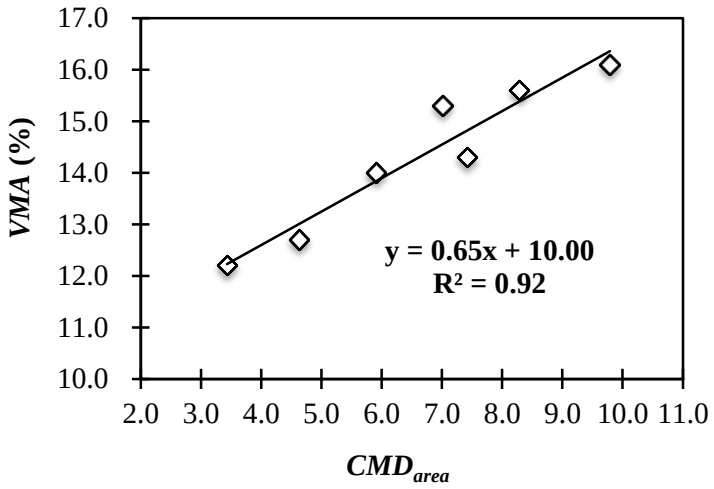

Figure 13. Relationship of CMD_{area} with *VMA*

3.4.3. Analysis of the effect of CMD on the VMA with different factors

3.4.3.1. Analysis of the effect of CMD on the VMA in the Superpave method

This study evaluated the data performed by the former graduate students at Highway Engineering Laboratory, Nagaoka University of Technology, Japan. The Superpave method was applied to design 19-mm NMPS wearing course mixtures for airport pavements. In the Superpave method, the design AC can be determined when the air voids content of the HMA mixture is 4.0%.

The Superpave gyratory compactor (SGC) was employed to compact the Superpave samples. Two aggregate sources, i.e., natural sand and manufactured screening, were used to fabricate HMA samples. The Superpave samples of eighteen aggregate gradations were compacted using both limestone screening and natural sand. On the other hand, the Superpave samples of twelve aggregate gradations were fabricated using natural sand sources only. Figure 14 also shows pictures of the limestone screening and granite sand. All the aggregate gradations are also depicted in Figure 15. Virgin straight asphalt of Pen 60/80 produced in Japan was used to fabricate all HMA samples.

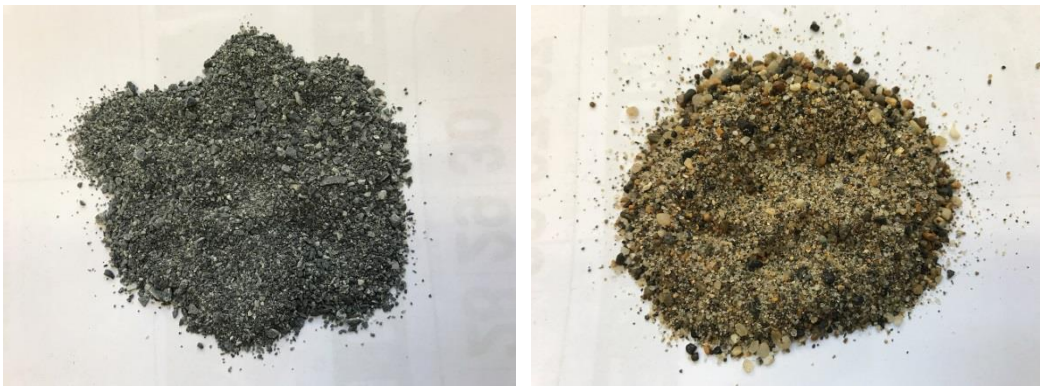

(a) (b)

Figure 14. Photographs of the (a) limestone screening and (b) granite sand

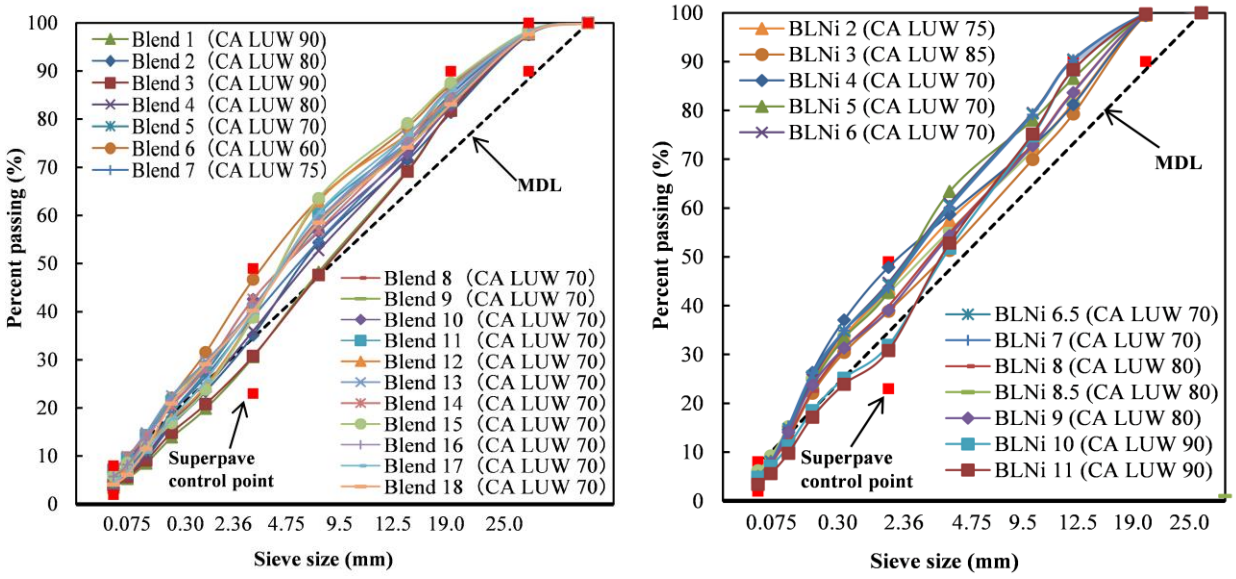

Figure 15. Eighteen limestone screening gradations and twelve granite sand gradations

Figure 16 and Figure 17 show the relationships of the CMD_{area} and Bailey parameters with the VMA for the eighteen screening and twelve sand mixtures. The results demonstrated that the VMA of mixtures had stronger relationships with CMD_{area} than with the Bailey parameters. The trend lines indicated that the mixtures having aggregate gradations that have higher CMD_{area} values showed greater VMA values. As shown in Figure 17**,** it is worth noting that the models demonstrated good R^2 values (0.75 and 0.69) for both the eighteen screening and twelve sand mixtures, regardless of aggregate source. In addition, the relationships of CMD_{area} with VMA for all thirty wearing course mixtures (Figure 18) had a reasonably correlation coefficient (good R^2: 0.69). In the Superpave method, The *VMA* values for 19-mm NMPS wearing course mixtures must be a minimum of 13% [10]. Figure 18 also suggests that the

CMD_{area} values of aggregate gradations should be higher than 4.0 to provide HMA mixtures with sufficient *VMA* values.

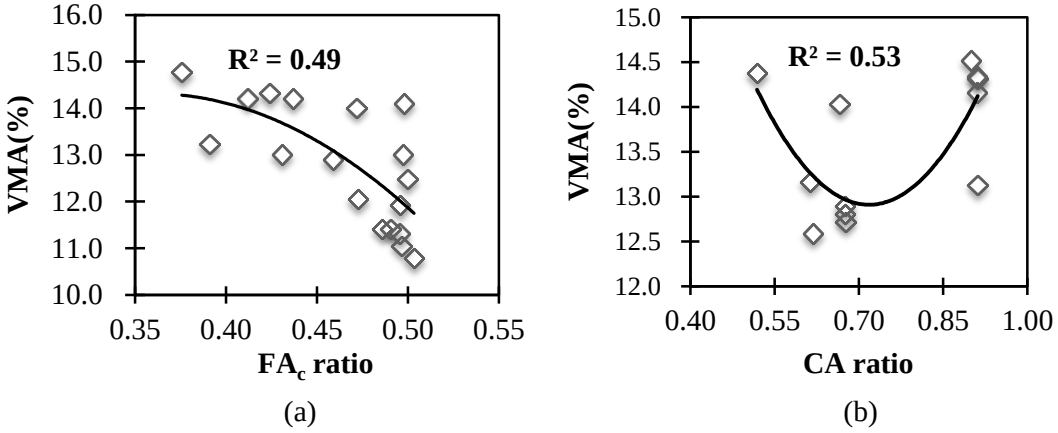

(a) (b)

Figure 16. The highest relationships of Bailey parameters with VMA for the (a) eighteen limestone screening blends and (b) twelve granite sand blends

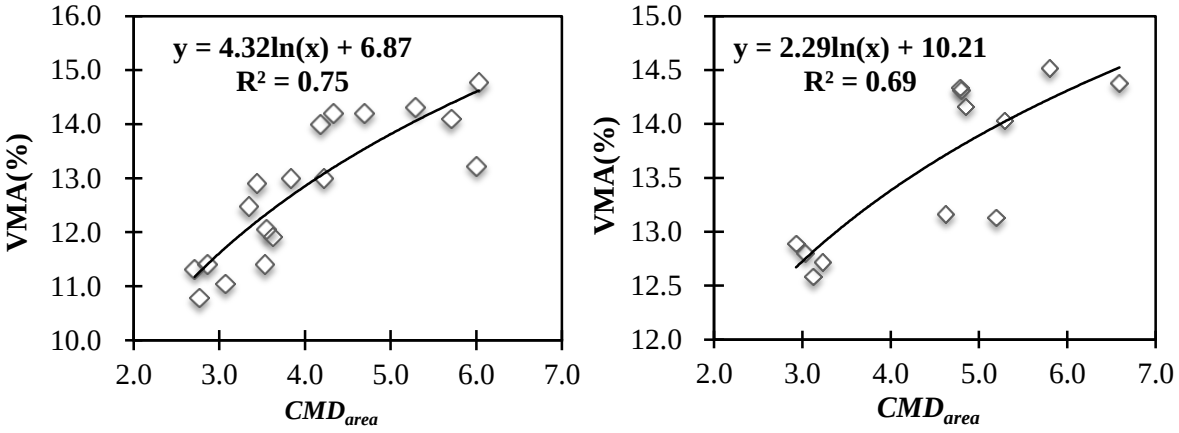

(a) (b)

Figure 17. Relationships of CMD_{area} with VMA for the (a) eighteen limestone screening blends and (b) twelve granite sand blends

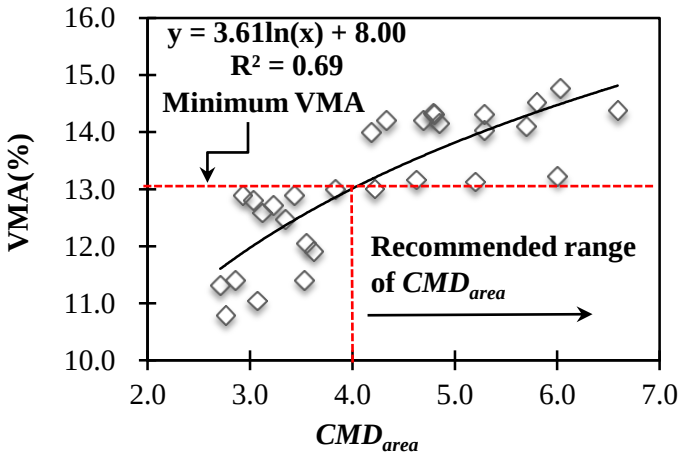

Figure 18. Relationship of of CMD_{area} with VMA for the thirty blends

3.4.3.2. Analysis of the effect of CMD theory on the VMA in the Marshall method

The present study evaluated the effect of CMD theory on the VMA in two groups of 12.5-mm NMPS wearing course mixtures using the Marshall method. The first group included seven aggregate gradations that were designed as Vietnamese wearing course mixtures, and these gradations were previously described in subsection 3.3. All the Vietnamese wearing course mixtures were fabricated using natural sand sources.

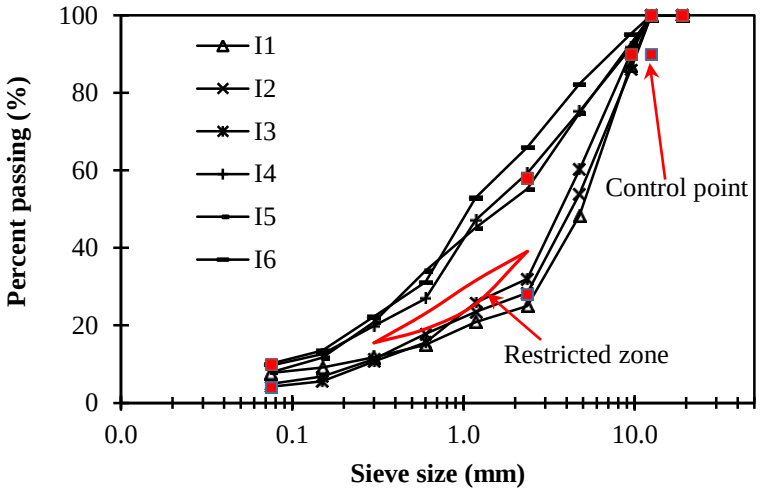

Figure 19. Six aggregate gradations for Indonesian wearing course mixtures

The second group included six aggregate gradations that were designed in accordance with the Indonesian standard for wearing course mixtures (designated Blends I1–I6) based on Iman et al. [1]. The

six aggregate gradations of this second group are presented in Figure 19. The Indonesian standard stipulates control points and a restricted zone to design aggregate gradation [1]. Three aggregate gradations (I1, I2, and I3) were designed to pass below the restricted zone, and the remaining three aggregate gradations (I4, I5, and I6) were designed to pass above the restricted zone. The HMA samples of Blends I1, I3, I4, and I6 were fabricated using the limestone screening and the natural sand. On the other hand, the samples of Blends I2 and I5 were compacted using the natural sand only.

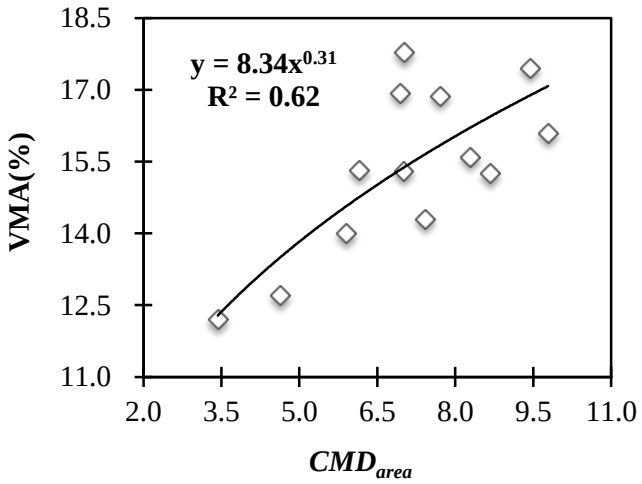

Figure 20. Relationship of of CMD_{area} with VMA for the thirteen blends using the Marshall method

Figure 20 presents the relationship between the CMD_{area} and VMA values for the thirteen mixtures. The trend line showed that the VMA of mixtures increased with the increases in CMD_{area} values of aggregate gradations. The analytical model showed a fair goodness of fit, where the R^2 value was 0.62 (A model with an R^2 above 0.4 is regarded as having fair goodness of fit [14]). The results indicated that the correlation coefficient of the CMD_{area} with the VMA for the Marshall mixtures was lower than that of the CMD_{area} with the VMA for the Superpave mixtures. This may be explained by the following reasons. First, in the Superpave method, the *VIM* value is designed at 4%. This means that only one value of the design AC or the VMA was found for the constant air void. As a result, the determination of the VMA of mixtures in the Superpave method follows the same protocol and only a VMA value is found for an aggregate gradation. In contrast, the Marshall method stipulates a range of values (3% to 6%) for *VIM*, thereby resulting in the large variability for the determination of the VMA. This means that there is a range of VMA values for an aggregate gradation. Next, because the Marshall requirements for 12.5-mm NMPS mixtures in Vietnamese and Indonesian standards (Table 7) are different, there is a principle difference in VMA determination between the two standards.

Table 7. Comparison of Marshall requirements for 12.5-mm NMPS mixtures for Vietnam and Indonesia

The properties of a HMA mixture	Required range	
	Vietnam	Indonesia
Voids in mineral aggregates (VMA)	≥ 14 (%)	≥ 15 (%)
Voids in mixture (VIM), after 75×2 blows	3 - 6 (%)	4.9 - 5.9 (%)
VIM at refusal density	–	4 - 6 (%)
Voids filled with asphalt (VFA)	–	≥ 65 (%)
Stability	≥ 8.0 (kN)	≥ 8.0 (kN)
Flow	2 - 4 (mm)	≥ 2 (mm)
Residual stability	≥ 75 (%)	≥ 85 (%)
Marshall quotient	–	≥ 2 (kN/mm)
Asphalt absorption	–	≤ 1.2 (%)

To gain a clearer understanding of the different mixtures, the aggregate gradations were evaluated using two methods where each blend was mixed with the same and distinct aggregate gradations. For the same aggregate gradation, we produced three pairs of duplicate aggregate gradations (Blends I1 and V4, I4 and V6, and I6 and V7); the blends in each pair generally showed the same passing percentage at each sieve. Table 8 presents the characteristics of all aggregate gradations investigated for the Marshall method.

The *VMA* of an asphalt mixture includes two components, i.e., the *VIM* and the effective AC (V_{be}). Table 8 shows that the design ACs or of Blends V4, V6, and V7 were higher than those of Blends I1, I4, and I6, respectively. As mentioned above, while the specimens of Blends I1, I4, and I6 were compacted using the limestone screening, the specimens of Blends V4, V6, and V7 were compacted using the granite sand. This corroborates the findings of a previous study that demonstrated that the design AC of HMA mixtures with limestone screening was lower than that of mixtures with granite material [15]. An increase in design AC in combination without controlling the VIM can lead to a difference in VMA determination. Consequently, three pairs of duplicate aggregate gradations (Blends I1 and V4, I4 and V6, and I6 and V7), which have same aggregate gradations or CMD_{area} values, may not necessarily provide same VMA values as shown in Table 8. Therefore, this may decrease the relationship of CMD_{area} with VMA when the same aggregate gradation was evaluated using different fine aggregates and the Marshall method.

Table 8. Aggregate gradations and mixture design results of the thirteen mixtures

	Sieve Size (mm)	19	12.5	9.5	4.75	2.36	1.18	0.6	0.3	0.15	0.075	CMD_{area}	Design AC (%)	*VIM* (%)	V_{be} (%)	*VMA* (%)
Vietnamese	V1	100	99.7	76.6	52	33.9	25.7	16.5	11.2	8.4	7	5.9	4.75	5.3	8.6	14.0
	V2	100	99.7	79	55.1	38.4	28.8	18.9	11.8	9	7.6	4.6	4.70	4.1	8.6	12.7
	V3	100	99.8	81.4	59.5	42.4	31.2	20	12.7	10	8.6	3.4	4.60	4.0	8.2	12.2
	V4	**100**	**99.8**	**85.2**	**47.6**	**25.5**	**20.5**	**15**	**10.6**	**8.2**	**6.9**	**8.3**	**6.00**	**4.0**	**11.6**	**15.6**
	V5	100	99.7	76.5	47	28.9	22.4	15.2	10.2	7.6	6.2	7.4	4.70	5.5	8.7	14.3
	V6	**100**	**99.9**	**91.7**	**75.5**	**59.3**	**43.2**	**26**	**14.8**	**10.2**	**8.1**	**7.0**	**6.00**	**4.2**	**11.1**	**15.3**
	V7	**100**	**99.9**	**95.1**	**82.4**	**66.3**	**48**	**27.8**	**15.7**	**10.2**	**8**	**9.8**	**6.35**	**4.3**	**11.7**	**16.1**
Indonesian	**I1**	**100**	**100**	**87.1**	**48.4**	**25**	**20.9**	**15**	**11.8**	**9.1**	**7.7**	**8.7**	**5.34**	**4.6**	**10.7**	**15.3**
	I2	100	100	86	53.9	28.4	23.5	17.8	11.3	6.8	4.9	7.7	5.83	5.6	11.3	16.9
	I3	100	100	90.2	60.2	32	25.9	15.6	10.7	5.6	4.2	6.9	5.31	5.9	11.0	16.9
	I4	**100**	**100**	**91.7**	**75.2**	**59.3**	**47.2**	**26.9**	**19.9**	**12.6**	**9.6**	**7.0**	**5.41**	**6.0**	**11.8**	**17.8**
	I5	100	100	92.7	74.8	55.2	45.2	34.1	20.9	11.7	7.9	6.2	5.62	5.2	10.2	15.3
	I6	**100**	**100**	**95.2**	**82.3**	**66**	**53**	**31.2**	**22.3**	**13.5**	**10.1**	**9.4**	**5.37**	**5.9**	**11.6**	**17.5**

Note: Identical colors indicate the same aggregate gradations.

3.4.3.3. Evaluation of the effect of CMD_{area} with VMA with different fine aggregate sources, mixture design methods, and nominal maximum particle size

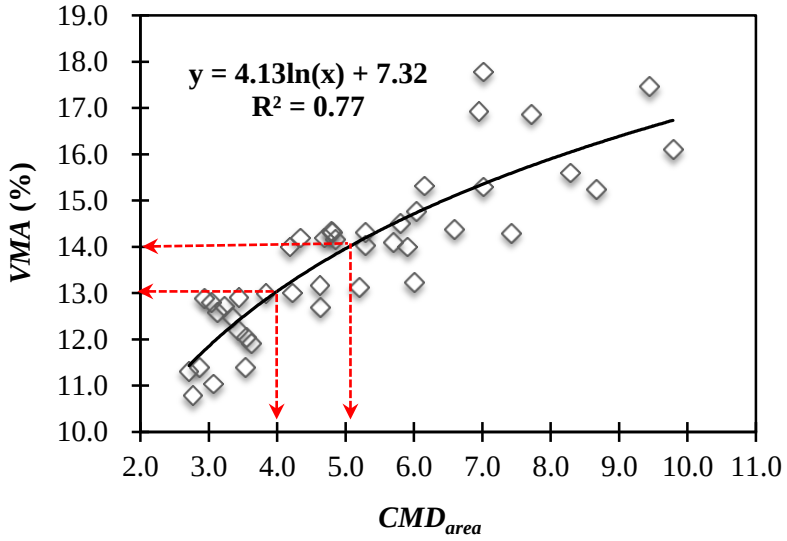

Figure 21. Relationship of CMD_{area} with the VMA for forty-three blends.

Figure 21 shows the effect of the CMD_{area} on VMA values for the forty-three mixtures. The data indicate a wide variety of asphalt mixtures for different fine aggregate sources (limestone screening and granite sand), mixture design methods (Superpave and Marshall), and nominal maximum particle size (19-mm and 12.5-mm NMPS). As expected, the coefficient of determination (R^2) of the regression was 0.77, which indicates that approximately 77% of the variability in the VMA observed from those forty-three mixtures can be explained by the sole independent variable, the CMD_{area} of aggregate gradation. Therefore, the CMD_{area} is a potential parameter that indicates a positive effect of aggregate gradation on the VMA of HMA mixtures. Based on Figure 21, the CMD_{area} value of aggregate gradation should be more than 4.0 and 5.0 to comply with the minimum *VMA* requirement of 13.0 % and 14.0 % for 12.5-mm and 19.0-mm NMPS mixtures, respectively.

3.4.3.4. Evaluation of the effect of CMD_{area} with the rutting resistance of HMA mixtures

This section evaluated the relationship between CMD_{area} of aggregate gradation and rutting resistance of HMA mixtures using two types of rutting test. First, for Superpave mixtures, the asphalt pavement analyzer (APA) test was conducted to characterize the resistance of the HMA mixtures to permanent deformation using SGC specimens. Prior to the test, the SGC specimens were heated for six hours at a temperature of 60 °C. The APA machine automatically stops when the wheel traverse reaches 8000 cycles [16]. Rut depth of specimens was measured at every traverse. Second, for Marshall mixtures,

the wheel tracking test was performed to evaluate the rutting resistance of asphalt mixtures. The test was also conducted at 60 °C using slab samples. Based on the relationship between the rut depth and the cycle of the wheel, the dynamic stability (DS) was estimated, which indicates the cycles of the wheel per 1-mm rut depth.

The present study investigated the relationship of CMD_{area} of aggregate gradation with rutting resistance of HMA mixtures using linear regression analysis. Table 9 summaries the regression results, and Figure 22 and Figure 23 depict the relationships of CMD_{area} with rutting resistance for each test. *P*-values and coefficients in the linear regression analysis determine whether there are statistically significant relationships and the characteristics of those relationships between variables. The sign of the coefficient indicates if there is a positive or negative relationship between each independent variable and the dependent variable. The *p*-value for each coefficient describes whether the relationship between each independent variable and the dependent variable is statistically significant. If the *p*-value is smaller than the chosen significance level (0.05 was chosen in this present study), the sample data sufficiently illustrates the statistically significant relationships between variables.

Table 9. Regression analysis between CMD_{area} and rutting resistance

Model	Term	Coefficient	Se	*t* value	*p* value	R^2
Rut depth ~ CMD_{area}	Intercept	2.01	0.69	2.93	0.010	0.232
(Superpave - with screening)	CMD_{area}	0.36	0.16	2.20	0.043	
Rut depth ~ CMD_{area}	Intercept	6.91	1.10	6.31	< 0.001	0.069
(Superpave - with natural sand)	CMD_{area}	-0.20	0.24	-0.86	0.410	
DS ~ CMD_{area}	Intercept	229.41	684.36	0.34	0.754	0.157
(Marshall - with screening)	CMD_{area}	76.40	88.55	0.86	0.437	
DS ~ CMD_{area}	Intercept	1716.10	202.48	8.48	< 0.001	0.846
(Marshall - with natural sand)	CMD_{area}	-153.27	29.22	-5.25	0.003	

Note: Se is standard error.

Table 9 shows that while the relationship of CMD_{area} with the rut depth was statistically significant for eighteen Superpave-screening blends (*p*-value < 0.05), this relationship was not statistically significant for twelve Superpave-sand blends (*p*-value > 0.05). In contrast, the relationship between the CMD_{area} and the *DS* was not statistically significant for six Marshall-screening blends, and this relationship was statistically significant for seven Marshall-sand blends. Furthermore, there were differences between the signs of regression coefficients for each group, indicating both positive and negative correlations between the CMD_{area} and the rutting resistance. The positive relationships of CMD_{area} with rutting resistance were not statistically significant while the negative relationships of

CMD_{area} with rutting resistance were statistically significant. In most cases, the low coefficients of determination (R^2) indicate that the sole CMD_{area} is insufficient to explain the percentage of variance in the rutting resistance of HMA mixtures.

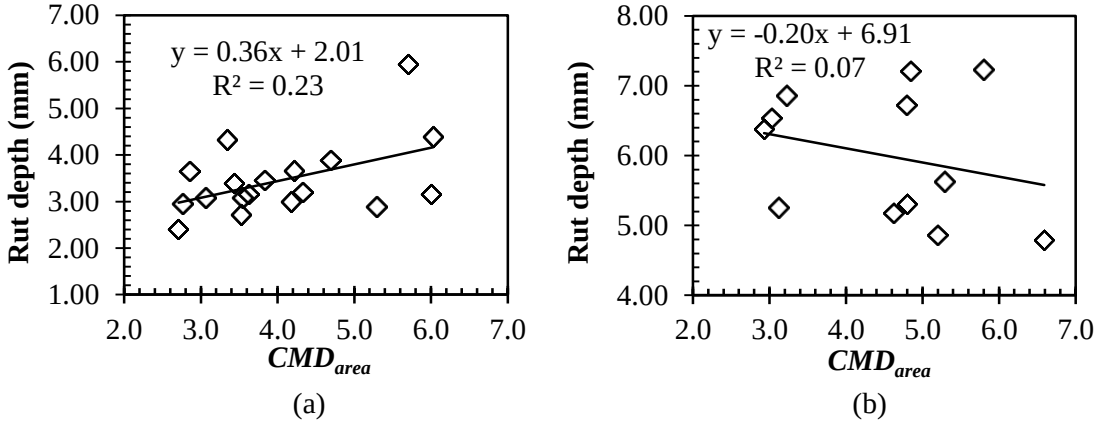

Figure 22. Relationships of CMD_{area} with rut depth for the (a) eighteen limestone screening blends and (b) twelve granite sand blends using Superpave method

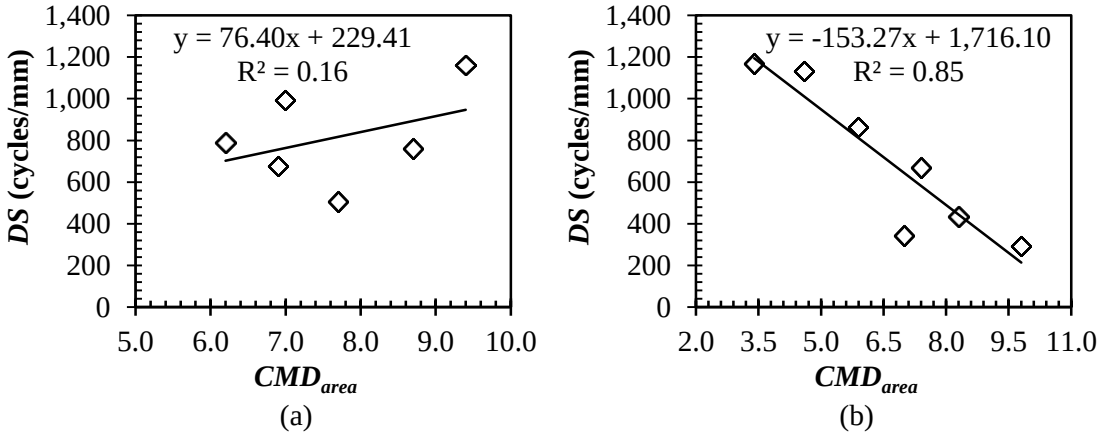

Figure 23. Relationships of CMD_{area} with *DS* for the (a) six limestone screening blends and (b) seven granite sand blends using Marshall method

As described in the previous section, the increase in CMD_{area} of aggregate gradation increases the VMA of HMA mixtures. It has been reported that the VMA has a fair negative relationship with the rutting resistance of HMA mixtures [8, 17]. Therefore, the CMD_{area} may have a negative effect on the rutting resistance of asphalt mixtures. The complicated relationship between the CMD_{area} and the rutting resistance of HMA mixtures may be explained through components of the VMA. The *VMA* includes two components, i.e., the effective asphalt content (V_{be}) and the voids in the mixture (*VIM*). While most

studies have consistently reported a negative relationship between the V_{be} and rutting resistance [2, 8], the influence of the *VIM* on rutting resistance is more ambiguous. It has been reported that increasing the *VIM* at a range of 2.6 to 5.7% improved the rutting resistance of HMA mixtures [18] while another study reported that increasing the *VIM* at a range of 2 to 7% reduced the rutting resistance of HMA mixtures [19]. In the Superpave mixtures, the *VIM* has a constant value of 4% [8]. Therefore, increasing CMD_{area} only increases the remaining component of the *VMA*, i.e., the V_{be}. When the CMD_{area} increases, the VMA of HMA mixtures increases and additional air voids within are created. The extra air voids in aggregate structure may be occupied by increasing asphalt binder to obtain the target air voids content (4%). As a result, the CMD_{area} may influence the rutting resistance of HMA mixtures through the V_{be} only, leading to a negative effect of the CMD_{area} on the rutting resistance of HMA mixtures. On the other hand, the Marshall method requires a range of from 3 to 6% for the *VIM* [2, 8]. As a result, the relationships of CMD_{area} with the components of the *VMA* (*VIM* and V_{be}) become more complicated. The increase in *VMA* can result in the following five effects: (i) increase V_{be} only; (ii) increase *VIM* only; (iii) increase both V_{be} and *VIM*; (iv) increase V_{be} but decrease *VIM*; and (v) decrease V_{be} but increase *VIM*. Therefore, the unclear relationship of *VIM* with the rutting resistance in combination with the complicated relationship of CMD_{area} with the *VIM* may result in the low correlation coefficients between the CMD_{area} and the rutting resistance.

3.5. Summary

Based on the experiments presented in this chapter, the following conclusions are relevant:

- New seven blends of aggregate structures, namely coarse-, dense-, and fine-graded asphalt mixtures were investigated for 12.5 mm NMPS Vietnamese wearing course mixtures. In the Marshall design procedure, it was challenging to meet the minimum VMA requirement for the dense-graded mixtures. Only one of three blends in dense-graded mixtures complied with the minimum VMA requirement.
- The CMD_{area} parameter proposed from the concept of the CMD has a potential application to evaluate the effect of aggregate gradation on the VMA of asphalt mixtures. The VMA of asphalt mixtures increases with the increase in the CMD_{area} of aggregate gradation, regardless of aggregate source, mix design, and nominal aggregate particle size. The relationship of CMD_{area} with VMA decreased when the aggregate gradations were controlled to reach the same gradations using different fine aggregates and volumetric requirements of the Marshall method.
- The sole CMD_{area} may be insufficient to evaluate the rutting resistance of HMA mixtures. There is therefore a need to conduct in-depth investigations that clarify the effect of additional potential factors (properties of aggregates and asphalt binders) on rutting resistance.

References

[1] Haryanto, I., and Takahashi, O. Ductile Fracture Assessment of Indonesian Wearing Course Mixtures Using J Integral and Crack Tip Opening Angle, International Journal of Pavement Engineering 9 (3), pp. 165-176, 2008.

[2] Tran, N.T., and Takahashi, O. Improvement on aggregate gradation design and evaluation of rutting performance of Vietnamese wearing course mixtures, the 8th international conference on maintenance and rehabilitation of pavements, Singapore, pp. 212-221, 2016.

[3] Vietnam Institute of Transport Science and Technology, TCVN 8819. Specification for construction of hot mix asphalt concrete pavement and acceptance, 2011.

[4] Watson, D.E., Johnson A., and Jared, D. The Superpave gradation restricted zone and performance testing with Georgia loaded wheel tester, Transportation Research Record 1583, pp. 106-111, 1997.

[5] Nguyen, L.T.N. A Study on aggregate gradation design for Superpave method, Master thesis, Nagaoka University of Technology, Japan, 2015.

[6] Coree, B., and Hislop, W. Difficult nature of minimum voids in the mineral aggregate: historical perspective, Transportation Research Record 1681, pp. 148-156, 1999.

[7] Christensen, D.W., and Bonaquist, R.F. VMA: one key to mixture design, submitted to the South Central Superpave Center for publication in the National Superpave Newsletter, 2005.

[8] Christopher, W.J., et al. A manual for design of hot mix asphalt with commentary, Report NCHRP 673, Washington DC, 2011.

[9] AASHTO Designation, M 323-13. Standard specification for Superpave volumetric mix design, 2015.

[10] Goh, T.S., and Takahashi, O. Design evaluation of Superpave asphalt mixtures for Tokyo International Airport Pavement, International Journal of Pavement, 10 (1-2-3), pp. 27-38, 2011.

[11] AASHTO Designation, M 325-08. Standard specification for stone matrix asphalt (SMA), 2012.

[12] Haryanto, I., and Takahashi, O. A rutting potential assessment using shear strength properties for Indonesian wearing course asphalt mixtures, International Journal of Pavements, 6 (1-2-3), pp. 27-38, 2007.

[13] Vietnam Institute of Transport Science and Technology, TCVN 8820. Standard practice for asphalt concrete mix design using Marshall method, 2011.

[14] Witczak, M.W. et al. Simple performance test for Superpave mix design, Report NCHRP 465, Washington, D.C., 2002.

[15] Cooley, L. A. Jr. et al. Use of screenings to produce hot mix asphalt mixtures, Transportation Research Record 1832, pp. 59-66, 2003.

[16] AASHTO Designation, TP 63. Standard Method of Test for Determining Rutting Susceptibility of Hot Mix Asphalt (HMA) Using the Asphalt Pavement Analyzer (APA), 2009.

[17] Park, K. Optimization of aggregate gradation for high-performing Hot Mix Asphalt, PhD thesis, University of Rhode Island, 2008.

[18] Prowell, B. D., Zhang, J., and E. R. Brown, E. R. Aggregate properties and the performance of Superpave-designed hot mix asphalt, Report NCHRP 539, Washington DC, 2005.

[19] Roy, N., Veeraragavan, A., and MuraliKrishnan, J. Influence of air voids of hot mix asphalt on rutting within the framework of mechanistic-empirical pavement design 104 (2), pp. 99-108, 2013.

Chapter 4. Effect of aggregate gradation on the workability of asphalt mixtures

4.1. Introduction

Workability of HMA mixtures indicates characteristics associated with the construction of the HMA layer, e.g., being placed, worked by hand, and compacted [1]. An asphalt mixture, which has higher workability, can be more easily compacted. Low workability may affect the durability and stability of the HMA mixtures in field construction. On the other hand, it is not proper to use an HMA mixture which is very workable, because it may show a poor rutting performance under repeated traffic loads at high temperatures [2].

Previous studies reported that some compaction devices such as torque-meter, Superpave gyratory compactor (SGC) and modified roller compactor are able to measure the workability of HMA mixtures [1, 3, 4]. In addition, Asphalt Pavement Analyzer and Wheel Tracking Test (WTT) are commonly applied to assess rutting resistance of HMA mixtures. The dynamic stability (DS) of the WTT is a potential parameter for evaluating resistance of asphalt mixtures to rutting [5]. However, those devices are not widely available in developing countries such as Vietnam and Indonesia [6, 7]. The Marshall compactor is still basic equipment to fabricate asphalt samples. Therefore, based on the Marshall method, there is a need to develop HMA indices that have good relationships with the workability and the rutting resistance of HMA mixtures. Those indices may help asphalt designers to select a stable asphalt mixture.

Aggregate gradation significantly influences the workability properties of HMA mixtures. A previous study reported that asphalt mixtures having aggregate gradations that are close to the MDL may be compacted more easily [2]. Furthermore, asphalt mixtures having aggregate gradations that pass below the restricted zone could be more workable than mixtures having aggregate gradations that pass above the restricted zone [2, 3]. An asphalt mixture with a higher fraction of sand may show lower workability [2]. However, to the best of our knowledge, the search of the literature found no well-established research that evaluates the relationship of aggregate gradations with the workability of asphalt mixtures. There are not unique guidelines for designers who do not have enough experience in designing an adequate aggregate gradation that leads to proper workable mixtures.

This chapter aimed to develop a simple index and applied it to investigate the effect of aggregate gradations on the workability of 12.5 mm NMPS wearing course mixtures with three compactors, i.e., the

Marshall compactor, the SGC, and the roller compactor. The study also discussed another simple performance index for assessing rutting resistance of HMA mixtures. Moreover, relationships between the workability and the rutting susceptibility of HMA mixtures were also investigated. The present study also applied the proposed workability and rutting resistance indexes for other data.

4.2. Literature review of the workability of asphalt mixtures

In recent years, the SGC is the important equipment for compacting HMA samples in the Superpave mix design. The standard SGC provides a vertical pressure of 600 kPa and the angle of 1.25° to an asphalt sample during compaction [8]. The computer system automatically measures and records the height of the sample at each gyration. As a result, the change of the sample height can be used to evaluate the workability of HMA mixtures [1]. The previous study also used the SGC compaction curve to develop two indices associated with the field construction. The first index, namely the workability energy index (WEI), presents the workability of an asphalt mixture when the volume of the mixture changes from the beginning of compaction to 92% of the G_{mm} [1]. The second index, namely the compact ability energy index (CEI), is calculated by the change in the volume of sample from 92% to 96% of the G_{mm} [1]. The 96% of the G_{mm} indicates the air voids content in the mixture is 4 %, which is the requirement of the Superpave method. It has been reported that the *CEI* indicates the shear strength of HMA mixtures or the interlocking between aggregate particles [1]. The *WEI* and the *CEI* are described by the following equations [1]:

$$WEI = \frac{\pi d^2}{4} \times P \times \frac{h_0 - h_{92\%}}{N_{92\%}} \tag{6}$$

$$CEI = \frac{\pi d^2}{4} \times P \times \frac{h_{92\%} - h_f}{N_{des} - N_{92\%}} \tag{7}$$

Where, d is the diameter of sample; P is the compaction pressure of the SGC (600 kPa); h_0 is the height of the sample before compacting; $h_{92\%}$ is the height of the sample when air voids of the mixture reach 8%; h_f is the height of sample with N_{des}; $N_{92\%}$ is the number of gyrations as air voids of the mixture reaches 8%, and N_{des} is the number of design gyrations.

4.3. Development of workability index

Aggregate gradation plays an important role in determining the workability of HMA mixtures. The previous study reported that a stone fraction (aggregates retains on the 2.36-mm sieve for 12.5 NMPS mixtures) significantly influences the workability of asphalt mixtures [2]. Asphalt mixtures having high

stone fractions show low workability [2]. The CMD pilot illustrates how much the aggregate gradation is far from the Fuller MDL at each sieve [7, 9]. In addition, it has been reported that it is easy to compact an asphalt mixture having an aggregate gradation that fits the MDL [2]. Therefore, the present study posited that the area of CMD for stone proportion ($CMD_{area-stone}$) has a strong relationship with the workability of HMA mixtures. When the $CMD_{area-stone}$ of an aggregate gradation is high, this asphalt mixture may not be compacted easily. Figure 24 also shows the meaning of the $CMD_{area-stone}$ for an aggregate gradation.

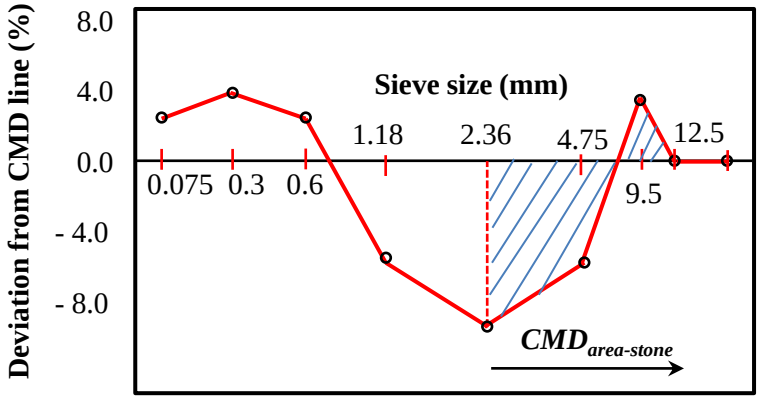

Figure 24. Meaning of $CMD_{area-stone}$

An asphalt mixture having a proper apparent film thickness (*AFT*) may be compacted easily. The *AFT* indicates an average thickness of asphalt binder that coats aggregate particles. It has been reported that when the effective asphalt content (V_{be}) increases, the *AFT* of the mixture also increases [10], thereby increasing the workability of HMA mixtures. Therefore, the V_{be} parameter may be a positive factor that affects the workability of HMA mixtures [2]. In addition, a proportion of fine aggregate has a strong effect on the *AFT*. When a proportion of fine aggregate in a mixture increases, the surface area of aggregates (S_s) within the mixture also increases [10]. As a result, the *AFT* value reduces due to the asphalt absorption by the fine aggregate. For this reason, the workability of the HMA mixture deteriorates.

Too many interceptor particles may disrupt dense packing of the aggregate structure and create additional voids. Asphalt binder may fill the new air voids, thereby improving the workability of the HMA mixture [2]. To the best of our knowledge, no studies have previously conducted an in-depth discussion on the effect of interceptors on the aggregate interlock which is related to the workability of asphalt mixtures. This study employed the disruption factor (*DF*) of the DASR model as a parameter to illustrate the effect of aggregate interlock on the workability of HMA mixtures. Coarse particles in the DASR model play the main role in forming a backbone aggregate structure. Aggregate particles that are

smaller than the DASR aggregates, i.e., asphalt binder and fine aggregates, tend to occupy the air voids created by the DASR particles. The *DF* value determines whether fine aggregate disrupts the coarse structure [11]. When the *DF* value is high, a high proportion of fine aggregates may reduce the backbone aggregate, thereby decreasing the aggregate interlock of asphalt structure and creating additional air voids within aggregate structures. As a result, compacted loads easily shift aggregate particles or the HMA mixture's workability increases [2].

The previous study has recommended the smallest sieve size for the aggregate particles of the DASR model to be 1.18 mm to calculate the *DF* [11]. In the Bailey method, a secondary control sieve (SCS) is used to split a sand fraction into coarse sand and fine sand. This means that at the SCS, the coarse sand fraction can still create air voids which can be occupied by fractions smaller than the coarse sand fraction (fine sand, asphalt binder). The SCS for 12.5 mm NMPS aggregate gradation is 0.6 mm sieve [12]. Therefore, the present study determined 0.6 mm as the smallest sieve size of coarse aggregate particles in the DASR model.

Based on the above analysis, this study investigated a new workability index (*WI*) that would describe the relationship between the aggregate gradation and workability of an HMA mixture. The present study hypothesized that an HMA mixture's workability increases with increasing values of *WI*. The *WI* is derived from three factors of aggregate gradation, i.e., $CMD_{area\text{-}stone}$, S_s, and *DF*, and one factor of asphalt binder, i.e., V_{be}; these respectively address the effects of stone content, aggregate-surface areas, aggregate interlock, and the proportion of asphalt binder on the workability performance of a mixture. The present study built a hypothesis that *WEI* increases with increasing *WI*. The *WI* value can be obtained from the stage of the mix design procedure. The *WI* can be calculated by the following equation and other associated variables.

$$WI = \left(\frac{1}{CMD_{area\text{-}stone}} \right) \times \left(\frac{V_{be}}{S_s} \right) \times DF \tag{8}$$

$$S_s = \frac{P_{0.30} + P_{0.15} + P_{0.075}}{5} \tag{9}$$

Where, $P_{0.30}$, $P_{0.15}$, and $P_{0.075}$ are the aggregate contents passing 0.30-mm, 0.15-mm, and 0.075-mm sieves, respectively. The equation (9), which was proposed the previous study, indicates an effect of fine aggregates on the area of the aggregate surfaces [9].

4.4. Development of rutting resistance index

The past study reported that the resistivity property of asphalt mixtures is an effective parameter to evaluate the rutting resistance of HMA mixtures. At high temperatures, because of the reduction in

viscosity, asphalt binder tends to flow through aggregate structures [10]. The resistivity property indicates the resistance of an aggregate structure to oppose asphalt binder that flows in the mixture. The resistivity also illustrates a contrary characteristic of permeability for an HMA mixture [10]. The resistivity of an asphalt mixture, which is derived from the S_s, the bulk specific gravity of aggregates (G_{sb}), and the *VMA*, simultaneously expresses rutting resistance of HMA mixtures [10]. The relationship between the mixture resistivity and the rutting resistance of HMA mixtures may be explained as follows. The strength of adhesion existing in HMA mixtures increases with increasing S_s. As a result, the indirect tensile strength of HMA mixtures increases when the adhesion strength of mixtures increases [13]. The indirect tensile strength is strongly associated with the cohesion of asphalt mixtures, which is one of shear strength properties and has a good relationship with the rutting resistance of HMA mixtures [6, 14]. Therefore, the rutting resistance of HMA mixtures increases with increasing the mixture resistivity.

Characteristics of aggregate gradation have significant effects on the *VMA* of asphalt mixtures. The previous study showed that the *VMA* value of HMA mixtures increases as the CMD_{area} value of aggregate gradations increases [7]. Therefore, the CMD_{area} parameter indicates the effects of aggregate gradation on the resistivity of the mixture. As a result, when calculating mixture resistivity, the present study used the CMD_{area} parameter instead of the *VMA*. The mixture resistivity increases with decreasing the CMD_{area} of aggregate gradation.

The volume of effective asphalt or the V_{be} also significantly influences rutting performance of asphalt mixtures. Asphalt mixtures with low V_{be} values generally show high resistivity values, thereby increasing the rutting resistance of the HMA mixtures [10]. This means that the V_{be} presents a negative effect of asphalt binder on the mixture resistivity. Furthermore, asphalt mixtures having higher V_{be} values have a greater *AFT* value, which further reduces rutting resistance of the HMA mixtures [9].

As mentioned above, when an HMA mixture has high workability, this mixture may show poor rutting performance under repeated traffic loads [2]. Equation (10) presents the rutting resistance index (RRI) formulation. The present study hypothesised that the rutting resistance of HMA mixtures increases as *RRI* increases. Equation (11) was modified based on the equation to calculate a resistivity of an asphalt mixture [10]. Because all the components are not enough to calculate mixture resistivity, Equation (11) was only used to determine resistivity index (*RI*), which presents the effect of aggregate gradation on the mixture resistivity.

$$RRI = RI \times \left(\frac{1}{V_{be}}\right) \times \left(\frac{1}{WI}\right) \tag{10}$$

$$RI = \frac{S_s^2 \times G_{sb}^2}{CMD_{area}^3} \tag{11}$$

4.5. Experience work

4.5.1. Preparation of HMA materials

Preparation of HMA materials had been described in chapter 3.

4.5.2. Design of aggregate gradation

Aggregate gradation design had been described in chapter 3.

4.5.3. Mix design procedure

Asphalt mixture design procedure had been described in chapter 3.

4.5.4. Superpave gyratory compactor

The present study compacted samples using the SGC to evaluate the workability of seven asphalt mixtures. Two samples at the design AC were fabricated to determine N_{des} for each blend. The N_{des} was regarded as the number of gyrations where the HMA mixture had the same G_{mb} as that of the Marshall specimen. Next, two samples were fabricated with the design AC and the N_{de} to check the G_{mb} value of the HMA mixture.

4.5.5. Roller compactor and wheel tracking test

This study also used a laboratory steel roller compactor to fabricate the slab specimen in order to evaluate workability of HMA mixtures. Slab samples of the mixtures with the dimension of 300×300×50 mm were prepared. The present study fabricated the slab samples at two methods. First, the compaction process was conducted at a passing number of 25 times, which was suggested from the previous study for investigating the workability of HMA mixtures [2]. Second, the passing number was set up where the slab samples have the same air voids (or G_{mb}) as the Marshall samples, which is commonly applied in Japan [5].

The present study also conducted the WTT for evaluating rutting resistance of slab samples. The WTT was performed at a temperature of 60 ^{o}C, a wheel speed of 42 passes/min, and a wheel load of 686 N [2, 5]. Based on the WTT data, the *DS* parameter, which indicates passage times of wheel load per 1-mm rut depth, was obtained. The *DS* is a common parameter in the Japanese WTT standard for the rutting evaluation of HMA mixtures [2, 5]. A value of *DS* is described by the following equation:

$$DS = C \times \frac{42 \times 15}{d_{60} - d_{45}} \tag{12}$$

Where, d_{45} and d_{60} are the rut depth at 45th and 60th minutes, respectively; and C is the index depending on the type of wheel load (C = 1 for one wheel, and C = 1.5 for chain wheels).

4.6. Results and discussions

4.6.1. Results of mix design

The results of mixture design had been described in chapter 3.

4.6.2. Effect of aggregate gradations on workability of HMA mixtures

Table 10. Properties of SGC samples at the design AC

Mixture		N_{des} (gyration)	G_{mb}	*VIM* (%)	V_{be} (%)	*WEI* (Nm)	*CEI* (Nm)
Dense-grade	1	70	2.366	5.2	8.6	6.99	0.96
	2	48	2.396	3.9	8.6	11.17	1.61
	3	48	2.394	4.2	8.2	11.56	1.61
Coarse-grade	4	120	2.341	4.3	11.6	5.84	0.36
	5	70	2.353	5.5	8.7	6.03	0.95
Fine-grade	6	45	2.335	4.4	11.1	10.68	1.62
	7	70	2.317	4.6	11.7	7.45	0.97

Table 11. Properties of slab-shaped samples at the design AC

Mixture		Slab samples at 25 passes			Slab samples at design air voids			
		G_{mb}	*VIM* (%)	V_{be} (%)	Passes	G_{mb}	*VIM* (%)	V_{be} (%)
Dense-grade	1	2.318	7.1	8.52	40	2.363	5.3	8.7
	2	2.372	4.9	8.54	25	2.372	4.9	8.5
	3	2.385	4.5	8.18	25	2.385	4.5	8.2
Coarse-grade	4	2.285	6.6	11.23	50	2.344	4.2	11.5
	5	2.307	7.4	8.62	45	2.351	5.7	8.8
Fine-grade	6	2.355	3.6	11.18	35	2.343	4.0	11.1
	7	2.296	5.5	11.61	45	2.319	4.5	11.7

Properties of SGC and slab samples for the seven mixtures are shown in Table 10 and Table 11. Among all the blends, Blend 4 having the coarsest aggregate gradation showed the smallest *WEI* value. This means that Blend 4 is the most difficult to be compacted. In general, the workability of the coarse-

graded HMA mixtures was lower than those of the dense- and fine-graded HMA mixtures. Figure 25 shows the effect of the stone content on the workability of seven HMA mixtures. The significantly reasonable correlation coefficient (R^2 = 0.84) was obtained between the stone content and the *WEI*. The trend line indicates that the workability of the HMA mixture is high when the aggregate gradation fits the MDL. It has been reported that when aggregate gradation is close to the MDL, individual aggregate particles easily interlock to fit together and create the densest packing of backbone aggregate [2]. Therefore, the findings of this study corroborate those from a previous analysis.

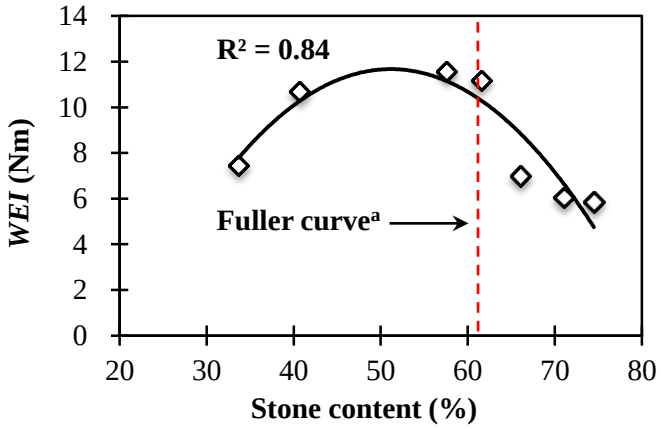

Figure 25. Relationship of stone content with *WEI*
[a] In Fuller curve, mineral aggregates retained on the 2.36-mm sieve size is 61% [2].

Table 12. *WI* of Marshall, SGC, and slab-shaped specimen

Mixture	S_s (m^2/kg)	$CMD_{area\text{-}stone}$	DASR (mm)	*DF*	*WI* ($\times 10^{-2}$) of Marshall and SGC samples	*WI* ($\times 10^{-2}$) of slab samples	
						25 passes	Design passes
1	5.32	4.28	9.5-0.6	0.70	26.52	26.20	26.66
2	5.68	3.00	9.5-0.6	0.89	44.68	44.58	44.59
3	6.26	1.61	9.5-0.6	0.83	67.33	67.29	67.28
4	5.14	6.50	4.75-0.6	0.72	24.99	24.19	24.86
5	4.80	5.98	9.5-0.6	0.75	22.83	22.53	22.99
6	6.62	3.18	9.5-0.6	0.95	50.15	50.47	50.30
7	6.78	4.81	4.75-0.6	0.91	32.72	32.38	32.79

Table 12 presents individual proportions that were used to calculate the *WI* of HMA mixtures. The *WI* value of each Marshall mixture was equal to that of the SGC mixture. The *WI* values of Marshall and SGC specimens were slightly different from that of slab-shaped specimens because of the little

difference in the V_{be}. At each mixture, the Marshall, SGC, and slab samples at the design air voids had the same V_{be} even though all the Marshall samples had the same compaction energy while the SGC and slab samples individually had the different compaction energy. In addition, the V_{be} values of the Marshall, SGC, and slab samples at the design air voids were generally higher than those of slab samples at the 25 passes. The V_{be} indicates the ratio between a volume of effective asphalt and the total volume of the mixture. During the compaction procedure, with the help of compaction energy, air voids in the mixture gradually reduce. This leads to a decrease in the total mixture volume and increases in both the V_{be} and the G_{mb} of HMA mixtures. Therefore, when fabricated various devices, asphalt mixtures with higher G_{mb} values generally have larger V_{be} values.

Figure 26 shows a linear relationship of the $CMD_{area-stone}$ with the *WEI* of seven mixtures. The correlation coefficient for the two parameters was high (R^2 = 0.89). The results indicated that when an aggregate gradation falls close to the MDL, the aggregate gradation of the mixture has a low $CMD_{area-stone}$ and the mixture can be more workable. Furthermore, the correlation coefficient between the $CMD_{area-stone}$ and the *WEI* was higher than that between the stone content and the *WEI*. This means that $CMD_{area-stone}$ is more proper parameter than the stone content in order to indicate the degree of the distance between an aggregate gradation and the MDL, which strongly affects the workability of HMA mixtures.

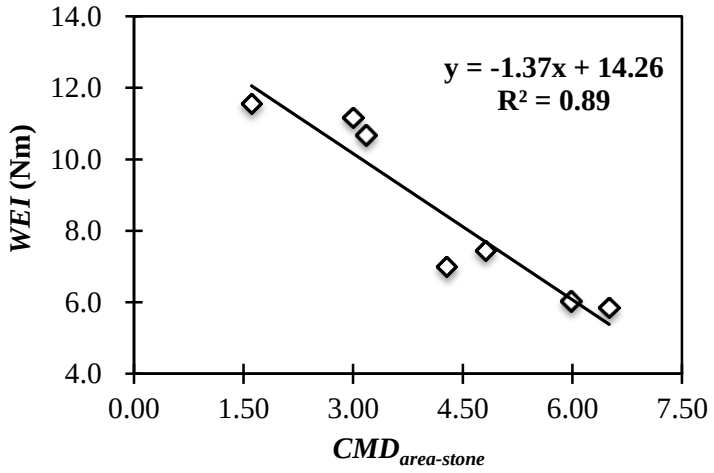

Figure 26. Relationship of $CMD_{area-stone}$ with *WEI*

Figure 27 presents relationships of *WI* values of samples using various devices with the *WEI*. The high correlation coefficients (Marshall, SGC, and slab samples with *WEI*: R^2 = 0.92; and slab samples at 25 passes with *WEI*: R^2 = 0.93) were obtained. The trend lines, as expected, indicated that the workability of HMA mixtures increases with the increase in the *WI*. It seems that the WI has a potential application to assess the workability of HMA mixtures even though the samples are fabricated with different devices and compaction energies.

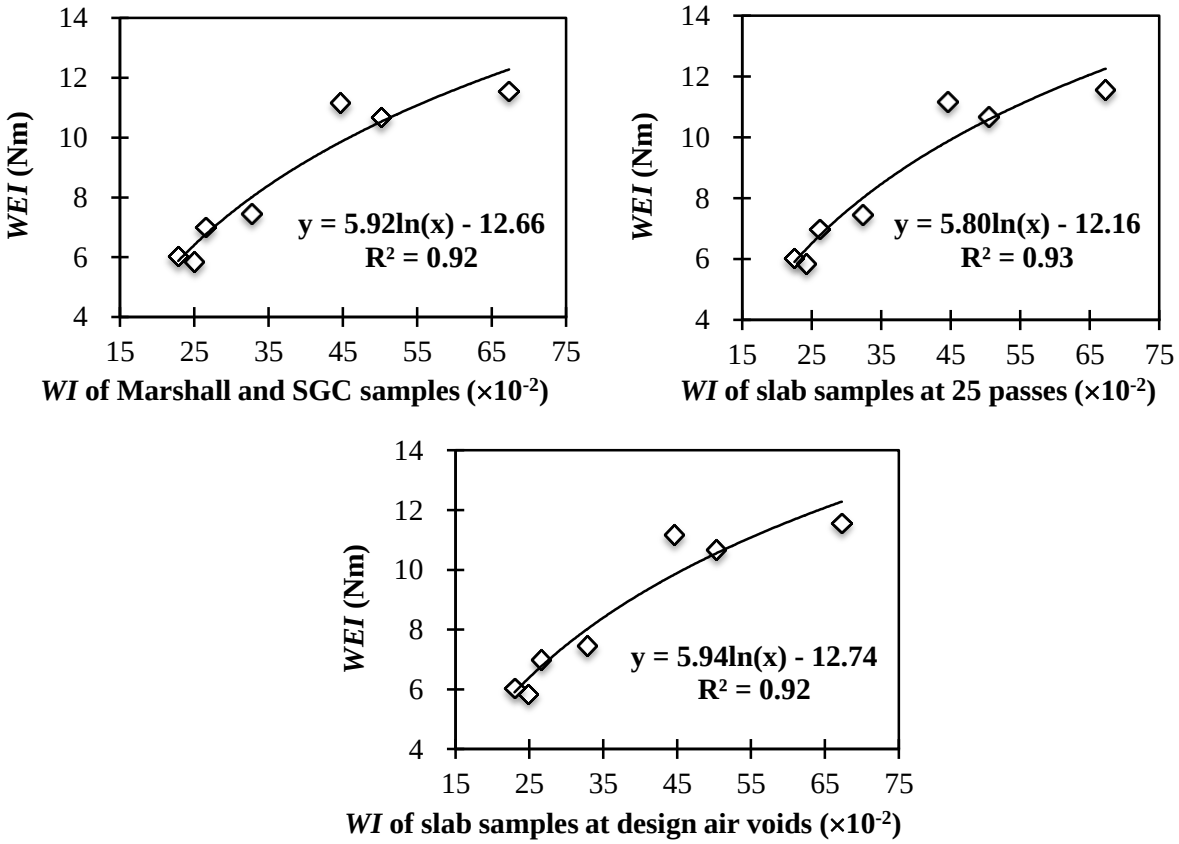

Figure 27. Relationships of *WI* of Marshall, SGC, and slab samples with *WEI*

4.6.3. Evaluation of relationship between rutting resistance index and dynamic stability

Table 13 shows *RRI* values of samples using various compactors and *DS* values for the seven mixtures. Relationships of *RRI* values with *DS* values are depicted in Figure 28 and Figure 29. The results showed that all relationships between *RRI* and *DS* had high correlation coefficients. As expected, the rutting resistance of HMA mixtures increases with increasing *RRI*. The experiments also illustrated that three *RRI* values of Marshall, SGC and slab-shaped specimens may be employed for the same objective, namely assessment of rutting resistance for 12.5 mm NMPS wearing course mixtures.

Table 13. Results of *RRI* and *DS* values

Mixture	*RRI* ($\times 10^{-2}$)			*DS* of slab samples at 25 passes (cycles/mm)	*DS* of slab samples at design air voids (cycles/mm)
	Marshall and SGC samples	Slab samples at 25 passes	Slab samples at design air voids		
1	41.06	42.09	40.63	755	863
2	57.96	58.23	58.24	1130	1130
3	119.41	119.58	119.67	1168	1168
4	10.94	11.67	11.05	422	435
5	19.37	19.9	19.10	667	670
6	15.38	15.19	15.28	340	342
7	8.59	8.78	8.56	284	293

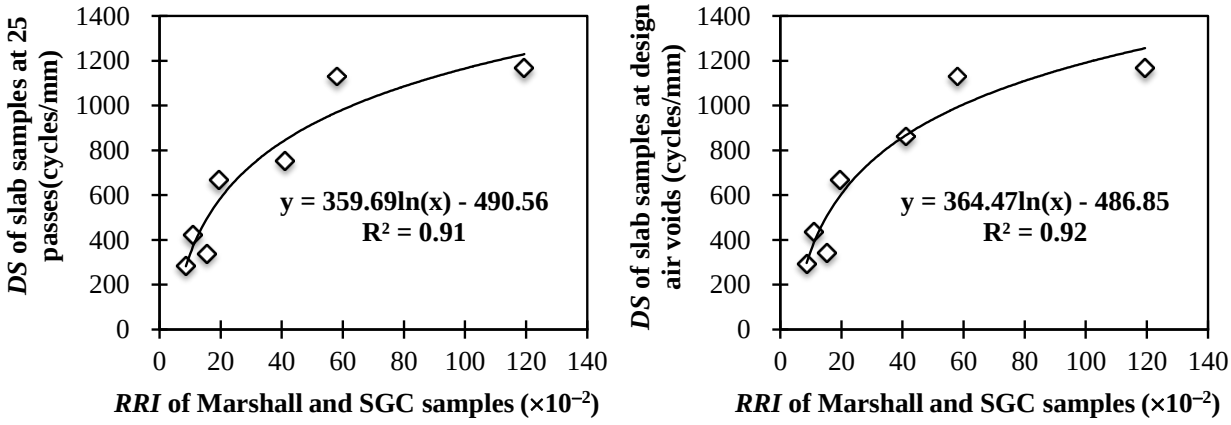

Figure 28. Relationships of *RRI* of Marshall, SGC with *DS*

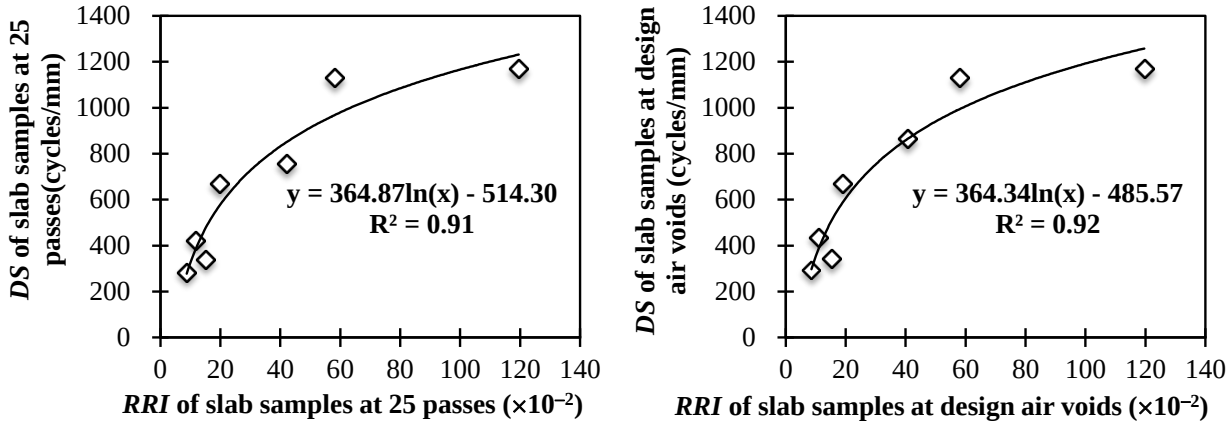

Figure 29. Relationships of *RRI* of slab samples with *DS*

4.6.4. Relationships of workability energy index and compact ability energy index with dynamic stability

Figure 30 presents relationships of SGC parameters (*WEI* and *CEI*) with the *DS* for the seven mixtures. It was found that the correlation coefficients of *WEI* and *CEI* values with *DS* values were low. This means that the *WEI* and the *CEI* were not potential parameters to evaluate rutting resistance of HMA mixtures. It has been reported that the gyration angle, i.e., 1.25 degree, in SGC is not adequate to assess the shear stress that can induce rutting in HMA mixtures [15]. This angle should increase to sufficiently characterise the rutting potential of HMA mixtures [15].

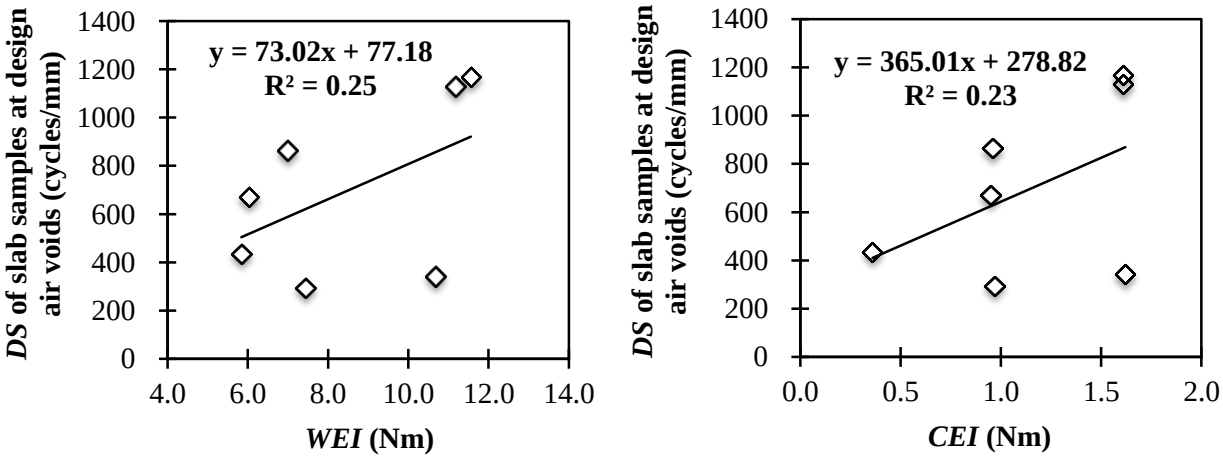

Figure 30. Relationships of *WEI* and *CEI* with *DS*

4.6.5. Potential practical use of workability and rutting resistance indexes

The present study examined the *WI* values proposed by the present study and by the previous study [2]. The previous study developed the *WI* and applied the index to evaluate the workability of six Indonesian mixtures that were previously described in section 3.4.3.2. The previous study calculated the *WI* based on the reduction in air voids of mixtures before and after compaction [2]. The air voids content of HMA mixtures before compaction were measured using the rodding procedure outlined in the AASHTO T-19 standard [2]. The determination of *WI* is detailed in the previous publish [2]. Table 14 also summaries all *WI* and *RRI* results for six Indonesian wearing course mixtures.

Figure 31 shows linear relationships between *WI* values for Marshall and slab samples proposed by the present study and Iman et al. The relationships show high coefficients of determination (Marshall samples: R^2 = 0.82; and slab samples: R^2 = 0.78). The results indicated that the *WI* proposed by the present study and Iman *et al*. may consistently characterise the workability property of HMA mixtures for

both the Marshall and slab samples. However, while the determination of *WI* proposed by the present study is essentially based on characteristics of aggregate gradation, the *WI* proposed by Iman *et al*. required the rodding test that determines individual porosity of the mineral aggregates source [2]. This may confirm that the *WI* proposed by the present study is cost-effective to describe the workability performance of HMA mixtures.

Table 14. *WI* results of six mixtures proposed by the present study and Iman et al

	Mixture					
	I1	I2	I3	I4	I5	I6
$CMD_{area\text{-}stone}$	6.49	4.91	3.56	3.12	2.18	4.71
S_s(m^2/kg)	5.72	4.6	4.1	8.42	8.1	9.18
DF	0.53	1.01	0.59	0.58	1.57	0.70
V_{be} of Marshall samples (%)	10.66	11.31	11.00	11.83	10.15	11.60
V_{be} of slab samples (%)	10.65	10.95	10.6	11.85	10.3	11.25
G_{sb}	2.623	2.606	2.644	2.673	2.598	2.670
WI of Marshall samples ($\times 10^{-2}$)	15.21	50.56	44.45	26.14	90.34	18.79
WI of Marshall samples - Iman	1.20	1.51	1.59	1.54	2.29	0.84
RRI of Marshall samples ($\times 10^{-2}$)	21.29	5.47	7.17	47.47	20.71	32.72
WI of slab samples ($\times 10^{-2}$)	15.19	48.95	42.83	26.18	91.67	18.23
WI of slab samples - Iman	1.20	1.46	1.46	1.22	1.97	0.66
RRI of Marshall samples ($\times 10^{-2}$)	21.33	5.84	7.72	47.31	20.11	34.79
DS (cycles/mm)	759	505	676	993	790	1160

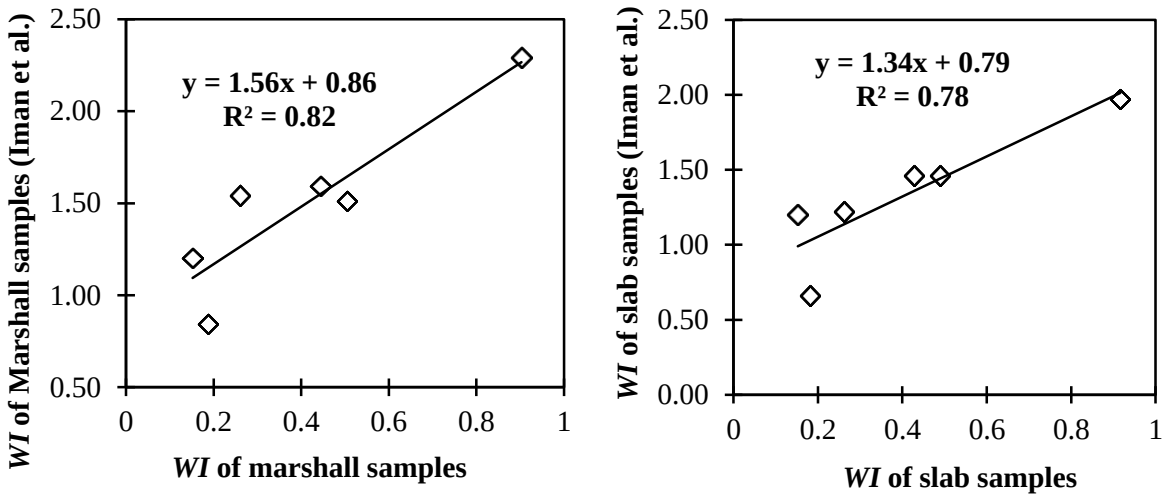

Figure 31. Comparison of *WI* values proposed by the present study and Iman et al

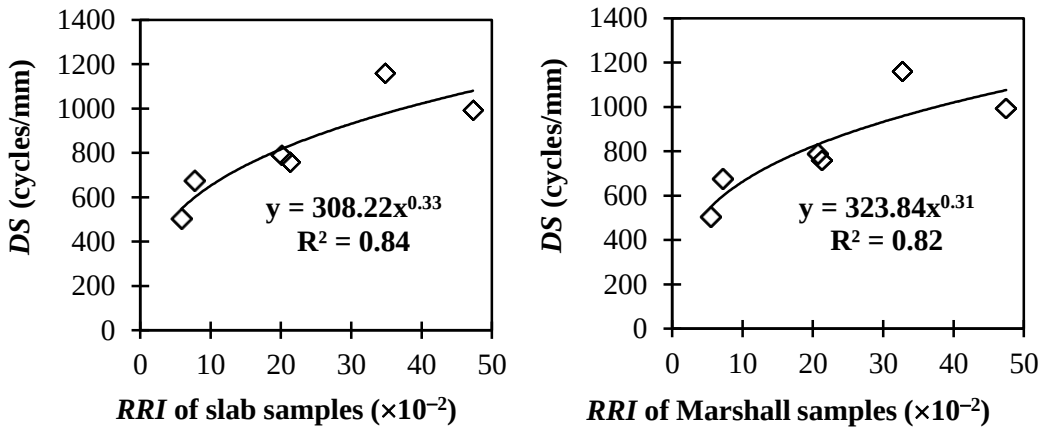

Figure 32. Relationships of RRI of slab and Marshall samples with *DS*

Figure 32 presents the relationships of *RRI* of the slab and Marshall samples with the *DS*. The results also demonstrated that the relationships of *RRI* of the slab and Marshall samples with the *DS* were high. The rutting resistance of HMA mixtures was low when the RRI value was small. This means that the *RRI* proposed by the present study is applicable for ranking the rutting performance of HMA mixtures.

4.7. Summary

The findings of this chapter can be summarized as follows.

- The present study has developed the *WI* for assessing the workability of HMA mixtures. The *WI* consisted of $CMD_{area-stone}$, V_{be}, S_s, and *DF* has a potential application for evaluating the workability of HMA mixtures.
- The strong relationship was observed between the $CMD_{area-stone}$ of aggregate gradations and the workability of HMA mixtures. When the $CMD_{area-stone}$ values of aggregate gradation are low, the HMA mixtures are properly workable under compaction energy.
- The relationships of *RRI* values and *DS* values were high, regardless of compaction energies or compactors. Rutting resistance of HMA mixtures tended to increase with the increases in *RRI* values. On the Marshall design, *RRI* can be easily obtained. Therefore, without requirements for any mechanical tests, the *RRI* value of Marshall cylindrical specimens has a potential application to evaluate rutting resistance of wearing course mixtures.

References

[1] Dessouky, S. et al. Laboratory evaluation of the workability and compactability of asphaltic materials prior to road construction, Journal of Materials in Civil Engineering 25(6), pp. 810-818, 2013.

[2] Haryanto, I., and Takahashi, O. Effect of gradation on workability of hot mix asphalt mixtures, The Baltic Journal of Road and Bridge Engineering 2(1): pp. 21-28, 2007.

[3] Gudimettla, J. M., Cooley, L. A., and Brown, E. R. Workability of hot mix asphalt, NCAT Report 03-03, Auburn Alabama, 2003.

[4] Oliver, J., and Alderson, Al. A development of an asphalt workability index: Pilot study, Austroads Technical Report AP-T59/06, Sydney, 2006.

[5] Japan Road Association, JRA-B003. Method of wheel tracking test, Standard Practice for Asphalt Concrete Mix Design (3), pp. 39-55, 2005.

[6] Haryanto, I., and Takahashi, O. A rutting potential assessment using shear strength properties for Indonesian wearing course asphalt mixtures, International Journal of Pavements, 6 (1-2-3), pp. 27-38, 2007.

[7] Tran, N.T., and Takahashi, O. Improvement on aggregate gradation design and evaluation of rutting performance of Vietnamese wearing course mixtures, the 8th international conference on maintenance and rehabilitation of pavements, Singapore, pp. 212-221, 2016.

[8] The Asphalt Institute, Superpave mix design: Superpave series No. 2, 3rd ed., 2001.

[9] Christopher, W.J., *et al*. A manual for design of hot mix asphalt with commentary, Report NCHRP 673, Washington DC, 2011.

[10] Christensen, W. D. Jr., and Bonaquist, R. F. A Volumetric requirements for Superpave mix, Report NCHRP 567, Washington DC, 2006.

[11] Chun, S., Roque, R., and Zou, J. Effect of gradation characteristics on performance of Superpave mixtures in the field, Journal of the Transportation Research Board, 2294, pp.43-52, 2012.

[12] Varik W.R et al. Bailey method for gradation selection in HMA mixture design, Transportation Research Circular, Number E-C044, TRB, Wasington D.C, USA, 2002.

[13] Chen, J-S.; and Liao, M.C. Evaluation of internal resistance in hot-mix asphalt (HMA) concrete, Construction and Building Materials 16 (6): 313-319, 2002.

[14] Christensen, D.W., *et al*. Indirect tension strength as a simple performance test. New simple performance tests for asphalt mixes, Report E–C068, Washington DC, pp. 44-57, 2004.

[15] Anderson, R.M., *et al*. Relationship of Superpave gyratory compaction properties to HMA rutting behavior, Report NCHRP 478, Washington DC, 2002.

Chapter 5. Effect of aggregate gradation on the cracking of asphalt mixtures at service temperatures

5.1. Introduction

Wearing course mixtures with low cracking resistance at normal service temperatures are susceptible to ductile fracture [1]. In Vietnam, a rise in the traffic volume of heavy vehicles in combination with high ambient temperature has increased the incidence of premature cracking in wearing course mixtures of asphalt pavements. However, current Vietnamese guidelines do not stipulate any evaluation procedures to ensure adequate cracking resistance for these mixtures. There is therefore a need to conduct rational evaluation tests for cracking performance under these conditions. These tests should be able to assess the tensile fracture characteristics of HMA mixtures.

For more than one decade, the simplicity of the notched semi-circular bending (SCB) test has gained increasing interest in evaluating the cracking behavior of HMA mixtures [1-4]. Several parameters have been specified for analyzing cracking performance of asphalt mixtures at two distinct stages. The first stage is cracking initiation, which occurs when a load reaches the bonding strength of the mixtures [1]. Based on the concept of elastic-plastic fracture mechanics (EPFM), the J-integral (J_c) parameter was introduced to evaluate the cracking resistance of asphalt mixtures during the cracking initiation stage [1, 2]. As this parameter indicates the accumulated fracture energy at the point where a crack originates in an asphalt mixture, it is therefore applicable for examining ductile fracture in HMA mixtures during cracking initiation [1]. It also has been reported that the J_c value is closely associated with the field cracking rate at construction sites [2]. The second stage for assessing cracking performance is cracking propagation. During the propagation stage, the crack length increases until the applied load decreases to the failure limit [1]. A fracture toughness parameter (K_{Ic}) was also developed to assess the potential for the cracking propagation [5].

In the flow of mix design procedures, cracking resistance of HMA mixtures may be improved through the design of an appropriate aggregate gradation. Aggregate interlock plays a critical role in preventing premature cracking. When backbone aggregate particles are in close contact with one another, aggregate interlock can occur more effectively and improve a mixture's frictional strength [1]. Because aggregate gradation has a strong effect on aggregate interlock, there is a need for an in-depth examination of the relationship between the characteristics of aggregate gradation and the cracking resistance of HMA mixtures. However, to the best of our knowledge, the effects of aggregate gradation on cracking

resistance in asphalt mixtures at normal temperatures have yet to be discussed in detail. Previous studies have generally focused on the influence of coarse aggregates, asphalt binders, and temperature on the cracking resistance of HMA mixtures [1-4, 6].

The present study aimed to develop a simple cracking performance index and to investigate the effects of aggregate gradation on the cracking performance of HMA mixtures with a 12.5-mm NMPS at the cracking initiation and propagation stages. The notched SCB test was conducted to evaluate cracking resistance in seven blends of HMA mixtures that were designed in accordance with Vietnamese guidelines for wearing course mixtures. In addition, this study examined the relationship between the J_c and the K_{Ic}. Furthermore, combinations of three different fine aggregates were examined to evaluate the effects of fine aggregate on the cracking resistance of HMA mixtures.

5.2. Literature review

5.2.1. Previously identified parameters of HMA mixture cracking resistance

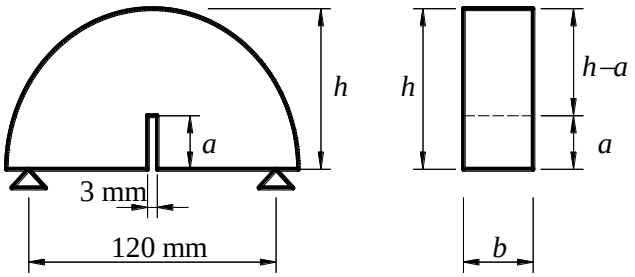

Figure 33. Configuration of the notched SCB test specimens

The cracking initiation stage occurs in an asphalt mixture when the applied load reaches the bonding strength of the mixture. J_c is defined as a path-independent line integral around the crack location, and has been used to measure the accumulated external energy required to form a new surface crack [1, 7]. A high J_c value illustrates high cracking resistance in a mixture [1, 2]. Based on a load-deformation curve obtained in the notched SCB test, the following equation is applied to determine the critical value of J_c [1-4, 7]:

$$J_c = \left(\frac{U_1}{b_1} - \frac{U_2}{b_2}\right) \times \frac{1}{a_1 - a_2} \tag{13}$$

Where, U_1 and U_2 are strain energy failure values obtained from the load-deformation curve for specimens with notch depths of a_1 and a_2, respectively; and b_1 and b_2 indicate the thickness of the

specimens with notch depths of a_1 and a_2, respectively. The strain energy value of an HMA specimen is determined as the area under the loading portion (from the initial load to the maximum load) of the load-deformation curve. The configuration and dimensional information of the notched SCB specimens are shown in Figure 33.

The cracking propagation stage describes an increase in crack length after cracking initiation. The European Standards utilize the notched SCB test to evaluate the cracking resistance of HMA mixtures during the cracking propagation stage. The tensile strength (or fracture toughness) parameter K_{Ic} is calculated by the following equations and other associated variables [5]:

$$K_{Ic} = \sigma_{max} \times f\left(\frac{a}{h}\right) \tag{14}$$

$$\sigma_{max} = \frac{4.263 \times P_{ult}}{D \times b} \tag{15}$$

$$f\left(\frac{a}{h}\right) = -4.9665 + 155.58 \times \left(\frac{a}{h}\right) - 799.94 \times \left(\frac{a}{h}\right)^2 + 2141.9 \times \left(\frac{a}{h}\right)^3 - 2709.1 \times \left(\frac{a}{h}\right)^4 + 1398.6 \times \left(\frac{a}{h}\right)^5 \tag{16}$$

Where, σ_{max} is the maximum horizontal stress at failure; P_{ult} is the maximum force; D is the diameter of the specimen; and $f\left(\frac{a}{h}\right)$ and h are the geometric factor and the height of the specimen, respectively.

5.2.2. Development of a novel parameter of HMA mixture cracking resistance

The presence of air voids within an asphalt mixture may negatively affect its cracking resistance, and increases in air voids reduce the fracture resistance and the fatigue life of a mixture at normal temperatures [7, 8]. The air voids content is a part of the VMA of HMA mixtures. Because the characteristics of aggregate gradation greatly influence the amount of air voids in an HMA mixture, it may be possible to obtain the target VMA by controlling these characteristics. A previous study investigated the relationship between aggregate gradation and the VMA using the area of continuous maximum density (CMD_{area}) [9]. It has been reported that the VMA of asphalt mixtures increases with increasing CMD_{area} [9]. Another study demonstrated that the K_{Ic} of HMA mixtures decreases with increasing VMA [10]. The K_{Ic} and J_c parameters are used to indicate the cracking resistance of HMA mixtures and are closely correlated: when the K_{Ic} of a mixture decreases, J_c also decreases [11]. An increase in CMD_{area} may increase the amount of air voids in the aggregate structure and reduce cracking

resistance. The present study posited that CMD_{area} is a potential parameter that indicates a negative effect on the cracking resistance of HMA mixtures.

The DASR refers to the interactive size range of particles that form the backbone of an aggregate structure. Dominant particles of coarse aggregate in the DASR create a structural network and produce voids. The interstitial components (fine aggregate, filler, and asphalt binder) or the IC fill the void spaces between the DASR aggregate particles [12]. Among these, fine aggregate has a particularly substantial effect on cracking resistance [13]. Figure 34 shows the effects of fine aggregate on cracking performance of HMA mixtures. When the proportion of fine aggregate is low, there is inadequate interaction among the DASR particles. The fine aggregate does not support any applied loads and does not contribute frictional strength to the DASR aggregate [13]. Therefore, low IC aggregates result in low cracking resistance. In contrast, an excessively large quantity of IC particles may disrupt the coarse aggregate structure and cause the mixture to become more brittle [13]. Consequently, there is a reduction in the points of contact among the DASR aggregate particles, thereby reducing the cracking resistance of HMA mixtures [13]. An optimal amount of IC aggregate may provide high cracking resistance to an asphalt mixture [13].

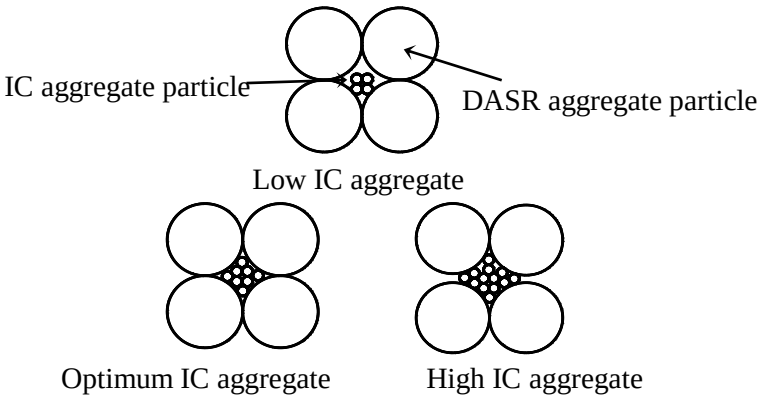

Figure 34. Effects of IC aggregate composition on cracking resistance in HMA mixtures [13]

It has been reported that the ratio of the aggregate fraction volume with a greater proportion to the aggregate fraction volume with a smaller proportion is a potential parameter that indicates the degree of aggregate interlock in HMA mixtures [14]. Based on that study, this study assumed that the ratio of the CMD area of DASR aggregate particles ($CMD_{area-DASR}$) to the CMD area of IC aggregate particles ($CMD_{area-IC}$) would be a useful indicator of interlocking strength for asphalt mixtures. Figure 35 shows an illustration of $CMD_{area-DASR}$ and $CMD_{area-IC}$ when the DASR ranges from 9.5 mm to 0.6 mm. It should be

noted that the CMD_{area} has been previously introduced to evaluate the effect of aggregate gradation on the VMA of asphalt mixtures [9].

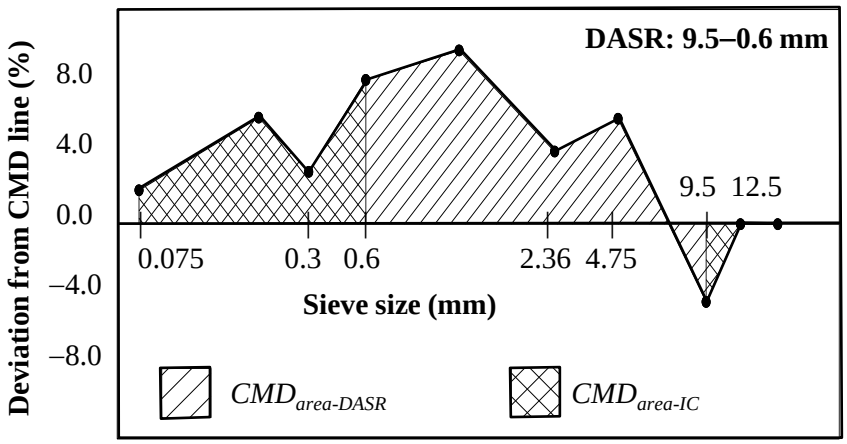

Figure 35. $CMD_{area\text{-}DASR}$ and $CMD_{area\text{-}IC}$

Therefore, the $CMD_{area–DASR}$ and $CMD_{area–IC}$ parameters may indicate the relative volumes of air voids in mixtures due to the DASR aggregate particles and IC aggregate particles, respectively. When the DASR aggregate particles have good contact with one another, the DASR aggregate fraction acts as a backbone aggregate and is the predominant cause of voids. In this case, the value of $CMD_{area–DASR}$ is significantly larger than that of $CMD_{area–IC}$ when the proportion of IC aggregate particles is low. However, when the proportion of IC aggregate particles is high, the amount of air voids created by the IC aggregates is also large. A high proportion of IC aggregate particles may therefore interfere with the dense packing of the backbone aggregate [13]. Figure 34 also presents that the DASR aggregate particles tend to separate when the quantity of IC aggregate particles is too high. This means that there is an increase in the amount of air voids created by the DASR aggregate particles as the IC aggregate particles disrupt aggregate structure. A previous study also noted that the disruption of aggregate structure by fine aggregate leads to the creation of additional voids in the mixture [14].

In all HMA mixtures, the $CMD_{area–IC}$ value cannot be higher than the $CMD_{area–DASR}$ value. In the DASR model, DASR aggregate particles are defined as the main aggregate fraction that creates voids in a mixture [12]. Therefore, the present study assumed a larger amount of air voids created by DASR aggregate particles than those created by IC aggregate particles. This means that the $CMD_{area–DASR}$ value (which signifies the relative volume of air voids in a mixture created by DASR aggregate particles) must be higher than the $CMD_{area–IC}$ value (which signifies the relative volume of air voids in a mixture created by IC aggregate particles). The ratio of $CMD_{area–DASR}$ to $CMD_{area–IC}$ ($CMD_{area–DASR}$ / $CMD_{area–IC}$) may illustrate the balance between the volumes of air voids created by the DASR aggregate and IC aggregate

particles. This ratio is expected to be high as the IC aggregate fraction is substantially lower and does not completely fill the voids between the DASR aggregate. In addition, when the IC aggregate fraction is too high, the DASR structure will become unstable and additional air voids are created within the DASR aggregate; this would result in a high $CMD_{area-DASR}$ / $CMD_{area-IC}$ value. Based on this assumption, the present study proposes the $CMD_{area-DASR}$ / $CMD_{area-IC}$ ratio as a parameter to indicate the degree of aggregate interlock in crack resistance of HMA mixtures. The cracking resistance of mixtures decreases as $CMD_{area-DASR}$ / $CMD_{area-IC}$ increases.

The film thickness of the asphalt binder that coats aggregate particles is strongly associated with the cracking resistance of an HMA mixture. This is because tensile stress tends to be concentrated on the asphalt binder. Cracking can occur easily when the asphalt binder is thin [8]. Accordingly, film thickness should also be established to improve cracking resistance of asphalt mixtures. Enriching the fine aggregate fraction may reduce effective asphalt thickness [8]. When the amount of fine aggregate increases, the aggregate specific surface area (S_s) coated by the asphalt binder also increases [8]. As a result, the effective asphalt content may decrease due to an increase in aggregate surface voids that absorb the asphalt binder. Therefore, an increase in S_s may decrease effective asphalt content and reduce cracking resistance.

Based on the above, the present study investigated a new cracking resistance index that would describe the relationship between the aggregate gradation and cracking resistance of an asphalt mixture. This index was designated the "gradation-based cracking resistance index", or *GCI*. This study hypothesized that an HMA mixture's cracking resistance increases with increasing values of *GCI*. The *GCI* parameter is derived from three factors of aggregate gradation, i.e., CMD_{area}, $CMD_{area-DASR}$ / $CMD_{area-IC}$, and S_s; these address the effects of air voids, aggregate interlock, and film thickness of the asphalt binder, respectively, on the cracking performance of a mixture. The *GCI* value of aggregate gradations is calculated using the following equation:

$$GCI = \frac{1}{CMD_{area}} \times \frac{1}{\left(CMD_{area-DASR} \Big/ CMD_{area-IC} \right)} \times \frac{1}{S_s} \tag{17}$$

Where S_s is calculated using Equation (9) in chapter 4.

5.3. Experience work

5.3.1. Preparation of HMA materials

Preparation of HMA materials had been described in chapter 3.

5.3.2. Design of aggregate gradation

Aggregate gradation design had been described in chapter 3.

5.3.3. Mix design procedure

Asphalt mixture design procedure had been described in chapter 3.

5.3.4. Notched SCB test method

Figure 36 shows the configuration of a notched SCB specimen and the loading equipment. A series of notched SCB tests with different notch depths can determine the critical strain energy release rate, or J_c value. The specimens for these tests were fabricated using a Superpave gyratory compactor (SGC). The test employed two nominal notch depths (a_1 = 25 mm and a_2 = 32 mm) based on those reported in previous studies [2-4]. The number of design gyrations (N_{des}) was set as the gyration number where the HMA specimens have the same bulk specific gravity (G_{mb}) as specimens produced by Marshall compaction. The specimens had a thickness of 50 mm in accordance with the European Standards for the notched SCB test [5]. The thickness should be at least four times that of the NMPS of the mixtures [15]. As the present study investigated 12.5-mm NMPS wearing course mixtures, the 50-mm thickness fulfilled the above recommendations.

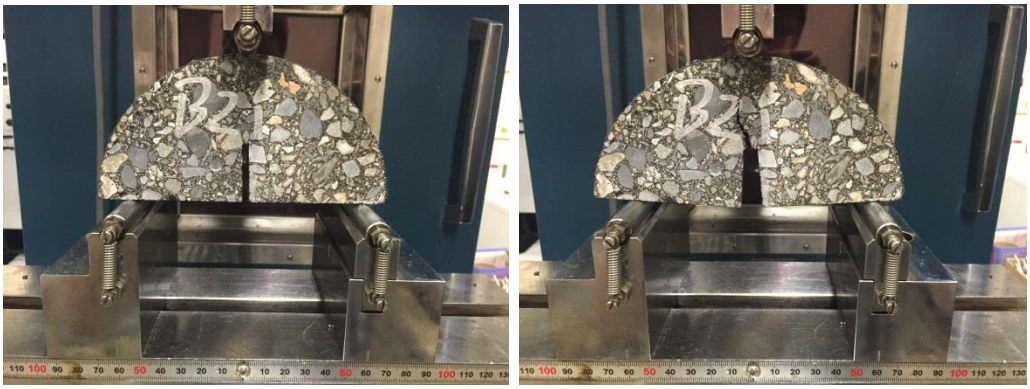

Figure 36. Photographs of the notched SCB test

The test was conducted at a temperature of 30 ^{o}C and a deformation rate of 2 mm/min. The deformation rate of the notched SCB test should range from 1 to 5 mm/min for analyses of cracking resistance at normal temperatures [15]. Before starting the test, the specimens were kept in an environmental chamber at the testing temperature for 15 hours. A minimum curing time of 12 hours has been recommended [16]. The temperature of the notched SCB test was set 20 ^{o}C lower than the highest

average pavement temperature in the southern region of Vietnam (i.e., 50 ^{o}C) [16]. The designated testing temperature was based on the test protocol proposed by Christensen *et al.*[17].

A previous study proposed the adjusted strain rate ($\dot{\varepsilon}_a$) to evaluate the validity of both the test temperature and the deformation rate that can induce ductile fracture of an asphalt film [1]; $\dot{\varepsilon}_a$ values were calculated using the following equations [1, 19]:

$$\dot{\varepsilon}_a = \dot{\varepsilon} \exp \frac{-Q}{R_g (T_0 - T_1)} \tag{18}$$

$$\dot{\varepsilon} = \frac{\text{deformation rate}}{R - a} \tag{19}$$

Where, $\dot{\varepsilon}$ is the normal strain rate; a is the notch depth; R is the radius of the notched SCB specimen (75 mm); Q is the activation energy, where Q = 210 kJ/mol is applied for HMA mixtures [1, 20]; R_g is the universal gas constant, where R_g = 8.314 J/mol/K [1]; T_0 is the reference temperature; and T_1 is a testing temperature. T_0 and T_1 were provided in Kelvin (T_0 = 273.15 K and T_1= 303.15 K).

The $\dot{\varepsilon}_a$ values for the notch depths of a_1 and a_2 were 0.0015 s^{-1} and 0.0018 s^{-1}, respectively. Past studies have also reported that ductile fracture of an asphalt film can occur when the $\dot{\varepsilon}_a$ value is lower than 0.01 s^{-1} [1, 19]. This indicates that both the test temperature and deformation rate were suitable for assessing the cracking resistance of the HMA mixtures.

5.4. Results and discussion

5.4.1. Results of mix design and the SGC parameters

Asphalt mixture design procedure had been described in chapter 3, and the SGC results had been presented in chapter 4.

5.4.2. Results of the notched SCB tests

Figure 37 presents the load-deformation curves obtained from the notched SCB tests. J_c values for all seven mixtures were also shown in Table 15. In general, the J_c values of the dense-graded HMA mixtures were generally higher than those of the coarse- and fine-graded HMA mixtures. The J_c values ranged from 0.13 to 0.89 kJ/m^2. A previous study reported that the J_c values for 12.5-mm NMPS mixtures ranged from 0.13 to 0.76 kJ/m^2 using notched SCB tests conducted at 30 ^{o}C with a 2.4-mm/min deformation rate [1]. Therefore, there is a large degree of overlap between the notched SCB test results of the present study and the previous study.

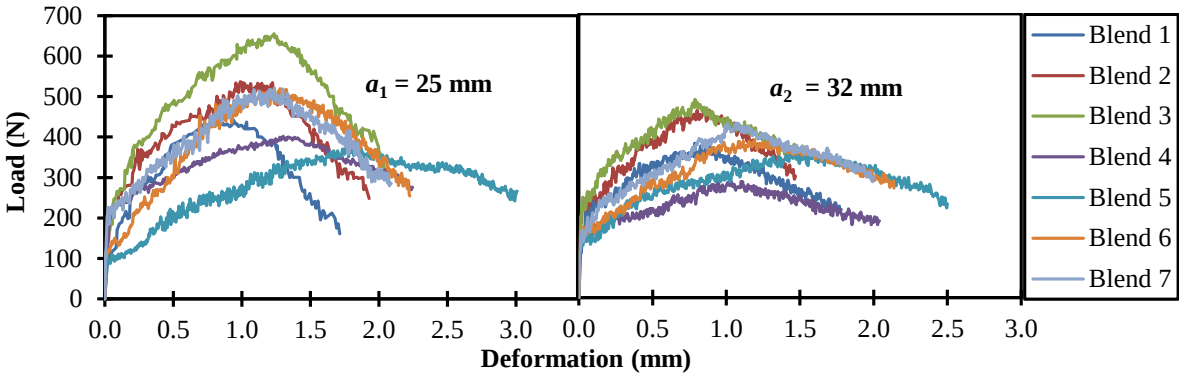

Figure 37. The load-deformation curves obtained from the notched SCB tests

Table 15. J_c values calculated from the results of the notched SCB tests

Mixture			U_i (J)	b_i (mm)	U_i/b_i (J/m)	Average of U_i / b_i (J/m)	J_c (kJ/m^2)
Dense - graded	1	a_1-1	0.449	48.2	9.326	8.121	0.44
		a_1-2	0.329	47.6	6.915		
		a_2-1	0.280	48.7	5.759	5.060	
		a_2-2	0.216	49.5	4.361		
	2	a_1-1	0.478	47.2	10.133	11.740	0.70
		a_1-2	0.621	46.5	13.347		
		a_2-1	0.380	48.3	7.858	6.812	
		a_2-2	0.294	51.0	5.767		
	3	a_1-1	0.738	51.3	14.378	13.016	0.89
		a_1-2	0.557	47.8	11.654		
		a_2-1	0.208	46.8	4.451	6.763	
		a_2-2	0.437	48.2	9.076		
Coarse - graded	4	a_1-1	0.506	48.5	10.441	9.546	0.61
		a_1-2	0.430	49.7	8.650		
		a_2-1	0.235	47.8	4.913	5.275	
		a_2-2	0.272	48.2	5.637		
	5	a_1-1	0.446	51.5	8.657	9.593	0.13
		a_1-2	0.509	48.3	10.528		
		a_2-1	0.478	50.7	9.440	8.690	
		a_2-2	0.388	48.8	7.941		
Fine - graded	6	a_1-1	0.552	50.3	10.965	10.208	0.39
		a_1-2	0.447	47.3	9.451		
		a_2-1	0.410	51.8	7.909	7.474	
		a_2-2	0.367	52.2	7.040		
	7	a_1-1	0.483	51.8	9.313	9.634	0.44
		a_1-2	0.503	50.5	9.956		
		a_2-1	0.375	51.8	7.244	6.530	
		a_2-2	0.297	51.0	5.816		

Table 16. K_{Ic} values calculated from the results of the notched SCB tests

Mixture			P_{ulti} (N)	b_i (mm)	h_i (mm)	σ_{max} (N/mm^2)	$f(a_i / h_i)$	K_{ici} (N/mm$^{1.5}$)	Average of K_{Ic} (N/mm$^{1.5}$)
Dense - graded	1	a_1-1	427	48.2	74.3	0.252	9.693	2.441	2.5
		a_1-2	419	47.6	74.2	0.250	9.703	2.425	
		a_2-1	377	48.7	74.1	0.220	12.290	2.706	
		a_2-2	334	49.5	73.2	0.192	12.471	2.390	
	2	a_1-1	496	47.2	74.5	0.299	9.668	2.887	3.1
		a_1-2	534	46.5	73.7	0.327	9.748	3.183	
		a_2-1	471	48.3	73.8	0.277	12.361	3.423	
		a_2-2	404	51.0	73.1	0.225	12.486	2.811	
	3	a_1-1	683	51.3	74.3	0.378	9.693	3.665	3.4
		a_1-2	537	47.8	73.9	0.319	9.727	3.106	
		a_2-1	339	46.8	74.1	0.206	12.292	2.526	
		a_2-2	582	48.2	73.6	0.343	12.389	4.253	
Coarse - graded	4	a_1-1	375	48.5	73.2	0.220	9.802	2.154	2.1
		a_1-2	396	49.7	73.2	0.218	9.804	2.223	
		a_2-1	258	47.8	73.2	0.147	12.484	1.911	
		a_2-2	279	48.2	72.5	0.155	12.626	2.075	
	5	a_1-1	344	51.5	73.0	0.190	9.822	1.863	2.2
		a_1-2	370	48.3	74.0	0.217	9.723	2.114	
		a_2-1	324	50.7	73.3	0.182	12.445	2.263	
		a_2-2	346	48.8	74.6	0.201	12.199	2.457	
Fine - graded	6	a_1-1	520	50.3	74.2	0.293	9.700	2.846	2.6
		a_1-2	484	47.3	74.2	0.291	9.701	2.820	
		a_2-1	389	51.8	73.2	0.213	12.471	2.659	
		a_2-2	326	52.2	75.1	0.177	12.100	2.148	
	7	a_1-1	463	51.8	73.8	0.254	9.743	2.473	2.7
		a_1-2	500	50.5	74.2	0.281	9.699	2.728	
		a_2-1	392	51.8	73.2	0.215	12.482	2.683	
		a_2-2	421	51.0	74.5	0.235	12.212	2.866	

Table 16 summarizes the calculated K_{Ic} values for all the mixtures; the values ranged from 2.1 to 3.4 N/mm$^{1.5}$. A previous study found that for 26.5-mm NMPS mixtures, the K_{Ic} value ranged from 4.0 to 13.0 N/mm$^{1.5}$ at 30 ^{o}C [10]. The disparity between our findings and those of the previous study may be due to the following: First, the previous study had conducted the tests with a deformation rate of 5 mm/min, whereas our experiment used a deformation rate of 2 mm/min. This higher deformation rate may result in higher cracking resistance [15]. Next, the notch depth used in the previous study was 10 mm, which was smaller than those used in our experiment. It has been reported that the failure load of the SCB test decreases with increasing notch depth [15]. This may account for the lower K_{Ic} values obtained in our study relative to those reported in the previous study.

As shown in Table 4 in chapter 3, the design AC values of Blends 4, 6, and 7 were high, which can lead to thicker films in the asphalt binder and improved cracking resistance. In addition, Blends 4, 6, and 7 had relatively high values of J_c. However, this trend was not observed in the K_{Ic} values. Among all the mixtures, Blend 4 showed the lowest K_{Ic} value. While an increase in AC may improve cracking resistance at cracking initiation [21], increases in the thickness of the asphalt binder may decrease the fracture toughness of mixtures at cracking propagation [10].

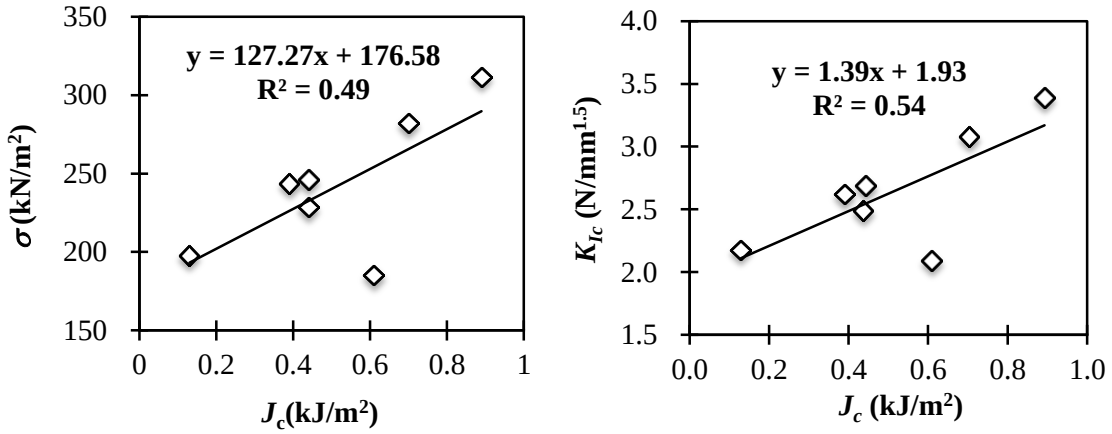

Figure 38. Relationships of J_c with σ_{max} and K_{Ic}

Figure 38 shows the relationship of J_c with σ_{max} and K_{Ic} for the notched SCB tests. These variables did not demonstrate a high correlation coefficient. J_c is commonly used in EPFM analyses, whereas K_{Ic} is used in linear-elastic fracture mechanics (LEFM) analyses [1, 6, 10]. Although the LEFM approach is generally not applicable for measuring J_c values, it can be adopted for calculating J_c values for laboratory evaluation purposes using load-deformation curves [1-4, 7]. The principle difference in J_c calculation between the LEFM and EPFM approaches is that a variety of notch depths for the notched SCB test are applied only in EPFM analyses [1-4, 7]. J_c values calculated with different notch depths provide insight into the cracking initiation stage, whereas K_{Ic} is more indicative of the fracture toughness of HMA mixtures during the cracking propagation stage [1, 5, 7]. As the cracking initiation and propagation stages are distinct, it is important to distinguish between the two during analyses [1]. A previous study reported a relatively weak linear correlation between J_c and K_{Ic} [11], and a recent analysis also found a low correlation coefficient between these two parameters [22]. However, the trend line in our analysis indicated that the K_{Ic} and J_c values of HMA mixtures increased or decreased together when the aggregate gradation of the mixtures was changed. The findings of this study corroborate those from a previous analysis [11].

5.4.3. Effect of aggregate gradation on cracking resistance

Table 17. Values of *GCI* and other associated variables

Mixture	DASR (mm)	CMD_{area}	$CMD_{area\text{-}DASR}$	$CMD_{area\text{-}IC}$	S_s (m^2/kg)	*GCI* ($\times 10^{-3}$)
1	9.5–0.6	5.91	4.43	1.48	5.32	10.62
2	9.5–0.6	4.63	2.97	1.66	5.68	21.30
3	9.5–0.6	3.43	1.75	1.68	6.26	44.69
4	4.75–0.6	8.29	5.10	3.19	5.14	14.68
5	9.5–0.6	7.42	6.17	1.25	4.80	5.69
6	9.5–0.6	7.01	4.68	2.33	6.62	10.74
7	4.75–0.6	9.79	4.94	4.84	6.78	14.76

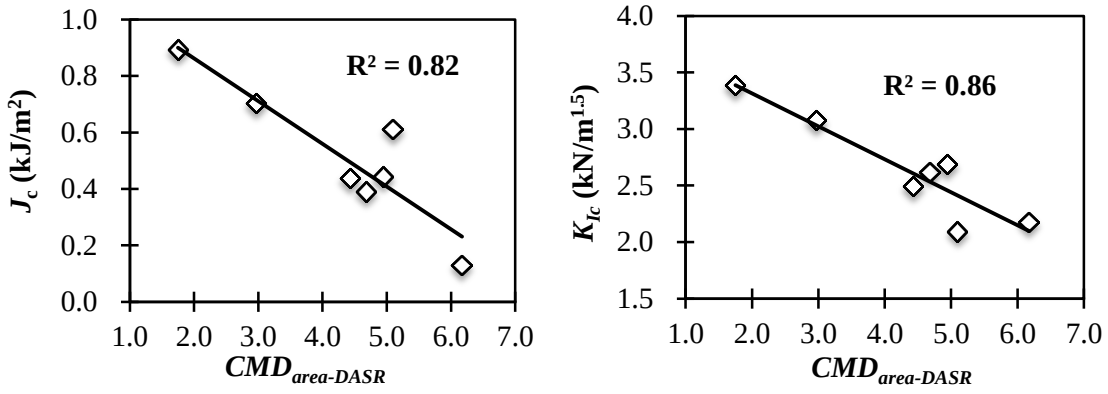

Figure 39. Relationships of $CMD_{area\text{-}DASR}$ with J_c and K_{Ic}

Table 17 shows the values of *GCI* for the seven HMA mixtures. The $CMD_{area\text{-}DASR}$ values are higher than the $CMD_{area\text{-}IC}$ values for all the mixtures, indicating that the DASR range in the study is compliant with the assumption of the DASR model described in subsection 5.2.2. Figure 39 shows the relationships of $CMD_{area\text{-}DASR}$ with the cracking resistance parameters at the cracking initiation and propagation stages. The correlation coefficients of $CMD_{area\text{-}DASR}$ were high for both parameters (J_c: R^2 = 0.82 and K_{Ic}: R^2 = 0.86). The trend lines indicated that the J_c and K_{Ic} values of the HMA mixtures increased as $CMD_{area\text{-}DASR}$ decreased. This tendency may be explained by the following reasons: Coarse aggregate in the DASR model forms the backbone of the aggregate structure and creates voids in HMA mixtures. When the $CMD_{area\text{-}DASR}$ value is high, the DASR aggregate creates a large quantity of air voids that may reduce cracking resistance [12]. Furthermore, when there are numerous air voids, the proportion of IC aggregate may be insufficient to fill these voids. This can interfere with the interlocking between the DASR and IC aggregates in HMA mixtures, thereby further reducing their cracking resistance [13]. The

results also showed that the $CMD_{area\text{-}DASR}$ of aggregate gradation has a stronger association with the cracking propagation stage than with the cracking initiation stage.

5.4.4. Relationships of *GCI* with J_c and K_{Ic}

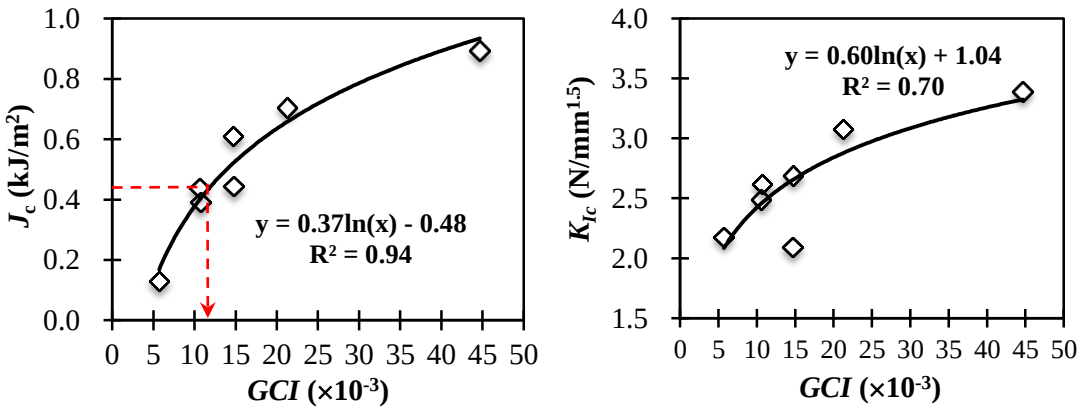

Figure 40. Relationships of *GCI* with J_c and K_{Ic}

Figure 40 shows the relationships of *GCI* with J_c and K_{Ic} values for the seven HMA mixtures. A high correlation coefficient (R^2 = 0.94) was obtained between *GCI* and J_c. However, contrary to the authors' expectations, the correlation coefficient between *GCI* and K_{Ic} was not as high (R^2 = 0.70). The trend lines, as expected, indicated that the J_c and K_{Ic} values are high when the *GCI* value of the aggregate gradation is high. It is therefore apparent that the *GCI* parameter is more closely associated with the cracking initiation stage than the cracking propagation stage. This is in direct contrast to the $CMD_{area\text{-}DASR}$ parameter of aggregate gradation. As described in subsection 5.2.2, S_s (one of components used to develop the *GCI* parameter) provides information on the effects of asphalt binder on crack resistance of HMA mixtures. The cracking initiation stage is significantly dependent on the asphalt binder component [22].

The J_c value indicates cracking resistance at the cracking initiation stage, which suggests that the *GCI* parameter has potential applications for evaluating the cracking performance of HMA mixtures. The previous study has noted that the J_c value of 12.5-mm NMPS mixtures should be higher than 0.43 kJ/m^2 to guarantee high cracking resistance [3]. Figure 40 presents that the aggregate gradation of HMA mixtures using the natural sands should be designed such that the value of *GCI* exceeds 12×10^{-3} in order to achieve an appropriate J_c value.

5.4.5. Evaluation of cracking resistance with different fine aggregate sources

The present study investigated the effects of fine aggregate on the cracking resistance of 12.5-mm NMPS mixtures by using two groups. The first group included seven aggregate gradations that were designed as Vietnamese wearing course mixtures (designated Blends V1–V7). The results of the cracking test were mention in section 5.4.2.

The second group included six aggregate gradations that were designed as Indonesian wearing course mixtures (designated Blends I1–I6) based on Iman *et al*. [1]. The gradation and mixture design were also mentioned in section 3.4.3.2. Iman et al. conducted the notched SCB test at a temperature of 30 ^{o}C and a deformation rate of 2.4 mm/min [1]. The test used the Marshall specimens with two nominal notch depths (a_1 = 15 mm and a_2 = 22.5 mm) [1]. The characteristics of aggregate gradations and the results of the notched SCB test conducted by Iman et al. were summarized in Table 18. Because the dimension of testing specimens was not enough, the present study determined the maximum horizontal stress at failure (σ_{max}) instead of the K_{Ic} for the six Indonesian mixtures.

Table 18. Cracking resistance parameters and results of the notched SCB test

	Mixture					
	I1	I2	I3	I4	I5	I6
DASR (mm)	4.75-0.6	9.5-0.6	4.75-0.6	9.5-0.6	9.5-0.6	4.75-0.6
CMD_{area}	8.67	7.71	6.95	7.01	6.16	9.44
$CMD_{area\text{-}DASR}$	5.56	6.63	4.69	5.32	3.81	5.39
$CMD_{area\text{-}IC}$	3.11	1.08	2.26	1.70	2.34	4.05
S_s (m^2/kg)	5.72	4.60	4.10	8.42	8.10	9.18
GCI ($\times 10^{-3}$)	11.29	4.59	16.93	5.41	12.32	8.67
σ_{max} (kN/m^2)	274	247	286	406	303	277
J_c(kJ/m^2)	0.76	0.60	0.23	0.23	0.13	0.76

To gain a clearer understanding of the effects of fine aggregate on cracking performance of asphalt mixtures, this study applied the fine aggregate angularity (FAA) as the main indicator of the degree of fine aggregate internal friction. The testing procedure outlined in the AASHTO T304-11 standard provides a method to determine the individual uncompacted void content of fine aggregate or the *FAA* of mineral aggregate sources [23]. The *FAA* value describes shape characteristics, i.e., the angularity and surface texture roughness, of fine aggregate particles. A high *FAA* value indicates that the aggregate particles have more angular and fractured faces, which increase the points of contact among the aggregate particles and promote shear strength [24]. The FAA testing procedure is shown in Figure 41.

Figure 41. Test setup for assessing fine aggregate angularity

Table 19. Individual fine aggregate angularity values for the mineral aggregate sources

	Fine aggregate		
	Limestone screening	Coarse granite sand	Fine granite sand
FAA (%)	46.0	43.4	38.5

Table 20. Summary of measured *FAA* values of the thirteen mixtures

	Mixture	Combination LS/ CGS/ FGS*	*FAA* (%)
Vietnamese	V1	0/ 100/ 0	43.2
	V2	0/ 75/ 25	43.1
	V3	0/ 68/ 32	42.9
	V4	0/ 100/ 0	42.9
	V5	0/ 100/ 0	42.7
	V6	0/ 80/ 20	42.3
	V7	0/ 89/ 11	43.0
Indonesian	I1	68/ 32/ 0	45.4
	I2	0/ 100/ 0	43.3
	I3	91/ 0/ 9	45.3
	I4	99/ 0/ 1	46.0
	I5	0/ 19 /81	39.2
	I6	91/ 6/ 3	45.9

*LS=limestone screening; CGS=coarse granite sand; FGS=fine granite sand.

The result of FAA test for each fine aggregate source is presented in Table 19. The *FAA* values of fine sand and coarse sand were 38.5% and 43.4%, respectively. These values were consistent with those of a previous study, which reported that the *FAA* values for natural sand ranged from 38.6% to 44.1% [25]. Only the limestone screening, which was used to fabricate the Indonesian mixtures, complied with the *FAA* requirements (≥45% of high traffic volume of heavy vehicles) for Superpave mix design [24].

Figure 42 presents the comparison of σ_{max} and J_c values between the Vietnamese and Indonesian wearing course mixtures. It should be noted that the aggregate gradation in each pair of mixtures presented in these figures has the same aggregate gradations. In accordance with expectations, the results indicated that the tensile strength and cracking resistance of Indonesian wearing course mixtures were higher than those of Vietnamese wearing course mixtures.

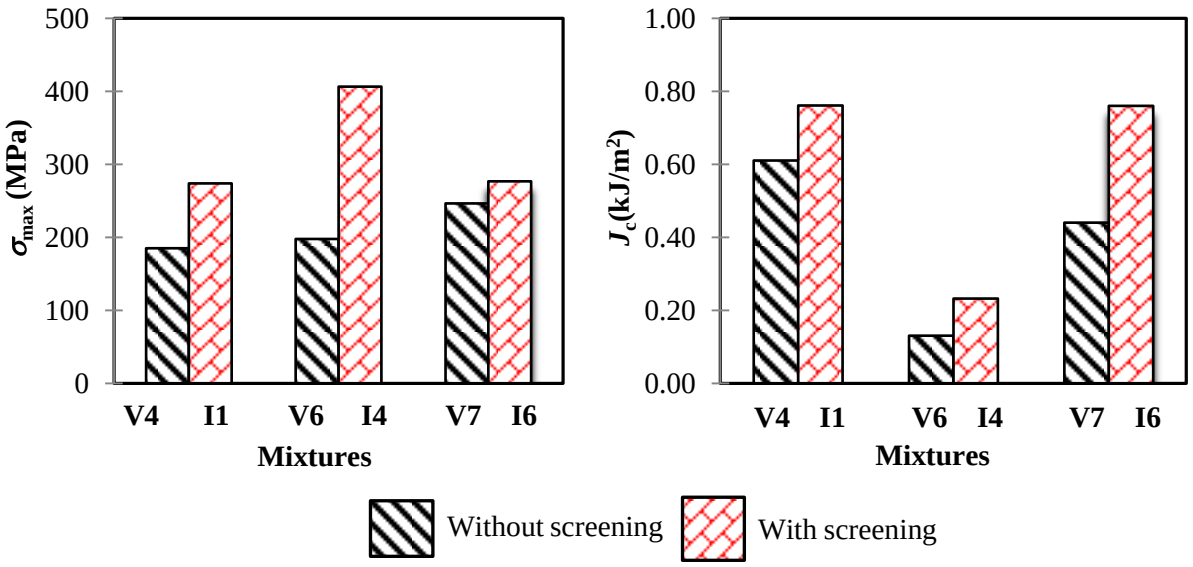

Figure 42. Comparison of σ_{max} and J_c values between the Vietnamese and Indonesian mixtures.

With the same aggregate gradation, the Indonesian mixtures had a higher cracking resistance than the Vietnamese mixtures, and these results may be explained by the following reasons. Firstly, the proportions of limestone screening (percentage of blend mass) in Blends I1, I4, and I6 were 15%, 72%, and 73%, respectively. When these mixtures were compared with Blends V4, V6, and V7, we found that higher quantities of limestone screening (relative to natural sands) were associated with improved cracking resistance. Consequently, as shown in Table 20, the *FAA* values of fine aggregate in the Indonesian blends were higher than those in the Vietnamese blends, which means that the fine aggregate particles in the former were more angular and fractured than those in the latter. Consequently, the aggregate particles in the Indonesian wearing course mixtures were able to form an adequate packing state, and the backbone aggregates improved their shearing resistance. Low tensile strength potentially

induces the initial cracking failure in HMA mixtures [26], and the use of limestone screening instead of natural sand may improve the tensile strength and interfacial strength of the asphalt mixtures [1, 27]. As a result, with the same aggregate gradation, the J_c and σ_{max} values of Indonesian mixtures were greater than those of Vietnamese mixtures. Secondly, the results may also be explained by the higher design ACs of the Vietnamese blends. Table 8 shows that the design ACs of Blends V4, V6, and V7 were higher than those of Blends I1, I4, and I6, respectively. As described in section 3.4.3.2, the present study used the granite sand to fabricate specimens of Blends V4, V6, and V7, while Iman et al. used the limestone screening to compact the specimens of Blends I1, I4, and I6. This finding was consistent with the finding of the previous study that indicated the design AC of asphalt mixtures with granite sand was higher than that of asphalt mixtures with limestone screening [28]. An increase in design AC can lead to an increase in the apparent film thickness of binding that coats aggregate particles in mixtures [8]. As a result, the excessively thick asphalt binder in combination with a decrease in viscosity at high temperatures may interfere with the points of contact among aggregate particles. Aggregate interlock is thus weakened and the aggregate particles are more easily shifted by the applied loads. This in turn reduces the peak load (P_{ult}) and σ_{max} values with high AC in the notched SCB test at normal temperatures.

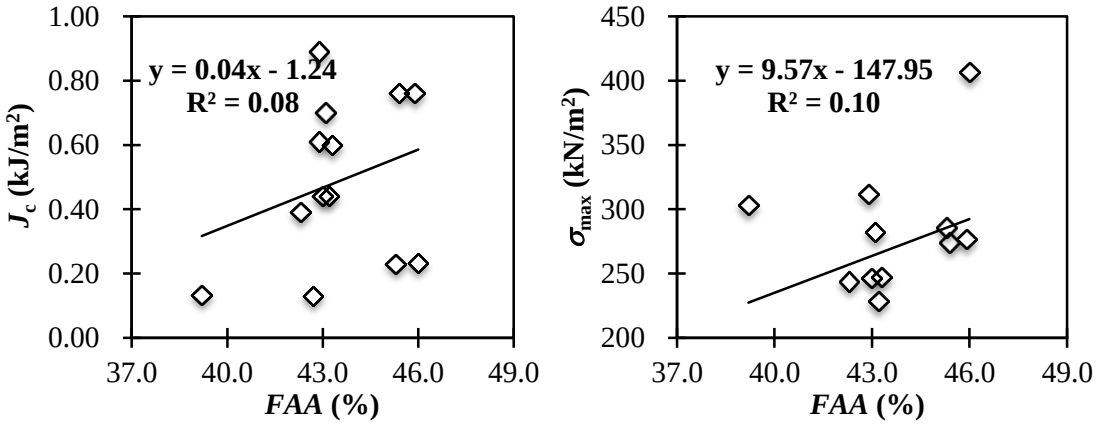

Figure 43. Relationships of *FAA* with J_c and σ_{max}

Figure 43 presents the relationships of *FAA* with J_c and σ_{max} for the thirteen mixtures. Contrary to the authors' expectations, the low correlation coefficients of these relationships were observed when mixtures with different aggregate gradations were compared. These results demonstrated that the *FAA* of fine aggregate alone may be insufficient to rank the J_c and σ_{max} of HMA mixtures with various aggregate gradations.

Figure 44 shows the relationship of J_c with σ_{max} in the notched SCB test for six Indonesian wearing course mixtures. Contrary to the authors' expectations, the results showed the negative

relationship between J_c and σ_{max} that was not consistent with the results obtained from seven Vietnamese wearing course mixtures and previous studies [11, 22]. Figure 45 and Figure 46 also show relationships of $CMD_{area-DASR}$ and *GIC* with J_c and σ_{max} for six Indonesian mixtures. The trend line, as expected, indicated that the $CMD_{area-DASR}$ and *GIC* had negative and positive effects on the σ_{max}, respectively. However, the data showed an outlier with excessively high σ_{max} (Mixture I4) which reduced the relationships of $CMD_{area-DASR}$ and *GIC* with σ_{max}. Comparing to Blend V6 that has the same aggregate gradation with the Blend I4, Blend I4 was comprised of a particularly large amount of limestone screening (72% of blend mass), which strongly increased the σ_{max} value but slightly increased the J_c value. In addition, the relationships $CMD_{area-DASR}$ and *GIC* with J_c were low and the trend lines did not corroborate those reported in the present study. Therefore, further research and more data are required to confirm the application of these cracking parameters for asphalt mixtures compacted with different aggregate sources.

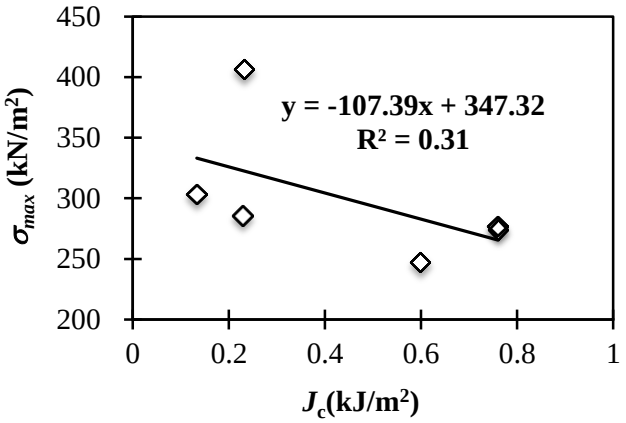

Figure 44. Relationship between J_c and σ_{max} for six Indonesian mixtures

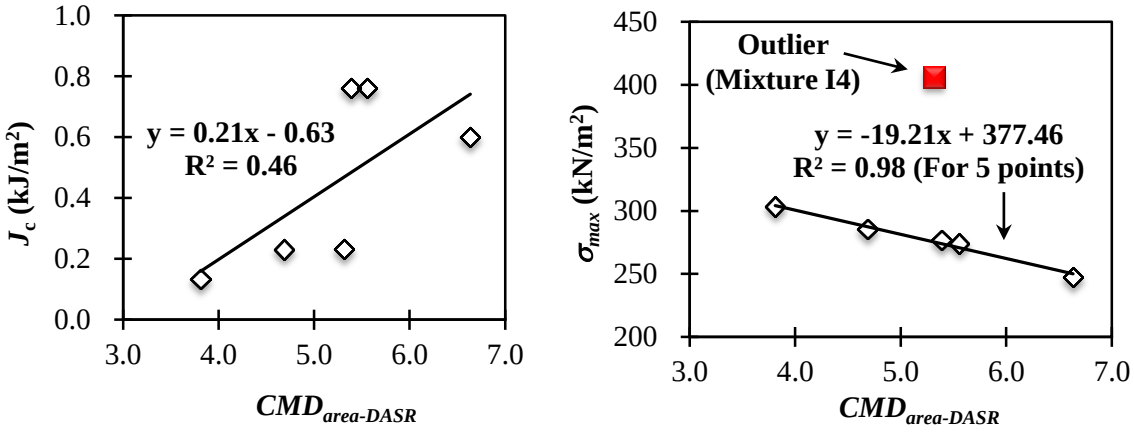

Figure 45. Relationships of $CMD_{area-DASR}$ with J_c and σ_{max} for six Indonesian mixtures

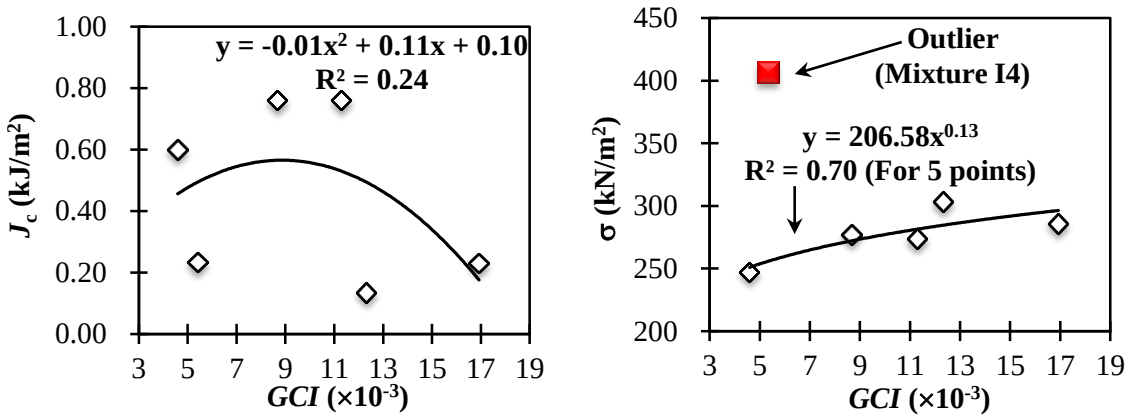

Figure 46. Relationships of *GIC* with J_c and σ_{max} for six Indonesian mixtures

5.5. Summary

The summaries of this chapter are the following.

- The present study found a high relationship between the $CMD_{area-DASR}$ of aggregate gradation and cracking resistance in HMA mixtures at a normal temperature. An asphalt mixture with a higher $CMD_{area-DASR}$ value may have lower cracking resistance at the cracking initiation and propagation stages. The $CMD_{area-DASR}$ parameter, which is indicative of the amount of air voids created by the DASR aggregate in the mixtures, had a stronger association with the cracking propagation stage than with the cracking initiation stage.
- A simple index, designated *GCI*, was developed to evaluate the cracking resistance of HMA mixtures at the cracking initiation and propagation stages. *GCI* values present a composite description of the effect of air voids, aggregate interlock, and the film thickness of asphalt binder on cracking performance. A strong correlation of the *GCI* with the J_c was observed, indicating that *GCI* was more strongly associated with the cracking initiation stage than with the cracking propagation stage. The analysis found that J_c and K_{Ic} values tended to increase with increases in *GCI*. *GCI* is a candidate indicator for assessing the cracking potential of wearing course HMA mixtures.
- The use of limestone screening instead of natural sands may improve cracking resistance of HMA mixtures. The combination of different fine aggregate source reduced the relationships of $CMD_{area-DASR}$ and *GCI* with J_c and σ_{max}.

References

[1] Haryanto, I., and Takahashi, O. Assessment of Indonesian wearing course mixtures using J

integral and crack tip opening angle, International Journal of Pavement Engineering 9(3), pp. 165-176, 2008.

[2] Mohammad, L.N, Kim, M., and Elseifi, M. Characterization of asphalt mixture's fracture resistance using the Semi-Circular Bending (SCB) test, 7th RILEM International Conference on Cracking in Pavements, on 20-22 June 2013, Delft, The Netherlands, pp. 1-10, 2012.

[3] Shamsi, K.A. et al. Compactability and performance of Superpave mixtures with aggregate structures designed using the Bailey method, Journal of the Association of Asphalt Paving Technologists 75, pp. 91-132, 2006.

[4] Othman, A.M. Fracture resistance of rubber-modified asphaltic mixtures exposed to high-temperature cyclic aging, Journal of Elastomers and Plastics 38, pp. 19-30, 2006.

[5] The European Committee for Standardization, EN 12697-44:2010. Bituminous mixtures-Test methods for hot mix asphalt-Part 44: Crack Propagation by Semi-Circular Bending Test, 2010.

[6] Saha, G., and Biligiri, K.P. Homothetic behaviour investigation on fracture toughness of asphalt mixtures using semicircular bending test, Construction and Building Materials 114, pp. 423-433, 2016.

[7] Saha, G., and Biligiri, K.P. Fracture properties of asphalt mixtures using semi-circular bending test: A state-of-the-art review and future research, Construction and Building Materials number 105, pp. 103-112, 2016.

[8] Christopher, W.J., *et al*. A manual for design of hot mix asphalt with commentary, Report NCHRP 673, Washington DC, 2011.

[9] Tran, N.T., and Takahashi, O. Improvement on aggregate gradation design and evaluation of rutting performance of Vietnamese wearing course mixtures, the 8th international conference on maintenance and rehabilitation of pavements, Singapore, pp. 212-221, 2016.

[10] Minhajuddin, M., Saha, G., and Biligiri, K.P. Crack propagation parametric assessment of modified asphalt mixtures using linear elastic fracture mechanics approach, Journal of Testing and Evaluation 44 (1), pp. 471-483, 2016.

[11] Abdo, A.M.A. et al. Semi-circular notched beam testing procedure for hot mixture asphalt, Proceedings of the Institution of Civil Engineers-Transport 167 (1), pp. 48-58, 2014.

[12] Kim, S. et al. Porosity of the dominant aggregate size range to evaluate coarse aggregate structure of asphalt mixtures, Journal of Materials in Civil Engineering ASCE 21 (1), pp. 32-39, 2009.

[13] Chun, S., Roque, R., and Zou, J. Effect of gradation characteristics on performance of Superpave mixtures in the field, Journal of the Transportation Research Board 2294, pp. 43-52, 2012.

[14] Haryanto, I., and Takahashi, O. Effect of gradation on workability of hot mix asphalt mixtures, The Baltic Journal of Road and Bridge Engineering 2 (1), pp. 21-28, 2007.

[15] Nsengiyumva, G. Development of semi-circular bending (SCB) fracture test for bituminous

mixtures, Master thesis, University of Nebraska, 2015.

[16] Erkens, S.M.J.G. Asphalt concrete response (ACRe): Determination, modelling and prediction. PhD thesis, Technical University Delft, Netherlands, 2002.

[17] Christensen, D.W. et al. Indirect tension strength as a simple performance test. New simple performance tests for asphalt mixes, Report E-C068, Washington DC, pp. 44-57, 2007.

[18] Nguyen, T. N., and Tran, V. T. Temperature distribution in asphalt pavement at the south area of vietnam, Journal of Vietnamese Transportation, 12, 30-31, 2015.

[19] Harvey, J.A.F, and Cebon, D. Failure mechanisms in viscoelastic films, Journal of Material Sciences 38(5), pp. 1021-1032, 2003.

[20] Montepara, A., Costa, A., and Tebaldi, G. The difference between the ASTM approach and the new AASHTO approach for dynamic (complex) modulus, the XV Congress SIIV, Bari, Italy, 22-24, 2005.

[21] Rowe, G.M. Performance of asphalt mixtures in the trapezoidal fatigue test, Journal of the Association of Asphalt Paving Technologists 62, pp. 344-384, 1993.

[22] Hakimelahi, H., Saadeh, Sh., and Harvey, J. Investigation of fracture properties of California asphalt mixtures using semicircular bending and beam fatigue tests, Road Materials and Pavement Design, 14 (S2), pp. 252-265, 2013.

[23] AASHTO Designation, T 304-11. Standard method of test for uncompacted void content of fine aggregate, 2015.

[24] The Asphalt Institute, Superpave Mix Design-Superpave Series No.2 (SP-2), third edition, Lexington, KY, 2001.

[25] Cross, S. A., and Purcell, E.M. Effects of fine aggregate angularity on VMA and rutting of Kansas HMA mixtures, Aggregate contribution to hot mix asphalt (HMA) performance, ASTMSTP 1412, T. D, pp. 95-109, 2001.

[26] Baladi, G.Y., Schorsch, M. and Svasdisant, T. Determining the causes of Top–down cracks in bituminous pavements, Report Number MDOTPRCE-MSU-2003-110, Pavement Research Center of Excellence, Michigan State University: East Lansing, Michigan, USA, August 2003.

[27] Masad, E.A. et al. Evaluation of aggregate characteristics affecting HMA concrete performance, Research Report ICAR 203-1, Texas Transportation Institute, The Texas A&M University System: Texas, USA, December 2003.

[28] Cooley, L. A. Jr. et al. Use of screenings to produce hot mix asphalt mixtures, Transportation Research Record 1832, pp. 59-66, 2003

Chapter 6. Effect of aggregate gradation on the cracking of asphalt mixtures design at low service temperatures

6.1. Introduction

The surface layer of asphalt pavements (i.e., the wearing course mixture) is directly exposed to repeated traffic loads and a variety of temperature conditions. A high volume of heavy vehicle traffic combined with seasonal climatic effects can lead to dramatic energy-dissipation processes in asphalt mixtures. These processes can reduce the adhesion and ductility of the asphalt binder, thereby inducing cracks in the mixtures [1, 2]. Current asphalt design procedures in developing countries (such as Vietnam and Indonesia) tend to follow the Marshall method, which focuses on the volumetric properties of HMA mixtures [1, 3]. However, the specification of volumetric parameters alone is insufficient to ensure high cracking resistance in asphalt mixtures [1].

In recent years, researchers have explored experimental fracture mechanics to link laboratory tests with the actual cracking performance of asphalt mixtures in the field. To evaluate the fracture behaviour of HMA mixtures, the Japanese standard uses the three-point bending beam (TPBB) test [4]. In contrast, the notched SCB test is more frequently employed in European and American standards [5-7]. For the TPBB test, slab-shaped specimens are compacted using a laboratory steel roller compactor. However, this type of specimen fabrication is complex, tedious, and time-consuming. In fact, it is difficult to control the characteristics of air voids in the slab-shaped specimens during this process. On the other hand, notched SCB specimens can be directly cored from a pavement or fabricated using the SGC designed for laboratory evaluation purposes. It should be noted that the SGC used to prepare the notched SCB specimens makes it easier to achieve the desired air voids than the roller compactor used to prepare the TPBB specimens.

The notched SCB test may potentially replace the TPBB test as a mechanical test for evaluating the cracking performance of HMA mixtures. Several distinctions in the analytical criteria must first be addressed before investigating the correlations between the TPBB test and the notched SCB test. First, there is a difference in directions between the compaction and stress–strain analyses used in these tests. For slab-shaped specimens in the TPBB test, the direction is identical between these two types of analyses. In contrast, the direction of the stress-strain analysis on notched SCB specimens is perpendicular to that of the compaction method [8]. Next, the TPBB test only specifies a deformation rate of 50 mm/min, whereas the notched SCB test can be performed under a variety of deformation rates and sample

thicknesses (Table 21). It has been reported that different deformation rates and sample thicknesses can lead to different cracking resistances in HMA mixtures [9, 10]. To the best of our knowledge, no studies have previously conducted an in-depth comparative discussion of the cracking resistance parameters between the two tests.

Table 21. Testing conditions of the notched SCB test among the different standards

	Deformation rate (mm/min)	Specimen thickness (mm)
AASHTO TP 105-13	0.03*	25
AASHTO TP 124-16	50	50
EN 12697-44	5	50

Note: *Crack mouth opening displacement

Aggregate gradation plays a fundamental role in improving the cracking resistance of HMA mixtures [1, 11]. First, the characteristics of aggregate gradation significantly affect aggregate interlock. Close contact between backbone aggregates can promote adequate aggregate interlock, which helps to avoid premature cracking [1, 12]. Furthermore, the interlocking of coarse aggregate particles decreases when the fine aggregate fraction is excessively high [1, 12]. Despite the recognized importance of aggregate gradation in cracking resistance, the search of the literature found no well-established research that evaluates the relationship between aggregate gradation and the cracking resistance of HMA mixtures at low intermediate temperature conditions.

Here, the present study conducted an experimental study to compare the fracture properties of HMA mixtures at an intermediate temperature between the TPBB test and the notched SCB test. The TPBB test was performed in accordance with the JRA B005 standard, whereas the notched SCB test was conducted in accordance with three different standards (EN 12697-44, AASHTO TP 105-13, and provisional AASHTO TP 124-16). The experiments were conducted using seven asphalt mixtures (dense-, coarse-, and fine-graded) representing wearing course mixtures with a 12.5-mm NMPS. In addition, this study examined the relationships of aggregate gradation and asphalt composition with the cracking resistance of asphalt mixtures based on the characteristics of continuous maximum density (CMD), the dominant aggregate size range (DASR) model, and apparent film thickness. This study was conducted from the perspective of asphalt mixtures with potential applications in Vietnam.

6.2. Literature review

6.2.1. The role of aggregate gradation in the cracking performance of HMA mixtures

The characteristics of aggregate gradation have been reported to be strongly associated with the voids in mineral aggregate (*VMA*) of asphalt mixtures [3, 13]. A previous study found a strong correlation between the area of CMD (CMD_{area}) and the *VMA* of HMA mixtures [3], where CMD_{area} indicates a degree of total deviation from the CMD line. Higher CMD_{area} values of aggregate gradation may result in higher *VMA* values [3].

The DASR is the interactive size range of aggregate particles that form the primary network of the aggregate structure [14]. Dominant coarse aggregate particles in the DASR model constitute the backbone of the aggregate structure and create void spaces in the asphalt mixture. The air voids within the DASR aggregate particles are occupied by interstitial components (IC), which are composed of fine aggregates, fillers, and asphalt binders [14, 15]. The interaction of aggregate particles occurs within the HMA mixtures when relative proportions between contiguous size particles are lower than 70/30 [14, 15]. For a 12.5-mm NMPS aggregate gradation, the previous study has suggested the smallest sieve size for the aggregate particles of the DASR model to be 0.6 mm [3].

Based on CMD properties and the DASR model, chapter 5 introduced the $CMD_{area\text{-}DASR}$ and $CMD_{area\text{–}IC}$ parameters to evaluate the effects of aggregate gradation on the cracking resistance of HMA mixtures at a normal temperature. The $CMD_{area\text{-}DASR}$ and $CMD_{area\text{-}IC}$ parameters represent the CMD areas of DASR aggregate particles and IC aggregate particles, respectively. A high $CMD_{area\text{-}DASR}$ value indicates that a DASR aggregate creates an excessively large proportion of air voids within the mixtures, which can reduce their cracking resistance [13]. In addition, when there is a large quantity of air voids, the proportion of IC aggregate particles may not sufficiently fill these voids. This reduces the points of contact or aggregate interlock between the DASR and IC aggregate particles, which subsequently leads to lower cracking resistance [15].

6.2.2. Effect of apparent film thickness on the cracking performance of HMA mixtures

Apparent film thickness (*AFT*) refers to the average thickness of the asphalt binder that coats aggregate particles in HMA mixtures [13]. In recent years, researchers have applied the *AFT* parameter instead of asphalt content (AC) to evaluate the rutting performance of asphalt mixtures [3, 13]. It has been reported that the cracking performance of HMA mixtures is also associated with the design AC [10, 13]. Although the fracture energy of asphalt mixtures was found to increase with increasing design AC, the correlation coefficient between these two parameters was not high [13]. To the best of our knowledge, the relationship between *AFT* and the cracking resistance of asphalt mixtures at low service temperatures has

yet to be established. Therefore, this study aimed to use the *AFT* parameter to characterize the effect of AC on cracking performance. The *AFT* value of each mixture can be calculated by the following equation.

$$AFT = \frac{1000 \times V_{be}}{S_s \times P_s \times G_{mb}} \tag{20}$$

Where, V_{be} is the effective AC; S_s is the aggregate specific surface area; P_s is the aggregate content; and G_{mb} is the bulk specific gravity of the asphalt mixture. Equations (20) can be applied to a wide range of mineral aggregates sources (slag, limestone, gravel, and granite) and asphalt binder types (virgin asphalt and modified asphalt) [16]. In addition, the equation has potential applications for calculating *AFT* in a variety of dense-, coarse-, and fine-graded mixtures [16].

6.3. Experimental work

6.3.1. Material sources and mixture design

The characteristics of materials and the results of mixture design had been described in chapter 3.

6.3.2. TPBB test method

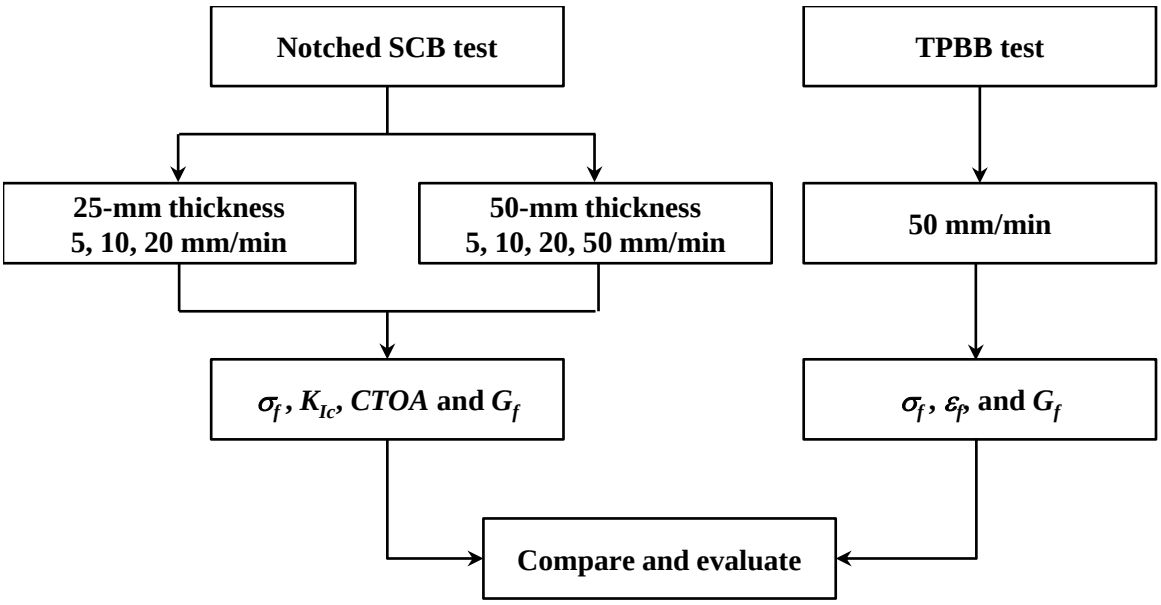

Figure 47. Experimental workflow

Figure 47 summarizes the workflow of the experiments conducted in this study. Slab-shaped specimens (dimensions: 300 × 300 × 50 mm) were prepared for the TPBB test using a laboratory steel

roller compactor. The steel roller compaction process used is commonly applied to fabricate slab-shaped specimens in Japan. The air void value of a Marshall specimen at the design AC is defined as the standard air void value when compacting slab-shaped specimens [4]. Therefore, at the design AC, the design number of passes for steel roller compaction was regarded as the number of passes required to produce a slab-shaped specimen with the same air void value (or G_{mb}) as a Marshall specimen. Each of the original slab-shaped specimens was trimmed into two prismatic TPBB specimens (dimensions: 300 × 100 × 50 mm). This specimen preparation process is depicted in Figure 48.

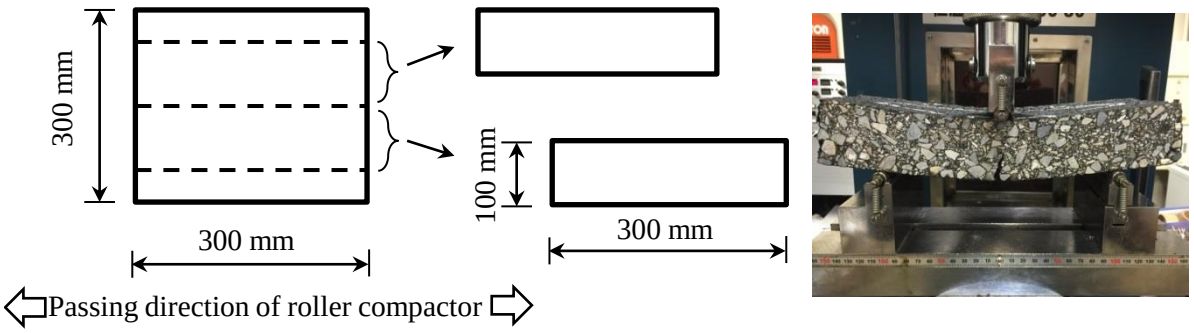

Figure 48. Prismatic TPBB specimen preparation and testing

Previous studies have generally conducted fracture tests at low temperatures to assess the mechanical properties of asphalt binders. However, under low-temperature conditions, asphalt mixtures become more brittle than they are at service temperatures [9]. The fracture tests for asphalt mixtures should therefore be performed at intermediate service temperatures to accurately evaluate fracture performance [9]. It has been reported that at intermediate service temperatures, the critical strain energy release rate of the notched SCB test is associated with the actual field cracking performance of asphalt mixtures [17]. In accordance with the AASHTO M 320-16 standard, a range of 4 ^{o}C to 31 ^{o}C is regarded as intermediate asphalt temperatures to evaluate the mechanical property of asphalt binder [18]. Based on average pavement temperatures in Vietnam, the Vietnamese standard recommends a low service temperature of 15 °C to evaluate the cracking performance of 12.5-mm NMPS wearing course mixtures [19]. Therefore, the TPBB test in this study was also conducted at this temperature. In addition, the TPBB test was performed at a deformation rate of 50 mm/min in accordance with JRA B005 standards. In order to match these conditions, the prismatic TPBB specimens were placed in an environmental chamber at the test temperature for 6 h before being used in the experiments [4].

Table 22. Requirements of cracking resistance parameters among the different standards

Parameter	JRA B005	EN 12697-44	AASHTO TP 124-16	AASHTO TP 105-13
Fracture toughness	σ_f	σ_f and K_{Ic}	σ_f and K_{Ic}*	σ_f and K_{Ic}
Cracking propagation	ε_f	*CTOA**	*CTOA**	*CTOA**
Fracture energy	G_f*	G_f*	G_f	G_f

Note: * These parameters are not required in the indicated standards.

Table 22 shows the requirements of the cracking resistance parameters among the different standards. Maximum horizontal tension stress at failure (σ_f) and tension strain at failure (ε_f) were evaluated for the TPBB test. The JRA B005 standard does not require the determination of fracture energy (G_f) for asphalt mixtures. Nevertheless, this study determined the G_f of the TPBB test to enable comparisons with the G_f of the notched SCB test. The three parameters of the TPBB test can be calculated as follows [4]:

$$\sigma_f = \frac{3}{2} \times \frac{P_{ult} \times L}{b \times h^2} \tag{21}$$

$$\varepsilon_f = \frac{6 \times h}{L^2} \times u \tag{22}$$

$$G_f = \frac{W_f}{A_{lig}} \tag{23}$$

Where, P_{ult} is the maximum force; L is the span of the bending support (200 mm); h is the height or thickness of the prismatic specimen; b is the width of the prismatic specimen; u is the deformation at the peak load; W_f is the work of fracture or the area under the load-deformation curve; and A_{lig} is the ligament area. For the calculation of W_f, the area under the extrapolated tail of the load-deformation curve can be reasonably calculated by fitting data in the post-peak region; this process is detailed in the AASHTO TP 105-13 standard [5].

6.3.3. Notched SCB test method

6.3.3.1. Notched SCB specimen preparation and testing conditions

Standard specimens with a 150-mm diameter and 115-mm thickness were fabricated using the SGC [20]. These specimens were also prepared to achieve the same degree of compaction as the slab-shaped specimens and Marshall specimens at the design AC. Therefore, at the design AC, the design

gyration number (N_{des}) was set as the gyration number required to produce an SGC specimen with the same air void value (or G_{mb}) as a Marshall specimen. The SGC standard specimens were trimmed into SCB specimens with two different thicknesses: 50 mm [6, 7] and 25 mm [5]. Figure 49 illustrates the preparation procedure of these notched SCB specimens. Although the EN 12697-44 standard dictates a strict requirement for a notch width of 0.35 mm, it is difficult to cut the specimens to meet this requirement. Therefore, all SCB specimens were trimmed with a nominal notch depth of 15 mm and a notch width of 1.5 mm in accordance with the AASHTO TP 124-16 and AASHTO TP 105-13 standards.

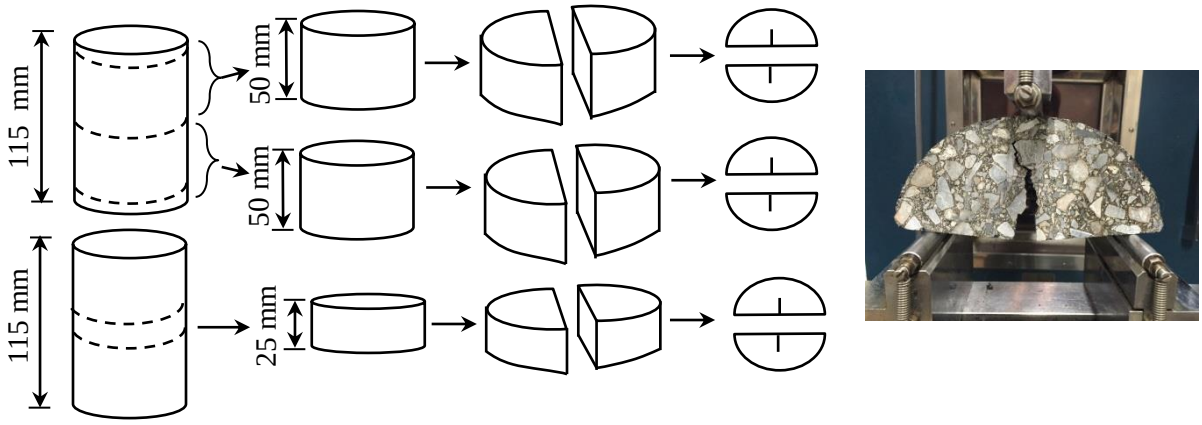

Figure 49. Notched SCB specimen preparation and testing

In order to conduct a comparison of various deformation rates, the notched SCB test using 50-mm–thick specimens was performed at the following four rates: 5, 10, 20 and 50 mm/min. As shown in Table 1, the deformation rates of 5 mm/min and 50 mm/min are recommended by the EN 12697-44 standard and the AASHTO TP 124-16 standard, respectively.

The loading conditions specified by the AASHTO TP 105-13 standard for notched SCB specimens with 25-mm thickness are complex (crack mouth opening displacement of 0.03 mm/min). In general, researchers have selected a deformation rate of 5 mm/min to conduct the notched SCB test when this standard is applied [21]. Therefore, the present study decided to test the 25-mm-thick specimens at three rates: 5, 10, and 20 mm/min. The deformation rate of 50 mm/min was not applied for the 25-mm-thick specimens because of the thinness of the specimens. A previous study found that the cohesive strength of the 25-mm-thick specimens is not sensitive to the deformation rate when the deformation rate is more than or equal to 50 mm/min [9]. As a result, this combination of parameters was not evaluated in the present study.

The notched SCB tests were also conducted at a temperature of 15 °C. Before the test, the specimens were placed in an environmental chamber at this test temperature. Curing times of 4 h and 2 h were used for specimens with thicknesses of 50 mm and 25 mm, respectively [5, 6].

6.3.3.2. Previously identified parameters of the cracking resistance of HMA mixtures

For 25-mm–thick specimens, the AASHTO TP 105-13 standard prescribes procedures to calculate the G_f and fracture toughness (K_{Ic}) of HMA mixtures. G_f can be determined using Equation (22), whereas K_{Ic} is calculated using the following equations and variables [5]:

$$K_{Ic} = \sigma_f \times \sqrt{\pi a} \times Y_{I(0.8)} \tag{24}$$

$$\sigma_f = \frac{P_{ult}}{D \times t} \tag{25}$$

$$Y_{I(0.8)} = 4.782 + 1.219 \times \left(\frac{a}{R}\right) + 0.063 \times \exp\left[7.045 \times \left(\frac{a}{R}\right)\right] \tag{26}$$

Where, D is the diameter of the specimen; t is the thickness of the specimen; a is the notch depth of the specimen; R is the radius of the specimen; and $Y_{I(0.8)}$ is the normalized stress intensity factor.

For 50-mm-thick specimens, the determination of K_{Ic} and other variables were described in section 5.2.1.

Table 22 shows that the EN 12697-44 standard only includes the procedure for calculating K_{Ic}. In this study, the determination of G_f as described in the AASHTO TP 105-13 standard was also applied to the specimens under the EN 12697-44 standard. In addition, the AASHTO TP 124-16 standard does not include the definition of K_{Ic}. For the purpose of laboratory-based evaluations, the calculation of K_{Ic} as outlined in the EN 12697-44 standard was also used for the AASHTO TP 124-16 specimens.

6.3.3.3. Application of the crack tip opening angle to evaluate the cracking propagation resistance of HMA mixtures

In this study, the notched SCB test did not use linear variable differential transducers to measure the strain at failure. A previous study proposed the use of the crack tip opening angle (*CTOA*) as a potential indicator for evaluating the cracking propagation of HMA mixtures [1]. Figure 50 provides a visual illustration of the *CTOA*, which has a constant value during the cracking propagation stage. Asphalt mixtures with higher *CTOA* values therefore demonstrate slower cracking propagation [1]. As shown in Figure 50, higher *CTOA* values indicate greater deflection at crack extension. Therefore, the present study

adopted the *CTOA* parameter from the notched SCB test for comparisons with the ε_f parameter of the TPBB test.

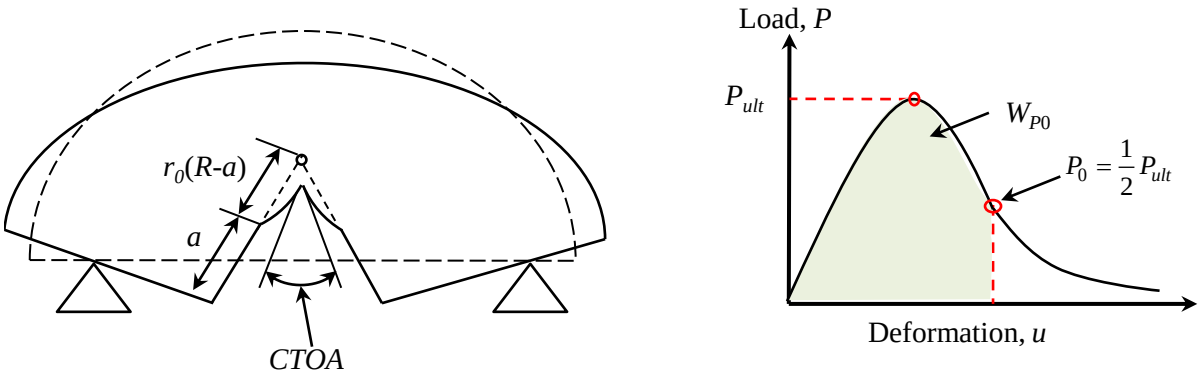

Figure 50. Descriptions of *CTOA*, r_0, P_0, and W_{P0}

It has also been reported that the procedure to calculate the *CTOA* is complicated, with various notch depths required in the notched SCB test [1]. Therefore, the present study decided to use the Martinelli-Venzi model to determine the *CTOA* of the notched SCB test. This model is commonly applied to ascertain the *CTOA* of ductile metals and soils [22]. Using only the load-deformation curve of the notched SCB test with the single notch depth, the *CTOA* is calculated through the following equations and variables [1, 22]:

$$CTOA = 2\tan^{-1}\frac{r_0 \times \left(W_f - W_{P0}\right)}{M_0} \tag{27}$$

$$M_0 = P_0\frac{L}{4} \tag{28}$$

$$P_0 = \frac{P_{ult}}{2} \tag{29}$$

Where, M_0 is the applied momentum; W_{P0} is the value of strain energy, which is calculated as the area under the load-deformation curve from the beginning of the test to point P_0; P_0 is the load value in the descending branch of the load-deformation curve; L is the distance between the two bottom supports (120 mm); and r_o is the plastic rotation parameter (0.45) [22]. Descriptions of W_{P0}, P_0, and r_0 are also provided in Figure 50.

The *CTOA* is commonly used in elastic-plastic fracture mechanics analyses to evaluate the ductile failure mechanisms of asphalt mixtures [1]. As mentioned in section 5.3.4, based on the test temperature and deformation rate, previous studies have proposed the adjusted strain rate ($\dot{\varepsilon}_a$) to determine if ductile fracture of a viscoelastic film can occur [1, 23]. At the test temperature of 15 °C, the $\dot{\varepsilon}_a$ values of the notched SCB at deformation rates of 5, 10, 20 and 50 mm/min were found to be 0.007, 0.015, 0.030 and 0.075 s^{-1}, respectively. It has been reported that an asphalt mixture undergoes ductile fracture when the $\dot{\varepsilon}_a$ value is lower than 0.01 s^{-1} [1, 23]. This means that at 15 °C, only the deformation rate of 5 mm/min has a potential application for assessing the ductile failure mechanisms of asphalt mixtures.

6.4. Results and discussion

6.4.1. Cracking resistance parameters

Table 23 shows the compaction properties of the seven HMA mixtures fabricated by the Marshall compactor, the SGC, and the steel roller compactor. The values for the SGC and slab-shaped specimens are mean values calculated from two samples. The cracking resistance parameters estimated from the TPBB test and the notched SCB test are also summarized in Tables 24 to 26. All cracking resistance parameters were obtained from four specimens for each mixture, and the mean values were calculated. In general, the fracture toughness (σ_f and K_{Ic}) values of the dense-graded HMA mixtures were higher than those of the coarse- and fine-graded HMA mixtures. In contrast, the cracking propagation (ε_f and *CTOA*) and G_f values of the dense-graded HMA mixtures were generally lower than those of the coarse- and fine-graded HMA mixtures.

Table 23. Compaction properties of the Marshall, SGC, and slab-shaped samples at the design AC

Mixture	Marshall Compactor	SGC		Steel roller compactor	
	G_{mb} (2×75 blows)	N_{des} (gyration)	G_{mb}	Passes	G_{mb}
1	2.364	70	2.363, 2.369 (2.366)	40	2.366, 2.371 (2.369)
2	2.392	48	2.395, 2.397 (2.396)	35	2.397, 2.401 (2.399)
3	2.398	48	2.390, 2.397 (2.394)	35	2.389, 2.400 (2.395)
4	2.347	120	2.338, 2.343 (2.341)	50	2.346, 2.341 (2.344)
5	2.356	70	2.348, 2.358 (2.353)	45	2.350, 2.352 (2.351)
6	2.339	45	2.334, 2.335 (2.335)	35	2.341, 2.345 (2.343)
7	2.324	70	2.314, 2.320 (2.317)	45	2.317, 2.321 (2.319)

Table 24. Cracking resistance parameters obtained from the TPBB test

Mixture		σ_f (MPa)	ε_f ($10^{-3}\times$ mm/ mm)	G_f (kJ/m^2)
Dense-graded	1	4.44	20.80	3.77
	2	5.26	21.18	4.16
	3	6.24	16.33	3.54
Coarse-graded	4	4.31	32.00	6.30
	5	4.40	19.38	3.85
Fine-graded	6	4.91	22.72	4.61
	7	4.63	25.95	4.91

Table 25. Cracking resistance parameters obtained from the notched SCB test using 50-mm-thick specimens

Deformation rate (mm/min)	Cracking resistance parameters	Mixture						
		1	2	3	4	5	6	7
5	σ_f (MPa)	2.19	2.37	2.70	1.87	1.95	2.12	2.09
	K_{Ic} (N/mm$^{1.5}$)	17.07	18.39	20.91	14.61	15.11	16.39	16.23
	G_f (kJ/m^2)	3.43	3.24	2.84	4.90	3.46	4.23	4.17
	CTOA (°)	3.16	2.57	1.70	5.29	3.35	3.61	3.74
10	σ_f (MPa)	2.68	2.80	3.16	2.30	2.62	2.66	2.50
	K_{Ic} (N/mm$^{1.5}$)	20.84	21.72	24.27	17.76	20.25	20.59	19.32
	G_f (kJ/m^2)	3.55	3.69	3.84	5.42	4.03	4.64	5.01
	CTOA (°)	2.30	2.26	1.79	4.10	2.75	2.99	3.21
20	σ_f (MPa)	3.32	3.55	3.81	2.81	3.11	3.23	2.94
	K_{Ic} (N/mm$^{1.5}$)	26.03	27.85	29.62	22.04	24.07	25.05	22.82
	G_f (kJ/m^2)	3.56	3.45	3.22	5.53	4.15	4.71	4.86
	CTOA (°)	1.68	1.53	1.15	3.20	2.04	2.24	2.61
50	σ_f (MPa)	4.60	4.83	4.79	4.04	4.08	3.97	3.53
	K_{Ic} (N/mm$^{1.5}$)	35.54	37.27	37.31	31.18	31.62	30.89	27.49
	G_f (kJ/m^2)	2.61	2.83	2.07	4.64	3.48	3.90	4.29
	CTOA (°)	0.75	0.87	0.46	1.68	1.22	1.07	1.55

Table 26. Cracking resistance parameters obtained from the notched SCB test using 25-mm-thick specimens

Deformation rate (mm/min)	Cracking resistance parameters	Mixture						
		1	2	3	4	5	6	7
5	σ_f (MPa)	0.54	0.63	0.62	0.42	0.55	0.5	0.45
	K_{Ic} (MPa×m$^{0.5}$)	0.66	0.77	0.76	0.51	0.67	0.61	0.56
	G_f (kJ/m^2)	4.01	3.49	3.62	6.37	4.37	4.51	4.37
	CTOA (°)	3.54	2.74	2.9	9.06	3.94	4.13	4.74
10	σ_f (MPa)	0.62	0.64	0.69	0.52	0.59	0.57	0.55
	K_{Ic} (MPa×m$^{0.5}$)	0.75	0.79	0.84	0.63	0.73	0.7	0.67
	G_f (kJ/m^2)	4.12	4.09	3.91	5.15	4.45	4.44	4.64
	CTOA (°)	3.11	3.1	2.51	6.11	3.81	3.79	4.16
20	σ_f (MPa)	0.84	0.85	0.94	0.74	0.68	0.68	0.59
	K_{Ic} (MPa×m$^{0.5}$)	1.02	1.04	1.15	0.91	0.83	0.82	0.73
	G_f (kJ/m^2)	4.2	4.62	3.89	6.08	4.62	4.58	5.38
	CTOA (°)	2.26	2.61	1.76	3.66	3.09	2.88	3.73

The experiments showed that increasing the deformation rates in the notched SCB test increased the fracture toughness (σ_f and K_{Ic}) and decreased the *CTOA* of the samples (Table 25 and Table 26). Because of the viscoelastic properties of asphalt binders, a decrease in deformation rates induces a reduction in the elastic component of asphalt mixtures [24]. This in turn reduces the stiffness of the asphalt binder and the cohesion strength of the HMA mixtures. Therefore, the lower deformation rate results in reduced fracture toughness and greater deformation at failure. These findings are consistent with those of previous studies [9, 24].

Table 25 and Table 26 also indicate that the G_f values of the notched SCB test generally increased with increasing deformation rates across a range of 5 mm/min to 20 mm/min. The findings corroborate those reported in a previous study [9]. However, when the deformation rate increased to 50 mm/min, the G_f value of the 50-mm-thick SCB specimens decreased. The results presented in Table 25 and Table 26 also indicate that the G_f values of the notched SCB tests were generally smaller than the G_f values of the TPBB tests at a deformation rate of 50 mm/min. G_f values generally increase with increasing size of specimens [25]. However, at each deformation rate in the notched SCB test, the G_f values of the 25-mm–thick specimens were generally higher than those of the 50-mm-thick specimens.

6.4.2. Comparison of cracking resistance between the notched SCB test and the TPBB test

6.4.2.1. Comparison of the accuracy and repeatability of the cracking resistance parameters

The present study compared and contrasted the accuracy and repeatability of cracking resistance parameters in the notched SCB test and the TPBB test using the coefficient of variation (COV). Table 27 presents the COV values of fracture toughness estimated from these two tests. Although a maximum COV value of 15% has been recommended [21], the σ_f values obtained from TPBB tests of the present study exhibited a lower COV (mean: 5.7%). The K_{Ic} estimated from the notched SCB tests also showed low COV values across a wide range of deformation rates, which corroborates previously reported findings [21]. These COV values tended to increase with increasing deformation rates, indicating reductions in the accuracy and repeatability of K_{Ic} in the notched SCB test. In addition, the COV values indicate that the K_{Ic} values of the notched SCB test using 50-mm-thick specimens were more precise than 25-mm-thick specimens at each deformation rate.

Table 27. COV of fracture toughness calculated for the notched SCB and TPBB tests

Fracture toughness		Deformation rate (mm/min)	COV of fracture toughness of each mixture (%)							Mean COV (%)	Ratio*
			1	2	3	4	5	6	7		
Notched SCB (50 mm)	K_{Ic}	5	6.7	4.8	5.1	7.8	5.5	5.3	4.3	5.6	7/7
		10	5.0	5.4	7.1	12.6	10.0	3.4	7.1	7.2	7/7
		20	9.7	8.5	1.5	6.5	17.5	4.7	3.7	7.4	6/7
		50	11.4	10.2	8.9	4.1	4.7	3.6	4.9	6.8	7/7
Notched SCB (25 mm)	K_{Ic}	5	4.6	7.2	11.4	1.5	11.6	5.4	10.4	7.4	7/7
		10	3.8	9.7	5.4	18.0	18.6	4.2	5.7	9.3	5/7
		20	12.3	9.4	10.7	9.3	14.8	9.5	4.7	10.1	7/7
TPBB	σ_f	50	5.6	11.0	3.5	4.9	10.3	0.8	3.5	5.7	7/7

* Ratio of mixtures with a COV below 15% to all mixtures.

Table 28 shows the COV values of cracking propagation obtained from the notched SCB and TPBB tests. The ε_f values of the TPBB test had a low COV, demonstrating that this method has a high repeatability for evaluating the cracking propagation stage of HMA mixtures. The results also indicate that the *CTOA* of the notched SCB test using 50-mm-thick specimens had a lower COV value (higher precision) than the 25-mm–thick specimens at each deformation rate. In addition, increasing the deformation rates of the notched SCB test increased the COV values of the *CTOA*, indicating the decreasing repeatability of the *CTOA*. This may be explained by the following: As described in section

6.3.3.3, ductile fracture may occur in asphalt mixtures at 15 °C when the notched SCB test is conducted at a deformation rate of 5 mm/min. As a result, this low deformation rate may be applicable for determining the *CTOA* when examining the ductile behaviour of asphalt mixtures. On the other hand, when the notched SCB test was conducted at higher deformation rates (10, 20, and 50 mm/min), brittle fracture may occur in the asphalt mixture. The higher deformation rates can therefore reduce the repeatability of the *CTOA* in the notched SCB test, and may not be appropriate for assessing ductile fracture properties.

Table 28. COV of cracking propagation calculated for the notched SCB and TPBB tests

Cracking propagation		Deformation rate (mm/min)	COV of cracking propagation of each mixture (%)							Mean COV (%)	Ratio*
			1	2	3	4	5	6	7		
Notched SCB (50 mm)	*CTOA*	5	17.0	5.9	4.6	5.3	15.7	8.1	6.3	9.0	5/7
		10	14.8	13.6	16.9	21.9	9.1	17.6	18.5	16.0	3/7
		20	19.3	9.5	11.4	2.5	29.4	27.4	8.3	15.4	4/7
		50	25.2	71.5	8.5	12.5	46.3	9.4	20.2	27.7	3/7
Notched SCB (25 mm)	*CTOA*	5	6.0	18.7	9.9	9.9	16.6	15.7	10.2	12.4	4/7
		10	15.5	19.1	20.3	23.5	16.4	18.8	4.4	16.8	1/7
		20	34.0	41.3	15.2	23.3	23.6	12.7	11.4	23.1	2/7
TPBB	ε_f	50	12.7	7.3	6.2	12.8	7.9	5.6	8.4	8.7	7/7

* Ratio of mixtures with a COV below 15% to all mixtures.

Table 29. COV of fracture energy calculated for the notched SCB and TPBB tests

Fracture energy		Deformation rate (mm/min)	COV of fracture energy of each mixture (%)							Mean COV (%)	Ratio*
			1	2	3	4	5	6	7		
Notched SCB (50 mm)	G_f	5	6.1	8.8	11.0	9.6	10.5	4.8	7.0	8.2	7/7
		10	7.5	11.7	20.2	7.9	10.9	7.7	9.1	10.7	6/7
		20	12.5	8.0	7.9	12.7	15.6	25.1	4.6	12.4	5/7
		50	18.1	28.4	5.7	14.8	24.5	10.0	13.5	16.4	4/7
Notched SCB (25 mm)	G_f	5	7.1	10.9	16.3	13.2	13.7	16.9	7.6	12.2	5/7
		10	14.4	16.8	11.9	10.5	14.3	13.5	9.1	12.9	6/7
		20	19.8	27.2	12.3	22.5	25.2	9.5	25.9	20.3	2/7
TPBB	G_f	50	24.3	5.3	9.7	8.7	11.2	6.4	6.7	10.3	6/7

* Ratio of mixtures with a COV below 15% to all mixtures.

Table 29 presents the COV values of fracture energy calculated from the notched SCB and TPBB tests. The G_f values obtained from the TPBB test showed low COV (<15%). Similarly, low COV values of G_f were also observed for the notched SCB test at deformation rates of 5 and 10 mm/min. The results indicate that at each deformation rate, the notched SCB test using 25-mm–thick specimens had less precise and repeatable G_f than 50-mm–thick specimens. These results may be explained by the following: The COV value of G_f is reported to increase with decreasing thickness of the notched SCB specimens [10]. Therefore, when the notched SCB test is conducted within a temperature range of 15 ^{o}C to 40 ^{o}C, the thickness of the notched SCB specimens should be at least four times (i.e., 40-50 mm) that of the NMPS of the test mixtures [10]. Because this study investigated 12.5-mm NMPS wearing course mixtures, only the 50-mm–thick specimens complied with the above recommendation. Moreover, a previous study also demonstrated that the AASHTO TP 105-13 standard (25-mm–thick specimens) offers a method to determine high COV, low precision, and low repeatability of G_f at intermediate temperature conditions [21]. In this way, the results of this study corroborate those of previous analyses.

These findings appear to confirm that the TPBB test using the JRA B005 standard and the notched SCB test using the EN 12697-44 standard are viable methods to measure the cracking resistance properties of HMA mixtures with high precision and repeatability.

6.4.2.2. Relationships of the cracking resistance parameters between the notched SCB test and the TPBB test

The present study investigated the relationships of the cracking resistance parameters between the notched SCB test and the TPBB test using the linear correlation coefficient (R^2) and Pearson correlation coefficient (PCC). PCC indicates the linear dependence between two different measurement systems, and ranges from –1 to +1. Values of –1 and +1 indicate that two variables have total negative correlation and total positive correlation, respectively; a value of 0 indicates that there is no correlation between the two variables.

Table 30 shows the correlations between the cracking resistance parameters from the notched SCB and TPBB tests estimated using linear regression analyses. The fracture toughness (σ_f and K_{Ic}) parameters from the TPBB test and the notched SCB test using 50-mm-thick specimens had the highest correlation coefficient when the latter was conducted at a deformation rate of 5 mm/min. The correlation coefficients of the fracture toughness parameters between the TPBB test and the notched SCB test using 50-mm–thick specimens decreased with increasing deformation rates in the latter. However, this trend was not observed for the notched SCB test using 25-mm-thick specimens. In addition, these parameters between the TPBB test and the notched SCB test using 25-mm-thick specimens had low correlation coefficients at all three deformation rates. In fact, in the notched SCB test using 25-mm-thick specimens,

the σ_f and K_{Ic} parameters may not be viable indicators for evaluating the cracking resistance of HMA mixtures at service temperatures [5, 21], as the temperature of this test should be 10 ^{o}C higher than the lower limit of the asphalt binder's performance grade [5].

Table 30. Correlations between the cracking resistance parameters of the notched SCB and TPBB tests

Test	Deformation rate (mm/min)	R^2 (PCC)			
		σ_{f_SCB} - σ_{f_TPBB}	K_{Ic_SCB} - σ_{f_TPBB}	$CTOA_{\_SCB}$ - ε_{f_TPBB}	G_{f_SCB} - G_{f_TPBB}
Notched SCB (50 mm)	5	0.89 (+0.94)	0.89 (+0.94)	0.87 (+0.93)	0.87 (+0.93)
	10	0.81 (+0.90)	0.80 (+0.89)	0.88 (+0.94)	0.82 (+0.91)
	20	0.76 (+0.87)	0.74 (+0.86)	0.89 (+0.94)	0.83 (+0.91)
	50	0.35 (+0.59)	0.38 (+0.61)	0.75 (+0.87)	0.76 (+0.87)
Notched SCB (25 mm)	5	0.49 (+0.70)	0.50 (+0.71)	0.68 (+0.82)	0.81 (+0.93)
	10	0.65 (+0.81)	0.64 (+0.80)	0.88 (+0.94)	0.86 (+0.93)
	20	0.45 (+0.67)	0.45 (+0.67)	0.83 (+0.91)	0.91 (+0.95)

Table 30 also shows strong correlations between the ε_f values from the TPBB test and the *CTOA* values of the notched SCB test at each deformation rate. In accordance with expectations, the PCC values indicate that ε_f tended to increase with increases in *CTOA*. In general, the *CTOA* parameter is used to evaluate the cracking propagation of metal alloys and metal composites instead of heterogeneous materials such as asphalt mixtures [1, 22]. However, the findings of the present study suggest that the *CTOA* parameter also has potential applications for investigating the cracking propagation stage of HMA mixtures.

The analysis also revealed strong linear correlations between the G_f values from the TPBB test and all notched SCB tests (Table 30), although the COV of the G_f values for the notched SCB test using 25-mm–thick specimens was inordinately high at the deformation rate of 20 mm/min (Table 29). These strong correlations indicate that the G_f estimates from the notched SCB and TPBB tests may be employed for the same objective of evaluating the cracking performance of HMA mixtures. These results may be explained by the following: G_f has been found to be less sensitive to the linear elasticity and homogeneity of materials than other cracking resistance parameters, such as the K_{Ic} and the J-integral [10, 26]. Therefore, although asphalt mixtures are heterogeneous and nonlinear inelastic, the G_f parameter may have potential applications for assessing and evaluating their fracture characteristics.

The experiments found that the pairs of cracking resistance parameters between the TPBB test using the JRA B005 standard and the notched SCB test using the EN 12697-44 standard had the highest correlation coefficients. Based on the COVs and linear regression analysis results, the notched SCB test

using the EN 12697-44 standard may present a viable alternative to the TPBB test for assessing the cracking resistance of HMA mixtures. Therefore, agencies or organizations may use the TPBB test using the JRA B005 standard or the notched SCB test using the EN 12697-44 standard depending on their experience and equipment.

6.4.3. Effect of mixture composition on the cracking resistance of HMA mixtures

Based on the results described in section 6.4.2, this study investigated the effects of aggregate gradation and AC on the cracking performance of HMA mixtures estimated from the TPBB test using the JRA B005 standard and the notched SCB test using the EN 12697-44 standard.

6.4.3.1. Effect of aggregate gradation on the cracking resistance of HMA mixtures

Table 31 presents the aggregate gradation parameters and *AFT* values for the seven HMA mixtures, and Table 32 shows the correlations of the aggregate gradation and asphalt binder parameters with the fracture characteristics of these mixtures. Increasing the CMD_{area} reduced the fracture toughness (σ_f and K_{Ic}) and increased the cracking propagation resistance (ε_f and *CTOA*) and G_f of the HMA mixtures. These relationships may be explained by the following: When the CMD_{area} of an aggregate gradation increases, the *VMA* of the HMA mixture also increases, thereby creating additional air voids in the mixture (*VIM*) [3]. To obtain the desired *VIM*, the additional voids in the aggregate structure are occupied by increasing the AC. This means that increasing *VMA* increases the viscoelastic property of asphalt mixtures. Accordingly, the asphalt mixtures become softer and have more extended deformation at the crack tip [2]. This may manifest as reductions in fracture toughness (σ_f and K_{Ic}) and increases in cracking propagation resistance (ε_f and *CTOA*) and G_f. The observed correlations between *VMA* and the cracking resistance parameters are consistent with the findings of a previous study [2].

Table 31. Gradation and asphalt binder parameters for the seven HMA mixtures

Mixture	DASR (mm)	CMD_{area}	$CMD_{area\text{-}DASR}$	*AFT* (mm)
1	9.5-0.6	5.91	4.43	7.2
2	9.5-0.6	4.63	2.97	6.61
3	9.5-0.6	3.43	1.75	5.71
4	4.75-0.6	8.29	5.10	10.23
5	9.5-0.6	7.42	6.17	8.11
6	9.5-0.6	7.01	4.68	7.63
7	4.75-0.6	9.79	4.94	7.99

Table 32. Correlations between the mixture compositions and fracture characteristics of the mixtures

Parameter	R^2 (PCC)					
	JRA B005			EN 12697-44		
	σ_f	ε_f	G_f	K_{Ic}	*CTOA*	G_f
CMD_{area}	0.60 (–0.77)	0.52 (+0.72)	0.43 (+0.66)	0.71 (–0.84)	0.64 (+0.80)	0.64 (+0.80)
$CMD_{\text{area-DASR}}$	0.84 (–0.92)	0.23 (+0.48)	0.16 (+0.40)	0.91 (–0.95)	0.53 (+0.73)	0.37 (+0.61)
VMA	0.55 (–0.74)	0.59 (+0.77)	0.51 (+0.71)	0.68 (–0.82)	0.71 (+0.84)	0.79 (+0.89)
VIM	0.26 (–0.51)	0.11 (–0.33)	0.20 (–0.45)	0.12 (–0.35)	0.00 (–0.03)	0.07 (–0.26)
V_{be}	0.22 (–0.47)	0.70 (+0.84)	0.71 (+0.84)	0.38 (–0.62)	0.63 (+0.79)	0.85 (+0.92)
Design AC	0.16 (–0.40)	0.61 (+0.78)	0.61 (+0.78)	0.29 (–0.54)	0.51 (+0.71)	0.77 (+0.88)
AFT	0.63 (–0.79)	0.79 (+0.89)	0.76 (+0.87)	0.81 (–0.91)	0.96 (+0.98)	0.81 (+0.90)

The correlation coefficients of the CMD_{area} with the cracking resistance parameters were lower than expected. This may be due to the following: the *VMA* of an asphalt mixture comprises two components, i.e., the *VIM* and the effective AC (V_{be}). As shown in Table 32, *VIM* negatively affects all cracking resistance parameters. On the other hand, V_{be} negatively affects fracture toughness (σ_f and K_{Ic}), but increases cracking propagation resistance (ε_f and *CTOA*) and G_f. In the Superpave method, the *VIM* value is controlled at 4%. When the value of *VIM* is constant, increasing the CMD_{area} of aggregate gradations only increases the remaining component of *VMA*, i.e., the V_{be} of asphalt mixtures. This means that the CMD_{area} may affect the cracking resistance of HMA mixtures only through V_{be}. In contrast, the Marshall method stipulates a range of values (3% to 6%) for *VIM* [27]. Therefore, CMD_{area} may influence the cracking resistance of HMA mixtures through both V_{be} and *VIM*. The results presented in Table 5 in chapter 3 indicate that when *VMA* increases due to increases in CMD_{area}, the following four effects can occur: (i) increase in V_{be} (e.g., Blends 3 and 4), (ii) increase in *VIM* (e.g., Blends 1 and 2), (iii) increase in both V_{be} and *VIM* (e.g., Blends 3 and 5), and (iv) increase in V_{be} but decrease in *VIM* (e.g., Blends 1 and 4). Consequently, increasing CMD_{area} may affect asphalt mixtures positively or negatively, and results in decreases or increases to cracking resistance. Therefore, the relationships of CMD_{area} with the fracture characteristics of asphalt mixtures may not have high correlation coefficients when applying the Marshall method.

$CMD_{area\text{-}DASR}$ had high correlation coefficients with the fracture toughness (σ_f and K_{Ic}) parameters obtained from the notched SCB and TPBB tests. The relationships between $CMD_{area\text{-}DASR}$ and the fracture toughness parameters are shown in Figure 51. By observing the trend lines, the HMA mixtures showed strong fracture toughness when the $CMD_{area-DASR}$ values of aggregate gradation were low. These findings were similar to those of a previous study, in which the notched SCB test was conducted at a normal

temperature of 30 °C [11]. However, the present study did not observe strong relationships between $CMD_{area-DASR}$ and the cracking propagation resistance (ε_f and *CTOA*) and G_f of HMA mixtures.

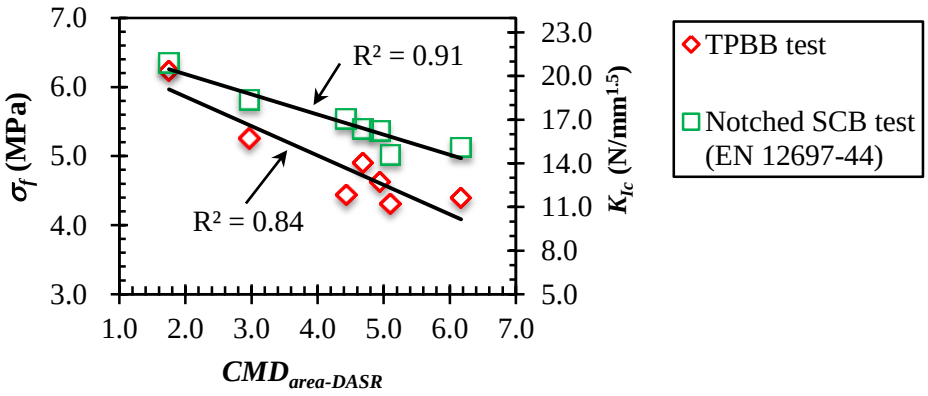

Figure 51. Relationships of $CMD_{area-DASR}$ with σ_f of the TPBB test and K_{Ic} of the notched SCB test

6.4.3.2. Effect of AC on the cracking resistance of HMA mixtures

Table 32 also presents the correlations between the asphalt binder parameters and the fracture characteristics of the HMA mixtures. The results highlighted that asphalt binder parameters (i.e., the V_{be}, design AC, and *AFT*) have the same effects on cracking resistance. These asphalt binder parameters negatively affect fracture toughness (σ_f and K_{Ic}), but positively affect cracking propagation resistance (ε_f and *CTOA*) and G_f. The correlation coefficients of V_{be} and the design AC with the cracking resistance parameters were not high, which corroborates findings from previous studies [2, 10]. The experiments showed that among the three asphalt binder parameters, *AFT* is a potential indicator of the effects of AC on the fracture mechanics of asphalt mixtures. The strong associations of *AFT* with cracking resistance are also shown in Figures 52 to 54.

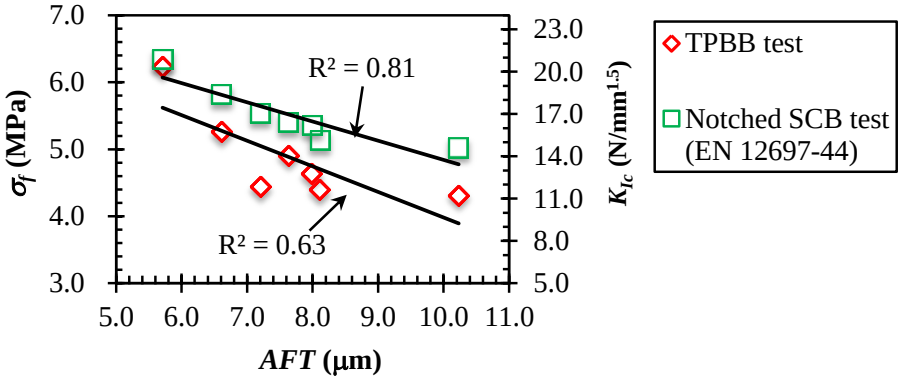

Figure 52. Relationships of *AFT* with σ_f of the TPBB test and K_{Ic} of the notched SCB test

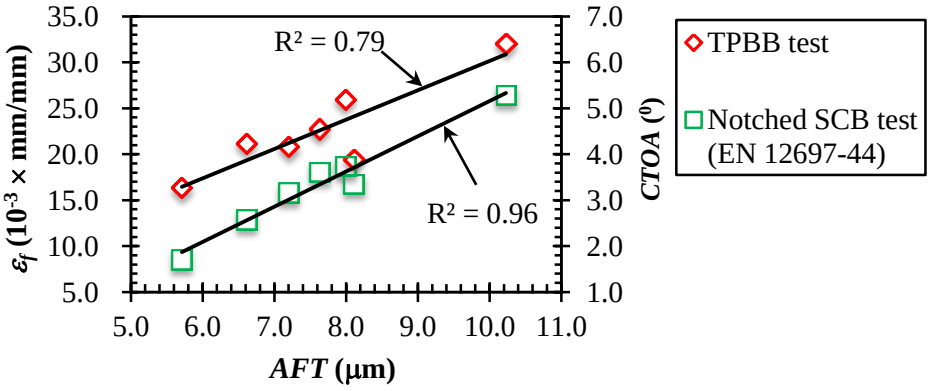

Figure 53. Relationships of *AFT* with ε_f of the TPBB test and *CTOA* of the notched SCB test

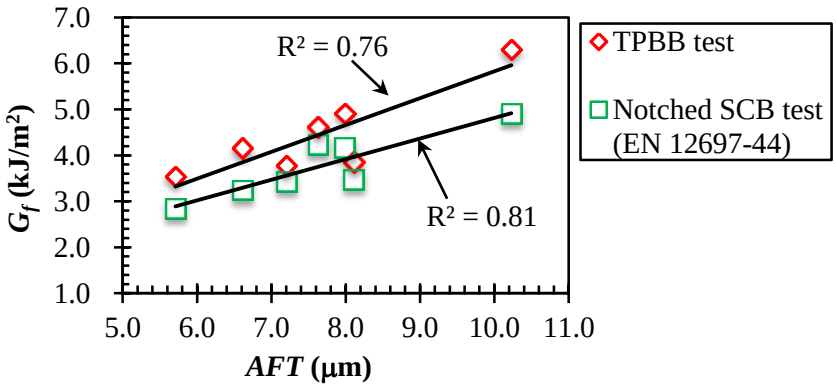

Figure 54. Relationships between *AFT* and G_f

The relationships between the asphalt binder parameters and the fracture characteristics of asphalt mixtures may be explained by the following: Increasing AC increases *AFT*, thereby increasing mixture viscosity, adhesion, and ductility [2]. High *AFT* may reduce the number of contact points between aggregate particles within the asphalt mixtures. As a result, the mixtures become softer and the aggregate particles are more easily moved or displaced when subjected to applied loads. Therefore, increasing AC can result in reductions in peak load (P_{ult}) and fracture toughness (σ_f and K_{Ic}). In addition, asphalt mixtures with increased viscoelasticity may increase the cracking propagation time before reaching failure [1, 2]. Therefore, asphalt mixtures with higher AC may have more protracted deformation at the crack tip and slower cracking propagation (ε_f and *CTOA*). Furthermore, slower deformation and cracking propagation may result in a larger area under the load-deformation curve [2], thereby leading to a higher G_f for HMA mixtures.

6.5. Summary

Based on the experiments presented in this chapter, the following conclusions are relevant:

- At a low service temperature, the cracking resistance parameters of the notched SCB test using the EN 12697-44 standard were most strongly correlated with those of the TPBB test using the JRA B005 standard. The experiments demonstrated that the notched SCB test using the EN 12697-44 standard provides a viable alternative to the TPBB test for evaluating the fracture characteristics of asphalt mixtures at intermediate temperatures.
- This study employed the *CTOA* parameter to assess the cracking propagation stage of HMA mixtures in the notched SCB test. *CTOA* from the notched SCB test was strongly associated with ε_f in the TPBB test. HMA mixtures with greater *CTOA* values also had higher ε_f values. *CTOA* is a potentially useful parameter for assessing the cracking propagation stage of asphalt mixtures.
- When the Marshall method is applied to design HMA mixtures, CMD_{area} may not be effective for evaluating the cracking resistance of these mixtures.
- There were strong correlations between the $CMD_{area-DASR}$ and the fracture toughness (σ_f and K_{Ic}) values calculated from the notched SCB and TPBB tests. Asphalt mixtures with higher $CMD_{area-DASR}$ values of aggregate gradations may have lower fracture toughness (σ_f and K_{Ic}).
- *AFT* is a candidate indicator of the effects of AC on the cracking performance of HMA mixtures. Increases in *AFT* reduced the fracture toughness (σ_f and K_{Ic}) values, but increased cracking propagation resistance (ε_f and *CTOA*) and G_f values.

References

[1] Haryanto, I., and Takahashi, O. Assessment of Indonesian wearing course mixtures using J integral and crack tip opening angle, International Journal of Pavement Engineering 9(3), pp. 165-176, 2008.

[2] Minhajuddin, M., Saha, G., and Biligiri K.P. Crack propagation parametric assessment of modified asphalt mixtures using linear elastic fracture mechanics approach, Journal of Testing and Evaluation 44 (1), pp. 471-483, 2006.

[3] Tran, N.T., and Takahashi, O. Improvement on aggregate gradation design and evaluation of rutting performance of Vietnamese wearing course mixtures, the 8th international conference on maintenance and rehabilitation of pavements, Singapore, pp. 212-221, 2016.

[4] Japan Road Association. Method of bending test for asphalt mixture, Standard practice for asphalt concrete mix design, 3 (B005), pp. 69-74, 2005.

[5] AASHTO Designation, TP 105-13. Determining the fracture energy of asphalt mixtures using the semicircular bend geometry (SCB). 2015

[6] AASHTO Designation, TP 124-16. Standard method of test for determining the fracture potential of asphalt mixtures using semicircular bend geometry (SCB) at intermediate temperature, 2016.

[7] The European Committee for Standardization, EN 12697-44:2010. Bituminous mixtures-Test methods for hot mix asphalt-Part 44: Crack propagation by semi-circular bending test, 2010.

[8] Lacroix, A., Kim, Y. R., and Arellano, C. Comparison of dynamic moduli for asphalt mixtures determined from different geometries and compactions, Journal of Testing and Evaluation 40 (6), 1-9, 2012.

[9] Aragão, F.T.S., and Kim, Y.-R. Mode I fracture characterization of bituminous paving mixtures at intermediate service temperatures, Experimental Mechanics, 52, 1423-1434, 2012.

[10] Nsengiyumva, G. Development of semi-circular bending (SCB) fracture test for bituminous mixtures, Master thesis, University of Nebraska, USA, 2015.

[11] Tran, N.T, and Takahashi, O. Effect of aggregate gradation on the cracking performance of wearing course mixtures, Construction and Building Materials 152, 520-528, 2017.

[12] Chun, S., Roque, R., and Zou, J. Effect of gradation characteristics on performance of Superpave mixtures in the field, Journal of the Transportation Research Board, 2294, 43-52, 2012.

[13] Christopher, W.J., et al. A manual for design of hot mix asphalt with commentary, Report NCHRP 673, Washington DC, 2011.

[14] Kim, S. et al. Porosity of the dominant aggregate size range to evaluate coarse aggregate structure of asphalt mixtures, Journal of Materials in Civil Engineering ASCE 21 (1), pp. 32-39, 2009.

[15] Chun, S., Roque, R., and Zou, J. Effect of gradation characteristics on performance of Superpave mixtures in the field, Journal of the Transportation Research Board 2294, pp. 43-52, 2012.

[16] Christensen, W. D. Jr., and Bonaquist, R. F. A Volumetric requirements for Superpave mix, Report NCHRP 567, Washington DC, 2006.

[17] Mohammad, L.N, Kim, M., and Elseifi, M. Characterization of asphalt mixture's fracture resistance using the Semi-Circular Bending (SCB) test, 7th RILEM International Conference on Cracking in Pavements, on 20-22 June 2013, Delft, The Netherlands, pp. 1-10, 2012.

[18] AASHTO Designation, TP 124-16. Standard method of test for determining the fracture potential of asphalt mixtures using semicircular bend geometry (SCB) at intermediate temperature, 2016.

[19] Vietnam Institute of Transport Science and Technology, 22TCN 211. Standard practice for asphalt pavements, 2016.

[20] AASHTO Designation, T-312. Standard method of test for preparing and determining the density of asphalt mixture specimens by means of the Superpave gyratory compactor, 2015.

[21] Stewart, C. M., Reyes, J. G., and Garcia, V. M. Comparison of fracture test standards for a Superpave dense-graded hot mix asphalt, Engineering Fracture Mechanics 169, 262-275, 2017.

[22] Martinelli, A., and Venzi, S. Tearing modulus, J integral, CTOA and crack profile shape obtained from the load-displacement curve only, Engineering Fracture Mechanics 53(2), 263-277, 1996.

[23] Harvey, J.A.F., and Cebon, D. Failure mechanisms in viscoelastic films, Journal of Materials Science 38 (5), 1021-1032, 2003.

[24] Saeidi, H., and Aghayan I. Investigating the effects of aging and loading rate on low-temperature cracking resistance of core-based asphalt samples using semi-circular bending test, Construction and Building Materials, 126, 682-690, 2016.

[25] Bjorn B., et al. Characterisation of asphalt mixture cracking behaviour using the three-point bending beam test, International Journal of Pavement Engineering, 12 (6), 569-578, 2011.

[26] Marasteanu, M. O., et al. Low temperature cracking of asphalt concrete pavement. Minnesota Department of Transportation, Report MN/RC-2004-23, 2004.

[27] Vietnam Institute of Transport Science and Technology, TCVN 8819. Specification for construction of hot mix asphalt concrete pavement and acceptance, 2011.

Chapter 7. Effect of aggregate gradation on the shear strength of asphalt mixtures

7.1. Introduction

The surface layer of asphalt pavements, i.e., the wearing course mixture, may be vulnerable to rutting at high service temperatures [1]. An increase in the traffic volume of heavy vehicles combined with high temperatures may increase the incidence of permanent deformation in wearing course mixtures. Therefore, the rutting resistance of asphalt mixtures has become one of the primary considerations in the mix design procedure. Previous studies have indicated that the shear strength of hot mix asphalt (HMA) mixtures is strongly associated with rutting performance of HMA mixtures [1-3]. In general, the viscosity of asphalt binder decreases with increasing temperatures. Consequently, asphalt mixtures become softer and aggregate particles are more easily shifted under repeated load applications, thereby inducing rutting [4]. It has been reported that HMA mixtures with higher shear strength may resist the applied loads more adequately, thereby decreasing the incidence of rutting in wearing course mixtures [1].

Recently, asphalt researchers have applied the Mohr-Coulomb theory to analyse shear strength properties of HMA mixtures [1, 3, 5, 6]. The Mohr-Coulomb theory characterizes the rutting performance of mixtures using the cohesion (C) and the internal friction angle (ϕ). In HMA mixtures, the C is related to the cementation of asphalt binder while the ϕ is associated with aggregate interlock [3, 6].

Previous studies also demonstrated that a compaction slope of a mixture (K) obtained from a Superpave gyratory compactor (SGC) can illustrate the ability of mineral aggregates in contributing to shear strength of the asphalt mixture at high temperatures [7, 8]. It has been reported that the K is markedly dependent on shape characteristics of aggregates, i.e. angularity and surface texture of aggregate particles [8]. On the other hand, the K is not associated with the content and the grade of asphalt binder [8].

Aggregate gradation significantly influences the internal friction property of HMA mixtures. When HMA mixtures have aggregate gradations that are closer to the maximum density line (MDL), the HMA mixtures show lower values of ϕ [3]. In addition, it has been reported that an increase in the sand content (SC) reduces the K values of HMA mixtures [2, 9]. Because the aggregate gradation has strong effects on the internal friction property of HMA mixtures, there is a need for an in-depth examination of the relationships of the aggregate gradation with the internal friction parameters (ϕ and K). However, there has been little discussion on the effects of aggregate gradation on the ϕ and the K of HMA mixtures.

In addition, to the best of our knowledge, no studies have previously investigated the relationship of aggregate gradation with the *C* of asphalt mixtures. The *C* is a function of asphalt binder, and the design asphalt content (AC) of HMA mixtures is strongly associated with the aggregate gradation. As a result, changes in aggregate gradation potentially affect the *C* of HMA mixtures through the asphalt binder component. Therefore, there is a need to conduct in-depth investigations that clarify the effects of aggregate gradation on the *C* of HMA mixtures.

The main objective of this study was to verify the effects of aggregate gradation on shear strength characteristics of HMA mixtures. In addition, this experimental study investigated the relationships of the shear strength properties with the rutting resistance of HMA mixtures. Seven HMA mixtures with a 12.5-mm NMPS were designed in accordance with the Marshall method. The unconfined compression (UC) test combined with the indirect tensile (IDT) test was performed to determine the *C* and ϕ values for those mixtures. In addition, the SGC was conducted to obtain *K* values for the seven wearing course mixtures. Rutting resistance of these mixtures was also evaluated using the wheel tracking test (WTT).

7.2. Literature review

7.2.1. Shear strength of HMA mixtures

Asphalt researchers have commonly conducted the triaxial test to determine *C* and ϕ of HMA mixtures [3, 5, 6]. However, the triaxial testing device is expensive, and the test procedure is complicated. Christensen *et al*. (2000) have proposed a combination of UC and IDT tests as an abbreviated protocol to calculate the *C* and the ϕ values [3]. It has been reported that this abbreviated protocol provides the *C* and ϕ estimates as good as or even better than those obtained from the triaxial test [3]. In this direction, the combination of UC and IDT tests has received increasing interest in assessing shear strength properties of HMA mixtures due to its simplicity [1, 3, 6, 10, 11]. Furthermore, it has been reported that the *C* property obtained from the abbreviated protocol had good relationships with rutting resistance of asphalt mixtures [1, 3]. Therefore, the combination of the UC and the IDT tests is a potential measure for evaluating both the shear strength and the rutting resistance of HMA mixtures. Figure 55 presents the combination of UC and IDT tests to determine Mohr-Coulomb parameters. *C* and ϕ values are calculated by the following equations [1, 3]:

$$\phi = \sin^{-1}\left(\frac{|\sigma_C| - 4|\sigma_T|}{|\sigma_C| - 2|\sigma_T|}\right) \tag{30}$$

$$C = \frac{(2 - \sin\phi) \times \sigma_T}{\cos\phi} \tag{31}$$

Where σ_T is the IDT strength; and σ_C is the uniaxial compressive strength.

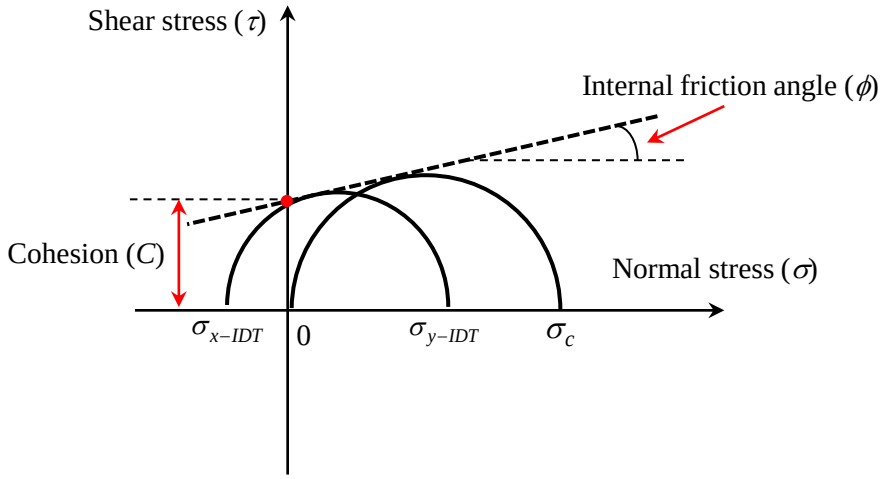

Figure 55. Mohr-Coulomb parameters using the UC and IDT tests [3]

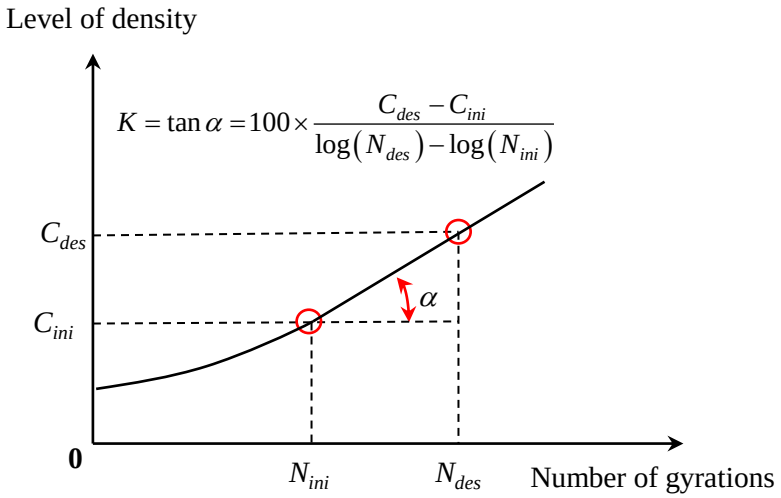

Figure 56. The determination of K

Previous studies also investigated the K obtained from the SGC data to evaluate the interaction among aggregate particles in HMA mixtures [7, 8]. The binder stiffness and the cohesion of HMA mixtures decrease with an increase in temperatures, thereby reducing the shear strength of mixtures [12]. At high temperatures, because asphalt binder apparently does not support any load and does not contribute to the mixture strength, aggregate interlock gradually plays a critical role in supporting the applied loads [7]. HMA mixtures with better interlocking of backbone aggregates generally have higher shear strength and better rutting resistance [1, 7, 8]. As shown in Figure 56, the following equation is used to determine the K value [7]:

$$K = 100 \times \frac{C_{des} - C_{ini}}{\log(N_{des}) - \log(N_{ini})} \quad (32)$$

Where, N_{des} and N_{ini} are the design and the initial number of gyrations, respectively; and C_{des} and C_{ini} are the level of density at N_{des} and N_{ini}, respectively.

7.2.2. Development of aggregate gradation parameters for the internal friction of HMA mixtures

It has been reported that the root-mean-square deviation between the aggregate gradation and the MDL (P_{rms}) has a significant influence on ϕ values of HMA mixtures [3]. The ϕ value of HMA mixtures tends to increase when the P_{rms} value of aggregate gradation increases [3]. Recent studies also investigated the fundamental role of aggregate gradation on voids in mineral aggregate (VMA) of HMA mixtures based on the concept of continuous maximum density (CMD) [13, 14]. An area of CMD, or CMD_{area}, was introduced to reflect the total deviation of aggregate gradation with the MDL [14]. The previous study found that the CMD_{area} is a potential parameter to provide information on a degree of the distance between the aggregate gradation and the MDL [14]. The determination of CMD_{area} was previously described in section 2.2.2.

In order to investigate the effects of the aggregate gradation on the ϕ property of HMA mixtures, this experimental study crucially compared the effects of P_{rms} and CMD_{area} on the ϕ of HMA mixtures. Even though the P_{rms} was introduced by the previous study [3], the discussion on the method for the determination of P_{rms} was not sufficient. Therefore, based on the concept of CMD, the present study proposed the following equation to calculate the P_{rms}:

$$P_{rms} = \sqrt{\frac{\sum_{0.075\text{-mm sieve}}^{NMPS} \left[P_{dev}(d_i)\right]^2}{n}} \quad (33)$$

Where, n is the number of sieves from the 0.075-mm sieve to the NMPS sieve.

A previous study reported that the sand fraction (the content of aggregates passing the 2.36-mm sieve) strongly influences the K of asphalt mixtures [2]. The mixtures with higher SC values generally show lower K values, resulting in poorer aggregate structures [2]. A previous study also noted that a high proportion of fine aggregate particles may interfere with the dense packing of the backbone aggregates [15]. Therefore, based on the concept of CMD, this study investigated a new aggregate gradation index that would describe the relationship between the aggregate gradation and the K of an asphalt mixture. This index was designated the "area of CMD for the sand fraction", or CMD_{sand}. The meaning of the

CMD_{sand} is also presented in Figure 57. This study hypothesized that the K of an asphalt mixture decreases with increasing values of CMD_{sand}. The CMD_{sand} is calculated as the following equation:

$$CMD_{sand} = \sum_{0.075\text{-mm sieve}}^{2.36\text{-mm sieve}} A_i \tag{34}$$

Where, A_i is the area between two contiguous sieve sizes (Figure 6).

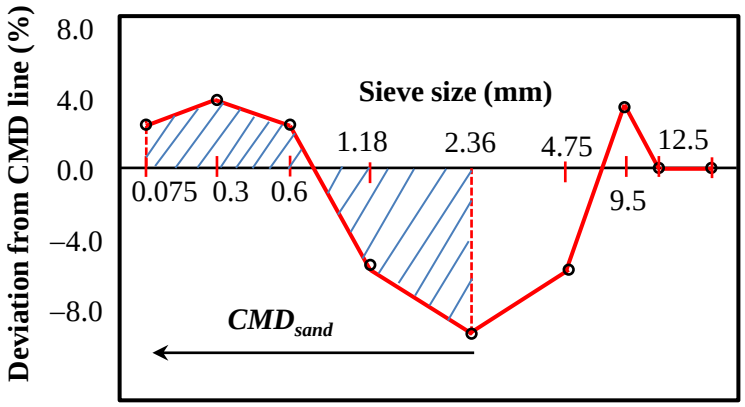

Figure 57. Meaning of CMD_{sand}

7.2.3. Application of aggregate gradation parameters for the cohesion of HMA mixtures

Aggregate gradation has a significant effect on the volumetric composition of asphalt mixtures, which in turn influences the C values of HMA mixtures. The previous studies showed that further distances between aggregate gradation and the MDL (or the higher values of the P_{rms} and the CMD_{area}) may lead to higher VMA values of HMA mixtures [13, 14, 16]. The VMA is subdivided into two components, namely, the effective asphalt content (V_{be}) and the air voids in mixture (VIM). The V_{be} presents the remaining volumetric composition of asphalt binder after aggregate surface voids absorb the asphalt binder. On the other hand, the VIM indicates the remaining air voids that exist within the asphalt binder and between aggregate particles in the mixtures [13]. The increase in VMA creates additional air voids within the aggregate structure, resulting in increasing the VIM. When an asphalt mixture has an excessively large quantity of air voids, fine aggregates and asphalt binder may be insufficient to fill these air voids. This can generate inadequate interaction among aggregate particles, thereby potentially disrupting the aggregate structure [15]. The previous study also noted that the increase in VIM can interfere with C properties of HMA mixtures [5]. In addition, the extra voids in aggregate structure can be occupied by increasing the proportion of asphalt binder in order to obtain the desired VIM. The increase in the proportion of asphalt binder generally reduces the C of mixtures at high temperatures [5, 12].

Consequently, both V_{be} and *VIM* components of the *VMA* negatively affect the *C* of mixtures. Therefore, the present study posited that the P_{rms} and the CMD_{area} are potential parameters that indicate a negative effect on the *C* of HMA mixtures.

HMA mix design methods may influence the relationships of P_{rms} and CMD_{area} with the *C*. The Superpave and the Marshall are common methods for designing HMA mixtures. In the Superpave method, the *VIM* value is held constant at 4% [13]. Therefore, the increases in P_{rms} and CMD_{area} only increase the remaining component of the *VMA*, i.e., the V_{be}. This means that the P_{rms} and the CMD_{area} may affect the *C* of HMA mixtures through the V_{be} only. In contrast, in the Marshall method, the *VIM* value is designed within a range of 3-6% [13]. As a result, the relationships between the gradation parameters (P_{rms} and CMD_{area}) and the components of the *VMA* (*VIM* and V_{be}) become more complicated. These complicated relationships may reduce the correlations of P_{rms} and CMD_{area} with the *C*. Therefore, this experimental study also aimed to verify the effect of the Marshall method on the relationships of aggregate gradation parameters (P_{rms} and CMD_{area}) with the *C* of HMA mixtures.

7.2.4. Relationship between asphalt composition and cohesion of HMA mixtures

The proportion of asphalt binder significantly affects the *C* of HMA mixtures at high temperatures. It has been reported that viscosity of asphalt binder decreases with increasing temperatures, thereby reducing the binder stiffness and the *C* of HMA mixtures [4, 12]. As a result, an excessive asphalt binder may reduce shear strength and rutting resistance of HMA mixtures at high temperatures [12]. Although the quantity of asphalt binder is widely considered to be the most important factor that strongly influences the *C*, the relationship of AC with the *C* has not been well established yet. The previous study demonstrated that the design AC cannot be a potential index to evaluate the *C* property [1]. Therefore, the present study determined to investigate the effect of asphalt composition on the *C* property of asphalt mixtures using another parameter, namely, the apparent film thickness (*AFT*).

The AFT indicates an average thickness of asphalt binder that covers aggregate particles in HMA mixtures [13]. The idea of applying the *AFT* parameter to evaluate rutting performance of HMA mixtures was actively pursued by recent asphalt researchers [13, 14]. The determination of *AFT* for an asphalt mixture was previously presented in section 6.2.2.

7.3. Experimental work

7.3.1. Material sources and mixture design

The material preparation and mixture design were described in chapter 3. Table 33 also summaries the characteristics of seven aggregate gradations and the results of mixture design.

Table 33. Aggregate gradations and results of the Marshall mix design

	Blend / Sieve (mm)	1	2	3	4	5	6	7
Percentage passing (%) at standard sieves	19.00	100.0	100.0	100.0	100.0	100.0	100.0	100.0
	12.50	99.7	99.7	99.8	99.8	99.7	99.9	99.9
	9.50	76.6	79.0	81.4	85.2	76.5	91.7	95.1
	4.75	52.0	55.1	59.5	47.6	47.0	75.5	82.4
	2.36	33.9	38.4	42.4	25.5	28.9	59.3	66.3
	1.18	25.7	28.8	31.2	20.5	22.4	43.2	48.0
	0.60	16.5	18.9	20.0	15.0	15.2	26.0	27.8
	0.30	11.2	11.8	12.7	10.6	10.2	14.8	15.7
	0.15	8.4	9.0	10.0	8.2	7.6	10.2	10.2
	0.075	7.0	7.6	8.6	6.9	6.2	8.1	8.0
Mixture	Design AC (%)	4.75	4.70	4.60	6.00	4.70	6.00	6.35
	VIM (%)	5.3	4.1	4.0	4.0	5.5	4.2	4.3
	V_{be} (%)	8.6	8.6	8.2	11.6	8.7	11.1	11.7
	VMA (%)	14.0	12.7	12.2	15.6	14.3	15.3	16.1

7.3.2. Indirect tensile strength test method

SGC samples with a dimension of 150 × 115 mm were prepared for the IDT test. The SGC sample preparation is based on the protocol outlined in the AASHTO T-312 standard [17]. At the design AC, the number of N_{des} and mass of the SGC sample were determined to obtain desired air voids, which were the same as the results obtained from the Marshall method. Two thinner specimens, as shown in Figure 58, were trimmed from the SGC sample. The thickness of testing specimens was 50 mm in accordance with the AASHTO T322-07 standard [18].

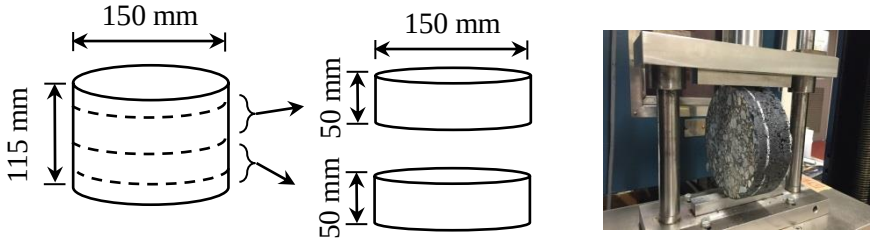

Figure 58. The IDT specimen preparation and test

The IDT test should be performed at a relatively slow deformation rate and an appropriate temperature to be approximately equal to the traffic loads and temperature conditions that can cause rutting to form [3, 11]. Therefore, this study conducted the IDT test at a temperature of 30 °C, which should be 20 °C lower than the highest average pavement temperature (50 °C for the southern region of Vietnam) [3, 11, 19]. The present study also performed the IDT test at a deformation rate of 3 mm/min. In order to determine the shear strength properties, the previous study conducted the IDT test at a deformation rate of 3.75 mm/min for SGC specimens with a dimension of 150 × 100 mm [3]. The deformation rate used in our study was slightly lower than that conducted by the past study, because the thickness of IDT specimens in our experiment was smaller than that used in the previous study. Before starting the test, the specimens were maintained in an environmental chamber at the same testing temperature for 15 hours. The curing time should be at least 12 hours [20]. The IDT strength (σ_T) is calculated using the following equation [18]:

$$\sigma_T = \frac{2P_{ult}}{\pi Dt} \tag{35}$$

Where, P_{ult} is the maximum force; D is the diameter of the specimen; and t is the thickness of the specimen.

7.3.3. Unconfined compression test method

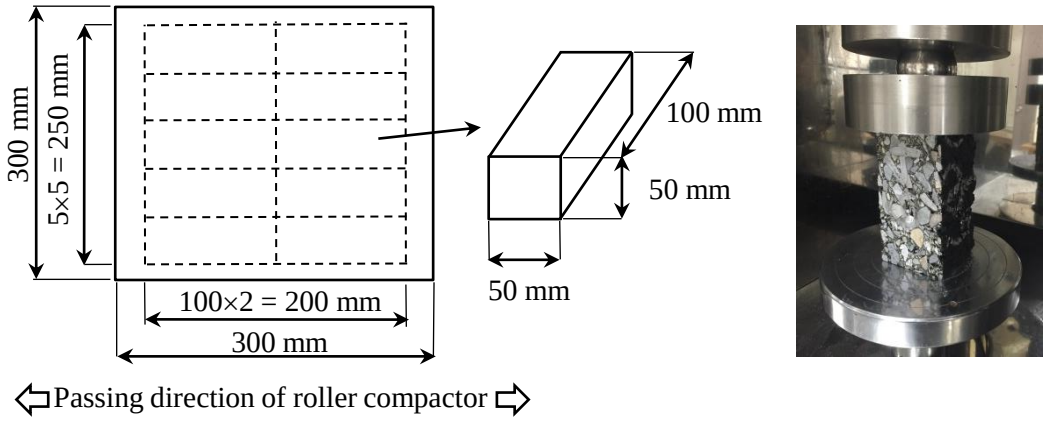

Figure 59. The compression specimen preparation and test

The present study conducted the UC test using prismatic specimens. In order to prepare the prismatic specimens, slab-shaped samples with a dimension of 300 × 300 × 50 mm were compacted using a laboratory steel roller compactor. At the design AC, the passing number for compaction was also determined as the appropriate number of passes, where the slab samples have the similar air voids as

samples fabricated by the Marshall compactor [21]. Next, the compacted slab-shaped samples were cut into prismatic specimens with a dimension of 100 × 50 × 50 mm as shown in Figure 59. In the UC test, the ratio of height to diameter for the specimens should be equal to 2.0 in order to obtain reliable strength values [20]. Therefore, this experimental study prepared the dimension of the testing specimens based on this suggestion.

The present study conducted the UC test at a deformation rate of 5 mm/min and a testing temperature of 30 °C. In order to assess the shear strength properties, the previous study conducted the UC test at a deformation rate of 7.5 mm/min using SGC specimens with dimensions of 70 × 140 mm and 150 × 150 mm [3]. The slightly lower deformation rate for the specimens used in our study was due to their smaller dimension. Prior to the test, the specimens were also placed in an environmental chamber at the testing temperature for 15 hours to make conditioning for the mixtures sufficiently. The following equation is applied to calculate the compression strength (σ_C):

$$\sigma_C = \frac{P_{ult}}{A} \tag{36}$$

Where, A is the cross-session area of the specimen.

7.3.4. Wheel tracking test method

The WTT was conducted to characterize the resistance of the HMA mixtures to permanent deformation under high temperatures. Slab-shaped samples having a dimension of 300 × 300 × 50 mm were prepared for the WTT in accordance with the JRA-B003 standard. The slab sample was also prepared to have similar air voids as samples fabricated by the Marshall compactor. Note that this chapter presents the slab sample preparation for the WTT that is different from chapter 4, which applied the same compaction energy (a constant passing number of 25 times) for all mixtures to evaluate the workability of the HMA mixtures. The WTT results of Blends 2 and 3 were obtained from chapter 4 because the differences in air voids of the slab samples and the Marshall samples were lower than 1%. On the other hand, the WTT for other blends was conducted again. A dynamic stability (*DS*) parameter was also determined to evaluate the rutting susceptibility of the HMA mixtures under the wheel-load.

7.4. Results and discussion

7.4.1. Results of shear strength parameters

Table 34 and Table 35 show the estimations of σ_C and σ_T for each mix type, respectively. The σ_C and the σ_T were determined with four replicates for seven asphalt mixtures. The accuracy and

repeatability of these parameters were evaluated using the coefficient of variation (COV), which empirically requires a maximum value of 15% [22]. The experiments indicated that both σ_C and σ_T obtained from the UC and IDT tests exhibited low COV values across a wide range of asphalt mixtures, demonstrating that the tests conducted in this experimental study have a high repeatability for evaluating the tensile and compressive strength of HMA mixtures.

Table 34. σ_C determination of seven asphalt mixtures

Mixture		Rep_1	Rep_2	Rep_3	Rep_4	Average (kPa)	COV (%)
Dense-graded	1	1137	1095	1049	1037	1080	4.2
	2	1262	1226	1256	1249	1248	1.3
	3	1330	1477	1363	1312	1371	5.4
Coarse-graded	4	804	913	820	836	843	5.7
	5	1014	952	943	920	957	4.2
Fine-graded	6	1047	1040	1035	1031	1038	0.7
	7	955	934	961	946	949	1.2

Table 35. σ_T determination of seven asphalt mixtures

Mixture		Rep_1	Rep_2	Rep_3	Rep_4	Average (kPa)	COV (%)
Dense-graded	1	161	164	164	166	164	1.4
	2	190	199	189	197	194	2.5
	3	206	221	197	223	212	5.9
Coarse-graded	4	115	105	104	110	108	4.8
	5	138	141	135	155	142	6.1
Fine-graded	6	140	149	154	143	147	4.0
	7	123	133	125	127	127	3.5

The values of shear strength parameters for seven HMA mixtures are summarized in Table 36. The results indicated that the *C* values of the dense-graded mixtures were higher than the *C* values of the coarse- and fine-graded mixtures, and this tendency was in direct contrast to the ϕ values. These results corroborated the findings reported by the previous study [9]. In addition, a range ratio of *C* to σ_T from 1.74 to 1.78 was found in our experiments. These values were consistent with those of previous studies, which reported that adequate ratios of *C* to σ_T ranged from 1.73 to 1.75 [3, 6]. The above experimental results also demonstrated that both the relatively low deformation rate and the moderate testing temperature performed in our study were appropriate to assess the shear strength of HMA mixtures.

Table 36. Shear strength properties the HMA mixtures

Mixture		σ_C (kPa)	σ_T (kPa)	C (kPa)	ϕ (°)	C/σ_T	K
Dense-graded	1	1080	164	285	34.3	1.74	7.96
	2	1248	194	337	33.3	1.74	7.59
	3	1371	212	368	33.5	1.74	7.86
Coarse-graded	4	843	108	192	41.0	1.78	7.96
	5	957	142	247	35.3	1.74	7.99
Fine-graded	6	1038	147	258	37.2	1.75	7.21
	7	949	127	224	39.4	1.77	6.72

Table 36 also shows *K* values of the seven mixtures. The *K* values were obtained from duplicate samples for each mixture, and the average values were calculated. The experiments showed that the *K* values ranged from 6.73 to 7.99. The results also corroborated findings from the previous study, which noted that the *K* values for 12.5-mm NMPS mixtures were from 6.14 to 8.84 [7]. Furthermore, the *K* values of the coarse-graded mixtures were found to be higher than the *K* values of the dense- and fine-graded mixtures. This finding was also consistent with the result that has been reported in the previous study [7].

7.4.2. Effect of aggregate gradation on the internal friction of HMA mixtures

Table 37 shows the values of aggregate gradation parameters and the *AFT* for each mixture, and Table 38 presents the *DS* values of the WTT. Table 39 also presents the coefficient of determination **(**R^2) matrix and the Pearson correlation coefficient (PCC) matrix of all parameters. The positive PCC values of P_{rms} and CMD_{area} with ϕ were obtained, indicating that the ϕ value of the HMA mixtures increased when the P_{rms} and the CMD_{area} of the aggregate gradation increased (P_{rms}: PCC = 0.806 and CMD_{area}: PCC = 0.856). This means that when aggregate gradation of an asphalt mixture is close to the MDL, the ϕ property of the asphalt mixture has a low value, which was also reported by the previous study [3]. In addition, the results shown in Table 39 demonstrated that the CMD_{area} is more proper than the P_{rms} to reflect the effect of aggregate gradation on the ϕ property of asphalt mixtures (P_{rms}: R^2 = 0.650 and CMD_{area}: R^2 = 0.733).

Table 37. Aggregate gradation parameters and *AFT* of the HMA mixtures

Mixture		P_{rms}	CMD_{area}	SC (%)	CMD_{sand}	*AFT* (μm)
Dense-graded	1	4.40	5.91	33.9	1.63	7.20
	2	3.40	4.63	38.4	1.63	6.61
	3	2.63	3.43	42.4	1.82	5.71
Coarse-graded	4	5.94	8.29	25.5	1.78	10.23
	5	5.26	7.42	28.9	1.44	8.11
Fine-graded	6	3.96	7.01	59.3	3.83	7.63
	7	5.62	9.79	66.3	4.98	7.99

Table 38. Results of wheel tracking test

Mixture			Air voids (%)	d_{45} (mm)	d_{60} (mm)	*DS* (cycles/mm)	Average of *DS* (cycles/mm)
Dense -graded	1	Rep_1	5.4	4.75	5.48	863	863
		Rep_2	5.1	4.94	5.67	863	
	2	Rep_1	5.4	4.15	4.65	1260	1130
		Rep_2	4.3	3.96	4.59	1000	
	3	Rep_1	4.4	3.47	4.07	1050	1168
		Rep_2	4.6	4.05	4.54	1286	
Coarse - graded	4	Rep_1	4.1	7.98	9.91	326	435
		Rep_2	4.3	6.36	7.52	543	
	5	Rep_1	5.6	5.62	6.56	670	670
		Rep_2	5.6	6.40	7.34	670	
Fine - graded	6	Rep_1	4.1	10.02	11.8	354	342
		Rep_2	3.9	10.20	12.11	330	
	7	Rep_1	4.4	13.83	15.98	293	293
		Rep_2	4.6	12.29	14.44	293	

Table 39 also shows relationships of SC and CMD_{sand} with *K* for the seven HMA mixtures. The negative PCC values, as the authors' expectations, indicated that HMA mixtures with higher values of the SC and the CMD_{sand} had lower values of the *K*. Both correlation coefficients of SC and CMD_{sand} with *K* were high, and the *K* has a slightly stronger association with the CMD_{sand} than with the SC (SC: R^2 = 0.887 and CMD_{sand}: R^2 = 0.916). This result may be explained by the following reason. While the SC value is analysed at one sieve (2.36-mm sieve) only, the CMD_{sand} value is calculated at six sieves (from

0.075-mm to 2.36-mm sieves) for the fine aggregate. The previous study has recommended that the 1.18-mm sieve is the smallest sieve size for the fine aggregate particles that potentially disrupt the coarse aggregate structure [15]. A recent analysis also suggested 0.6 mm as the smallest sieve size for a 12.5-mm NMPS aggregate gradation to evaluate the effects of fine aggregate on the coarse aggregate skeleton [14]. It has been reported that an excessively large quantity of fine aggregates at the 0.6-mm and the 1.18-mm sieves may interfere with the interlocking of the coarse aggregates [14, 15]. Therefore, this may account for the higher correlation coefficient obtained between the *K* and the CMD_{sand} relative to that obtained between the *K* and the SC.

7.4.3. Effect of the asphalt composition on the cohesion of HMA mixtures

Table 39 summaries the linear relationships of all asphalt binder parameters (i.e., V_{be}, design AC, and *AFT*) with *C* values of the seven HMA mixtures. The experiments demonstrated that all asphalt binder parameters negatively affect the *C* of asphalt mixtures. The low correlation coefficient between the design AC and the *C* (R^2 = 0.554) was consistent with the experimental results from the previous study [1]. The results also highlighted that among the three asphalt binder parameters, the *AFT* has promising applications to address the effect of the asphalt composition on the *C* property of HMA mixtures (R^2 = 0.876).

The high relationships between the *AFT* and the *C* may be explained by the following reason. Because the viscosity of asphalt binder decreases with increasing temperatures, asphalt binder tends to flow through aggregate particles under the applied loads at high temperatures [4]. When the *AFT* that coats the aggregate particles is excessively thick, there is a reduction in the points of contact among the aggregate particles. Therefore, this may lead to a weaker aggregate interlock and the mixtures become softer. As a result, the aggregate particles are more easily moved or displaced under load applications, thereby reducing the peak load at failure and the σ_T in the IDT test. The analysis presented in Table 39 also found a high correlation coefficient between the *AFT* and the σ_T (R^2 = 0.876). As described in section 7.4.1, the σ_T is strongly correlated with the *C* property of HMA mixtures. Therefore, HMA mixtures with greater *AFT* values may have lower *C* values.

Table 39. Coefficient of determination matrix (above main diagonal) and Person correlation matrix (below main diagonal) of all parameters

	P_{rms}	CMD_{area}	SC	CMD_{sand}	*VMA*	*VIM*	V_{be}	*AC*	*AFT*	σ_C	σ_T	*C*	ϕ	*K*
P_{rms}	1	0.845	0.011	0.062	0.711	0.075	0.440	0.355	0.803	0.925	0.903	0.908	0.650	0.017
CMD_{area}	0.919	1	0.082	0.362	0.918	0.016	0.687	0.646	0.604	0.835	0.876	0.874	0.733	0.241
SC	-0.105	0.287	1	0.870	0.120	0.118	0.207	0.319	0.068	0.004	0.000	0.000	0.036	0.887
CMD_{sand}	0.249	0.602	0.933	1	0.423	0.092	0.517	0.638	0.008	0.078	0.136	0.130	0.262	0.916
VMA	0.843	0.958	0.347	0.650	1	0.001	0.830	0.796	0.618	0.817	0.885	0.880	0.806	0.252
VIM	0.273	0.125	-0.344	-0.304	0.025	1	0.151	0.171	0.001	0.066	0.017	0.021	0.080	0.130
V_{be}	0.663	0.829	0.455	0.719	0.911	-0.389	1	0.982	0.514	0.531	0.663	0.648	0.893	0.365
AC	0.596	0.804	0.565	0.799	0.892	-0.413	0.991	1	0.389	0.437	0.569	0.554	0.817	0.477
AFT	0.896	0.777	-0.261	0.092	0.786	0.025	0.717	0.624	1	0.865	0.876	0.876	0.750	0.002
σ_C	-0.962	-0.914	0.067	-0.280	-0.904	-0.256	-0.729	-0.661	-0.930	1	0.980	0.984	0.691	0.019
σ_T	-0.950	-0.936	-0.019	-0.369	-0.941	-0.131	-0.814	-0.754	-0.936	0.990	1	1.000	0.812	0.048
C	-0.953	-0.935	-0.011	-0.361	-0.938	-0.146	-0.805	-0.744	-0.936	0.992	1.000	1	0.799	0.045
ϕ	0.806	0.856	0.189	0.512	0.898	-0.282	0.945	0.904	0.866	-0.831	-0.901	-0.894	1	0.134
K	-0.132	-0.491	-0.942	-0.957	-0.502	0.361	-0.604	-0.691	0.039	0.138	0.219	0.211	-0.366	1

7.4.4. Effect of aggregate gradation on the cohesion of HMA mixtures

The relationships of P_{rms} and CMD_{area} with C are shown in Table 39. The negative PPC values, as expected, showed that the C values of HMA mixtures decreased as the P_{rms} and the CMD_{area} values of aggregate gradation increased. The correlation coefficients of C were high for both parameters (P_{rms}: R^2 = 0.908 and CMD_{area}: R^2 = 0.874). The high correlation coefficients of P_{rms} and CMD_{area} with the C may be explained through the two components of the *VMA*, i.e., the V_{be} and the *VIM*. The results shown in Table 39 indicated that increases in P_{rms} and CMD_{area} of aggregate gradations increased *VMA* of HMA mixtures. As described in Table 33, the increase in *VMA* can result in the following four effects: (i) increase V_{be} only (e.g., Blends 3 and 4); (ii) increase *VIM* only (e.g., Blends 1 and 2); (iii) increase both V_{be} and *VIM* (e.g., Blends 3 and 5); and (iv) increase V_{be} but decrease *VIM* (e.g., Blends 1 and 4). As described in section 7.2.3 and as shown in Table 39, the V_{be} and the *VIM* negatively affect the C of HMA mixtures. As a result, the three effects from (i) to (iii) apparently lead to the reduction in the C of HMA mixtures. In addition, Table 39 indicates that the negative effect of *VIM* on the C was so small and then the V_{be} predominated in reflecting the effect of *VMA* on the C. Therefore, the increase in the V_{be} and the decrease in the *VIM* (the iv effect) may also reduce the C of HMA mixtures. The results of Blends 1 and 4 shown in Table 33 and Table 36 also confirmed the above finding. In Blends 1 and 4, the increase in *VMA* resulted in increasing the V_{be} and decreasing the *VIM*, but there was a reduction in the C.

The previous study reported good negative relationships of *VIM* with the C at four *VIM* levels with high deviations, i.e., 0%, 4%, 8%, and 12% [5]. However, our experiments demonstrated that when the Marshall method was applied to design HMA mixtures, the range of 3-6% for the *VIM* may be too small and insufficient to evaluate the negative effect of the *VIM* on the C. As a result, the Marshall method may not significantly influence the relationships of P_{rms} and CMD_{area} with the C.

The experiments also indicated that the C of HMA mixtures is more closely associated with the P_{rms} than with the CMD_{area}. This may be explained through the *AFT* of HMA mixtures. The results provided in Table 39 indicated that the *AFT* increased with increases in both P_{rms} and CMD_{area}, and the *AFT* had a stronger association with the P_{rms} than with the CMD_{area} (P_{rms}: R^2 = 0.803 and CMD_{area}: R^2 = 0.604). As described in section 7.4.3, the level of C provided by the asphalt binder is markedly dependent on the *AFT*. This may account for the relatively higher correlation coefficient of the P_{rms} with the C relative to that of the CMD_{area} with the C.

The low correlation coefficient between the CMD_{area} and the *AFT* can be explained by the mixture design method. The results shown in Table 39 indicated that the *VMA* of the HMA mixtures is more strongly associated with the CMD_{area} than with the P_{rms} (P_{rms}: R^2 = 0.711 and CMD_{area}: R^2 = 0.918). As mentioned above, because the Marshall method does not require a constant value of the *VIM*, the

CMD_{area} and the V_{be} are no longer perfectly correlated. This means that the increase in the CMD_{area} may not necessarily increase the V_{be} component of the *VMA* or the *AFT* of HMA mixtures. The results as shown in Table 37 also confirmed the above finding. The CMD_{area} value of Blend 7 was higher than the CMD_{area} values of Blends 4 and 5, whereas an opposite trend was observed for the *AFT* values.

7.4.5. Relationships of shear strength parameters with rutting resistance of HMA mixtures

Table 40 summarizes regression analyses of the shear strength parameters with the *DS*. Because the data includes seven mixtures only, the present study performed the regression analyses for understanding the relationships between the variables instead of precise predictions. Among all shear strength parameters, the relationship of *C* with *DS* had the highest correlation coefficient. The *DS* values of the HMA mixtures tended to increase as the *C* values of shear strength increased. However, contrary to the authors' expectations, the ϕ had a negative coefficient with the *DS*. The data as shown in Table 39 also highlighted that when the *C* values increased, the ϕ values decreased. The inverse relationship between the ϕ and the *C* obtained from the combination of UC and IDT tests also corroborated findings from the previous studies [1, 6, 11]. Therefore, this may account for the negative relationship of ϕ with *DS* obtained in the present study.

Table 40. Linear regression analysis of *DS* with shear strength properties

Model	Term	Coefficient	Se	*t* value	*p* value	R^2	R^2_{adj}
$DS \sim C$	Intercept	-733.96	325.29	-2.256	0.074	0.802	0.763
	C	5.25	1.17	4.505	0.006		
$DS \sim \phi$	Intercept	4522.95	967.86	4.673	0.005	0.758	0.710
	ϕ	-105.35	26.59	-3.961	0.011		
$DS \sim K$	Intercept	-2372.10	2166.50	-1.095	0.323	0.288	0.145
	K	403.60	284.10	1.420	0.215		
$DS \sim C+\phi$	Intercept	1298.37	2721.80	0.477	0.658	0.827	0.740
	C	3.42	2.72	1.258	0.277		
	ϕ	-42.24	56.13	-0.753	0.494		
$DS \sim C+K$	Intercept	-2692.59	769.45	-3.499	0.025	0.929	0.893
	C	4.80	0.80	5.986	0.004		
	K	273.41	102.97	2.655	0.057		

Note: Se is standard error.

The positive coefficient of *K* with *DS*, as expected, indicated that the *DS* values increased with increasing *K* value. However, the correlation coefficient of *K* with *DS* was low. Our experiments also confirmed the results in the previous study, which noted that the *K* alone is unable to ensure high rutting resistance of HMA mixtures [7].

The results highlighted that the *C* is a better indicator of the rutting resistance than the ϕ and the *K*. These results may be explained by the following reasons. First, the present study used an aggregate source with a high quality of shape and surface texture. The results shown in Table 36 indicated that most of the ϕ values had relatively good levels, which should be at least 35° [3]. As mentioned above, at high temperatures, rutting resistance of HMA mixtures is significantly sensitive to both aggregate interlock and the *AFT* [1, 3, 4]. When an aggregate source has a high quality, the *AFT* may be a dominant factor that negatively influences the rutting resistance of HMA mixtures. As described in section 7.4.3, the level of *C* provided by the asphalt binder also has a strong relationship with the *AFT*. Therefore, the rutting resistance of HMA mixtures is more closely associated with the *C* than with the ϕ and the *K*. Next, in a field rutting rate at construction sites, pressures of truck tires may create high tensile stresses in the asphalt surface layers, thereby inducing the combination of high shear stresses and low levels of confinement within the pavement structure [3]. This critical condition may lead wearing course mixtures to exhibit rutting at high temperatures [3]. The IDT test also induces the above stress condition when the test is performed at a reasonably low deformation rate and an adjusted testing temperature [3]. As mentioned in section 7.4.1, the IDT strength is strongly associated with the *C* property of HMA mixtures. Therefore, this may account for the strong relationship between the *C* and the rutting resistance of HMA mixtures.

The regression analyses also indicated that the model using *C* and *K* had a better goodness of fit than the model using *C* and ϕ to predict the rutting resistance of HMA mixtures (*C* and *K*: $R^2 = 0.929$; and *C* and ϕ : $R^2 = 0.827$). In addition, the standard error for independent variables illustrated that the precision in the former model was higher than that in the latter model. As shown in Table 39, while the *C* had a low correlation with the *K*, the *C* showed a strong relationship with the ϕ. This can lead to an effect of multicollinearity, thereby increasing the standard error of independent variables and reducing the precision in the model using *C* and ϕ.

In order to estimate rutting resistance of HMA mixtures, the previous studies performed statistical analyses using the IDT strength, the *VMA*, and the *K* [8, 23]. In their analytical models, the IDT strength presented the cohesion while the *K* indicated the internal friction of HMA mixtures [8, 23]. As a result, these analytical models had promising applications for evaluating the rutting resistance of HMA mixtures [8, 23]. Therefore, the good analytical model using the *C* and the *K* obtained in our study was consistent with the results from the previous analyses.

The analytical model also indicated that the *K* obtained from the SGC data tended to be more adequate indicator of aggregate interlock than the ϕ obtained from the combination of UC and IDT tests. This may be explained by the following reasons. First, it has been reported that the internal friction of HMA mixtures increases with an increase in the content of coarse aggregate [3]. This means that the internal friction values of fine-graded mixtures (Blends 6 and 7) should be lower than the internal friction values of the coarse- and dense-graded mixtures (Blends 1 to 5). As shown in Table 36, the *K* is more appropriate than the ϕ to reflect this trend. Next, as described in section 7.4.2, the ϕ calculated from the combination of UC and IDT tests is substantially dependent on the distance between the aggregate gradation and the MDL [3]. In general, the coarse-graded mixtures have aggregate gradations that fall below the MDL, whereas the fine-graded mixtures have aggregate gradations that fall above the MDL [13]. As a result, when aggregate gradations of the coarse-, and fine-graded mixtures have higher distances with the MDL, these mixtures may simultaneously have greater values of ϕ. Therefore, the ϕ value obtained from the combination of UC and IDT tests may not be sensitive to the coarse aggregate content. As shown in Table 36, the experiments demonstrated that both the coarse-, and fine-graded mixtures had high values of ϕ. However, there were significant differences in the coarse aggregate contents for these mixtures, and the rutting resistance of these mixtures was not as great as expected for the high ϕ values.

7.5. Summary

The findings of the present study can be summarized as follows:

- The combination of UC and IDT tests conducted in the present study has a potential application for assessing the shear strength properties (*C* and ϕ) of wearing course mixtures.
- The experimental results showed that the distance between the aggregate gradation and the MDL markedly affects the ϕ value of HMA mixtures. The ϕ value tended to increase with increases in CMD_{area} and P_{rms}. In addition, the CMD_{area} indicates a more adequate parameter than the P_{rms} to evaluate the effect of aggregate gradation on the ϕ of HMA mixtures.
- The fine aggregate has a substantial effect on the *K* of HMA mixtures. The *K* was found to decrease with increases in SC and CMD_{sand}. The experiments also demonstrated that the *K* is more strongly associated with the CMD_{sand} than with the SC.
- The *AFT* indicates a more appropriate parameter than the design AC and the V_{be} to provide information on the effect of the asphalt composition on the *C* of HMA mixtures. An asphalt mixture with a higher *AFT* value may have a lower *C* value.
- The analysis found that the P_{rms} and the CMD_{area} of aggregate gradations produce significant

influences on the *C* of HMA mixtures. The higher P_{rms} and CMD_{area} values strongly accelerate the reduction in the *C* values.

- The analytical model using *C* and *K* has a potential application to evaluate the rutting resistance of wearing course mixtures. In addition, the *K* indicates a more proper parameter than the ϕ to address the effect of aggregate interlock on the rutting performance of HMA mixtures.

References

[1] Haryanto, I., and Takahashi, O. A rutting potential assessment using shear strength properties for Indonesian wearing course asphalt mixtures, International Journal of Pavements, 6 (1-2-3), 27-38, 2007.

[2] Mc Gennis, R. Evaluation of materials from Northeast Texas using Superpave mix design technology, Transportation Research Board 1538, 98-105, 1997.

[3] Christensen, D.W, Bonaquist, R., and Jack, D. P. Evaluation of triaxial strength as a simple test for asphalt concrete rut resistance. FHWAPA-2000-010+97-04(19), Final Report, PTI 2K26, 2000.

[4] Christensen, W. D. Jr., and Bonaquist, R. F. A. Volumetric requirements for Superpave mix, Report NCHRP 567, Washington DC, 2006.

[5] Pellinen, T.K., Song, J., and Xiao, S. Characterization of hot mix asphalt with varying air voids content using triaxial shear strength test, Proceeding 8th Conference Asphalt Pavement for Southern Africa, Sun City, South Africa, 2004.

[6] Xiao, S. Investigation of performance parameters for hot-mix asphalt, PhD Thesis, Purdue University, West Lafayette Indiana, 2006.

[7] Anderson, R. M. et al. Relationship of Superpave gyratory compaction properties to HMA rutting behaviour. National Research Council, Washington, D.C, NCHRP Report 478, 2002.

[8] Anderson, R.M., Christensen, W. D., and Bonaquist, R. Estimating the rutting potential of asphalt mixtures using Superpave gyratory compaction properties and indirect tensile strength, Journal of Association of Asphalt Paving Technologists, 72, 1-26, 2003.

[9] Lei, Z., Zheren, W., and Yinping, D. Internal structure characterization of HMA using different compaction method, The 6th International Conference on Road and Airfield Pavement Technology, Sapporo, Japan, 129-135, 2008.

[10] Christensen, D. W., and Bonaquist R. Use of strength tests for evaluating the rut resistance of asphalt concrete, Journal of the Association of Asphalt Paving Technologists, 71, 692-711, 2002.

[11] Christensen, D.W., *et al*. Indirect tension strength as a simple performance test. New simple performance tests for asphalt mixes, Report E–C068, Washington DC, pp. 44-57, 2004.

[12] Wang, H., Liu, X., and Hao, P. Evaluating the shear resistance of hot mix asphalt by the direct

shear test, Journal of Testing and Evaluation 36 (6), 485-491, 2008.

[13] Christopher, W.J., et al. A manual for design of hot mix asphalt with commentary, Report NCHRP 673, Washington DC, 2011.

[14] Tran, N.T., and Takahashi, O. Improvement on aggregate gradation design and evaluation of rutting performance of Vietnamese wearing course mixtures, the 8th international conference on maintenance and rehabilitation of pavements, Singapore, pp. 212-221, 2016.

[15] Chun, S., Roque, R., and Zou, J. Effect of gradation characteristics on performance of Superpave mixtures in the field, Journal of the Transportation Research Board, 2294, 43-52, 2012.

[16] Anderson, R.M., and Bahia, H. Evaluation and selection of aggregate gradations for asphalt mixtures using Superpave, Journal of the Transportation Research Board, 1583, 91-97, 1997.

[17] AASHTO Designation, T 312. Preparing hot-mix asphalt (HMA) specimens by means of the Superpave gyratory compactor, 2015.

[18] AASHTO Designation, T 322. Standard method of test for determining the creep compliance and strength of hot-mix asphalt (HMA) using the indirect tensile test device, 2007.

[19] Nguyen, T. N., and Tran, V. T. Temperature distribution in asphalt pavement at the south area of vietnam, Journal of Vietnamese Transportation, 12, 30-31, 2015.

[20] Erkens, S.M.J.G. Asphalt concrete response (ACRe): Determination, modelling and prediction. PhD thesis, Technical University Delft, Netherlands, 2002.

[21] Japan Road Association, JRA-B003. Method of wheel tracking test, Standard Practice for Asphalt Concrete Mix Design (3), pp. 39-55, 2005.

[22] Stewart, C. M., Reyes, J. G., and Garcia, V. M. Comparison of fracture test standards for a Superpave dense-graded hot mix asphalt, Engineering Fracture Mechanics 169, 262-275, 2017.

[23] Zaniewski, J.P., and Srinivasan, G. Evaluation of indirect tensile strength to identify asphalt concrete rutting potential, Asphalt Technology Program, Department of Civil and Environmental Engineering, West Virginia University, Washington, 2004.

Chapter 8. Use of compression test, circle shear test, and indirect tensile test for rutting potential assessment of wearing course mixtures

8.1. Introduction

Wearing course mixtures, which are surface layer materials used in asphalt pavements, are directly susceptible to the effects of traffic volume and weather conditions. Accordingly, insufficient shear strength in these mixtures increases the risk of rutting when exposed to repeated heavy loads at high temperatures [1]. The rutting susceptibility of hot mix asphalt (HMA) mixtures is generally evaluated using specialized devices, such as the asphalt pavement analyzer (APA), the Hamburg wheel tracking device, and the Japanese wheel tracking test (WTT) device [1, 2]. Dynamic stability (*DS*) values of the WTT are used as a standardized parameter for assessing the rutting potential of HMA mixtures in Japan [1, 3]. However, these devices are expensive and not commonly available in developing countries such as Vietnam and Indonesia. These developing countries have continued to use the Marshall method to design HMA mixtures. Their design standards specify requirements for volumetric and Marshall properties, but do not stipulate the need for any empirical testing to ensure sufficient resistance of HMA mixtures to permanent deformation. However, the specified volumetric properties alone are unable to ensure high rutting resistance [1, 3].

Historically, pavement engineers have characterized rutting resistance of HMA mixtures using the Mohr-Coulomb theory [4-9]. Based on the Mohr-Coulomb theory, two parameters, i.e., the cohesion (C) and the internal friction angle (ϕ), are introduced to analyse the rutting performance of asphalt mixtures. It is regarded that the C indicates the function of asphalt binder, while the ϕ illustrates the degree of aggregate interlock within HMA structures [4].

In general, the triaxial strength test has been performed to characterize the Mohr-Coulomb parameters. However, the triaxial devices are expensive and complicated to handle. Therefore, pavement researchers have been investigated other alternative tests to determine the shear strength properties. In order to estimate the C and the ϕ of asphalt mixtures, previous studies developed the following two methods: the combination of the unconfined compression (UC) and the indirect tensile (IDT) tests [4-6], and the combination of the UC and the circle shear (CS) tests [7-9]. However, to the best of our knowledge, even though the two methods have differences between both temperatures and deformation rates, the comparison of the shear strength properties of the two methods has not been discussed in detail.

Previous studies investigated the Mohr-Coulomb parameters using HMA specimens fabricated by the Superpave gyratory compactor (SGC) and the roller compactor [4-9]. In developing countries such as Indonesia and Vietnam, the mixture design procedure has followed the Marshall method [1, 3]. The Marshall compactor is still common equipment to fabricate HMA specimens. Therefore, it is difficult to prepare the SGC specimens in developing countries. A previous study conducted the UC test combined with the IDT test using the Marshall cylindrical specimens to evaluate the shear strength of HMA mixtures [3]. However, as far as the authors know, none of previous studies has investigated the combination of the UC and the CS tests using the Marshall specimens to determine the shear strength properties.

It has been reported that the sole IDT test has a potential application to measure the *C* of HMA mixtures [1, 4, 6]. Within the same quality of aggregates, the rutting resistance of HMA mixtures is heavily dependent on the level of cohesion provided by the asphalt binder [4]. Therefore, the cohesion of HMA mixtures is considered to be an important indicator of rutting resistance [4, 6]. This suggests that the IDT strength test can be applied not only to the investigation of HMA mixture cohesion, but also to the evaluation of rutting resistance [1, 4-6, 10-12]. Previous studies also examined the relationship between IDT strength and rutting resistance using specimens fabricated by the SGC [4-6, 10-12]. However, it is difficult to carry out IDT strength tests using SGC-compacted specimens in developing countries because the Marshall compactor is still the prevalent device used to fabricate HMA specimens.

The main objective of the present study was to compare the shear strength properties of seven asphalt mixtures with a 12.5-mm nominal maximum particle size (NMPS) using two different methods, i.e., the combination of the UC and the IDT tests, and the combination of the UC and the CS tests. The UC test combined with the CS test was performed with the Marshall cylindrical specimens to validate the shear strength parameters obtained from this protocol. The present study also aimed to evaluate the relationship between the IDT strength of the conventional Marshall specimen and the rutting resistance of thirteen wearing course mixtures using different fine aggregate sources.

8.2. Literature review

8.2.1. Protocols to determine shear strength of HMA mixtures

The triaxial strength test has been actively pursued by pavement researchers in order to evaluate shear strength of HMA mixtures [4, 5]. Shear strength of asphalt mixtures comprises the *C* and the ϕ to indicate the relationship between a normal (confining) stress and failure stress. When the normal stress is zero, the shear strength of HMA mixtures is equal to the *C* [4]. Characteristics of asphalt binder significantly influence the *C* value. It has been reported that the *C* decreases with the increase in asphalt

content at high temperatures [10]. An asphalt mixture having a higher asphalt dust ratio generally shows a higher C value [1]. On the other hand, the ϕ parameter is strongly dependent on aggregate characteristics. When HMA mixtures have high values of ϕ, an adequate interaction is developed among aggregate particles within the mixtures [1, 4]. As a result, aggregate interlock occurs more strongly and improves the resistance of mixtures to shear deformation more effectively [1].

Because the triaxial devices are expensive and complicated, Christensen *et al*. (2000) developed a procedure of the UC test combined with the IDT test as an abbreviated protocol to determine shear strength properties [4]. Previous studies showed that the C values of shear strength properties found using this abbreviated protocol had a good relationship with rutting performance of HMA mixtures [1, 4]. Therefore, the combination of the UC and the IDT tests has potential applications for addressing shear strength properties of HMA mixtures. The determinations of the C and the ϕ obtained from the combination of the UC and the IDT were previously described in section 7.2.1.

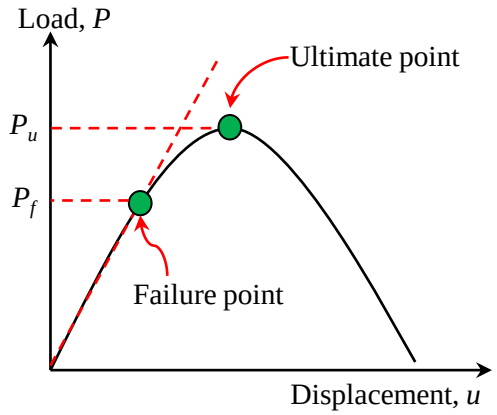

Figure 60. Meaning of P_f and P_u

Recently, the combination of the UC and the CS tests has been investigated to calculate the shear strength parameters [7-9]. Based on the relationship between load and displacement, this protocol has been specified for analysing shear strength properties of asphalt mixtures at two distinct stages [7]. The first stage is damage shear strength, which occurs when the relationship of the load with the displacement initially becomes nonlinear [7, 8]. The second stage for assessing shear strength is the ultimate damage shear strength, which occurs when the applied load increases to the failure limit [8]. In the load-displacement curve, the damage shear strength and the ultimate damage shear strength are, respectively, defined as the P_f and the P_u as shown in Figure 60. The shear strength parameters can be calculated by the following equations [4, 7, 8]:

$$\phi = \sin^{-1}\left(\frac{|\sigma_1| - |\sigma_3| + |\sigma_C|}{|\sigma_1| + |\sigma_3| + |\sigma_C|}\right) \quad (37)$$

$$C = \frac{(1 - \sin\phi) \times \sigma_C}{\cos\phi \times 2} \quad (38)$$

Where, σ_1 and σ_3 are the first and third principal stresses in the CS test, respectively.

Previous studies reported that to estimate the shear strength parameters, the combination of UC and IDT tests used the P_u [1, 4], whereas the combination of UC and CS tests applied the P_f [7-9]. In order to identify a clearer comparison between two different calculations, the present study calculated the shear strength of mixtures at both P_f and P_u for both methods.

8.2.2. Potential application of the IDT strength test to asphalt mixtures

Asphalt researchers have developed several empirical tests to accurately predict the performance of HMA mixtures. These empirical tests should not only elucidate the overall response of HMA mixtures to stress, but also shed light on the behavior of the individual components (i.e., the aggregate particles and asphalt binder) [12]. The IDT strength test was developed to investigate the relationship between the stress induced by these empirical tests and the stress experienced by field HMA mixtures [1, 4-6, 11-13]. In the IDT strength test, a cylindrical specimen is first subjected to vertical compression across its diameter [1]. Longitudinal and transverse tensions are then induced in the center of the specimen's face, which can cause structural failure when combined with vertical compression [4]. Previous studies have pointed out that the IDT strength test is able to assess fracture energy, as well as evaluate the stress and strain at failure in HMA mixtures [1, 4].

The IDT strength test is being increasingly applied to the evaluation of rutting resistance instead of cracking performance for HMA mixtures [1, 4, 6, 11-13]. However, the fundamental differences in failure mechanisms must be addressed before investigating the correlation between the IDT strength test and rutting resistance. Failure in the IDT test is typically caused by longitudinal and transverse tensions. In contrast, rutting in wearing course mixtures is caused by vertical compression or shear flow. The good relationship between the IDT strength test and the rutting resistance may be due to the following: First, the previous study indicated that the surface tensile stresses induced by truck tire pressures may create high shear stresses in combination with low levels of confinement in the pavement [4]. As a result, this condition has promoted rutting of the asphalt surface layers. The critical combination of high shear stresses and low levels of confinement also exists in the IDT strength test when the test is conducted at the relatively low deformation rate and moderate temperature [4]. Next, the relationship of the IDT strength test with the rutting resistance may be explained through the mixture cohesion. Both the cohesion

and the internal friction angle are important determinants of shear strength, which provides stability to oppose the plastic deformation generated by high traffic volume of heavy vehicles [1, 4]. However, the correlation between cohesion and rutting resistance was found to be generally stronger than the correlation between the internal friction angle and rutting resistance [1, 4]. This suggests that cohesion may be a better indicator of rutting resistance than the internal friction angle. Previous studies have also indicated that mixture cohesion can be accurately calculated using IDT strength (represented by the σ_T) [4, 6]. Figure 61 shows a combination of the unconfined compression test and the IDT strength test to determine Mohr-Coulomb parameters. $\sigma_{x\text{-}IDT}$ and $\sigma_{y\text{-}IDT}$ from the IDT strength test indicate the horizontal tensile stress and the vertical compression stress at failure, respectively. Stress analyses have indicated that the average normal stress, i.e., $p = (\sigma_{x\text{-}IDT} + \sigma_{y\text{-}IDT})/2$, is almost equal to zero in the IDT strength test [4]. As a result, the maximum shear stress, i.e., $q = (\sigma_{x\text{-}IDT} - \sigma_{y\text{-}IDT})/2$, is essentially dependent on the cohesion of mixtures [7]. When the Poisson's ratio of asphalt mixtures is 0.5, the magnitude of $\sigma_{y\text{-}IDT}$ will be three times that of $\sigma_{x\text{-}IDT}$ [4]. As a result, the value of q is simply equal to twice the absolute value of $\sigma_{x\text{-}IDT}$, and mixture cohesion is approximately twice that of $\sigma_{x\text{-}IDT}$. Experiments have also been previously conducted to validate the relationships of σ_T with the mixture cohesion and rutting resistance of HMA mixtures [7, 8]. Christensen *et al*. (2000) and Xiao (2006) reported a strong relationship between σ_T and mixture cohesion, and that the ratio of mixture cohesion to σ_T was 1.73-1.75 [4, 6]. In addition, the IDT strength test was reported to have potential as a practical and simple method to evaluate the resistance of HMA mixtures to permanent deformation [1, 4, 6, 11-13].

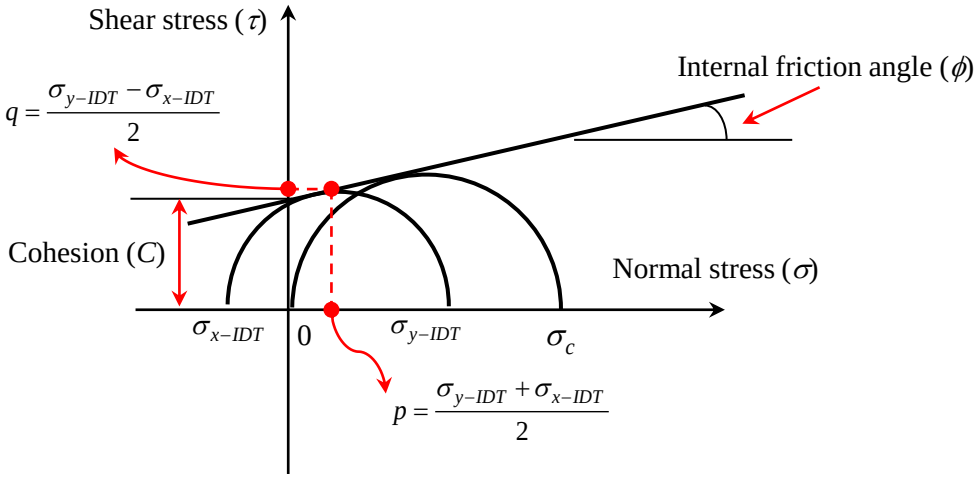

Figure 61. Mohr-Coulomb theory with the combination of the UC and IDT test [4]

The key factors of the IDT strength test for evaluating the rutting resistance of HMA mixtures are the test temperature and the deformation rate [4-6, 11-13]. The viscosity of the asphalt binder decreases in higher temperatures, which can lead to reduced binder stiffness and mixture cohesion. In this way, higher temperatures can lower the shear strength and rutting resistance of mixtures [10]. Christensen *et al.* (2000) proposed that the IDT strength test should be conducted at a temperature of 30 °C (i.e., 20 °C lower than the critical pavement temperature) and a deformation rate of 3.75 mm/min in order to assess σ_T [4]. This combination of test parameters has promising applications for describing the traffic load and temperature conditions for rutting [4]. A downstream analysis compared the results of the IDT strength test conducted at 30 °C and 3.75 mm/min with a test conducted at 40 °C and 50 mm/min [12]; that study demonstrated a correlation between the findings of both protocols, which indicated that they can be employed for the same objective of assessing rutting resistance [12]. Similarly, Zaniewski *et al*. (2004) conducted the IDT strength test at 60 °C and 50 mm/min, and the results also showed a high correlation between σ_T values and rutting resistance [6]. The specimens in all these tests were fabricated using an SGC [4, 6, 10-13].

8.3. Experimental work

8.3.1. Material sources and mixture design

Seven asphalt mixtures that were designed as Vietnamese wearing course mixtures (designated Blends V1–V7) were prepared for the combination of the UC and the IDT tests, and the combination of the UC and the CS tests. In addition, the IDT strength test using Marshall cylindrical specimens of thirteen mixtures was conducted to verify the validity of the IDT strength test as a potential indicator of rutting resistance in HMA mixtures. The Marshall cylindrical samples comprised seven Vietnamese and six Indonesian (designated Blends I1–I6) HMA mixtures with a 12.5-mm nominal maximum particle size. The properties of materials and the results of mixture design for the thirteen mixtures were previously described in chapter 3.

8.3.2. The UC and the IDT tests

The UC and IDT specimen preparations and tests were previously presented in section 7.3.

8.3.3. The UC and the CS tests for the Marshall specimen

The present study conducted the UC and the CS tests using the Marshall specimens with the standard dimension of 101.7 × 63.5 mm. Both tests were performed at a deformation rate of 1 mm/min, which was suggested from the previous studies [7-9]. The testing temperature was maintained at 60 °C,

which was specified for the WTT for evaluating rutting resistance of asphalt mixtures [7, 14]. Before the test, the specimens were also placed in an environmental chamber at the test temperature for over 6 h [7]. The testing conditions of the two protocols that were performed for assessing shear strength of mixtures are also summarized in Table 41.

Table 41. Testing conditions of two methods for determining shear strength of HMA mixtures

Testing condition	UC test	IDT test	UC test	CS test
Specimen	Slab	SGC	Marshall	Marshall
Temperature (^{o}C)	30	30	60	60
Deformation rate (mm/min)	5	3	1	1

Figure 62. The CS specimen and test

Figure 62 shows the configuration of the CS specimens and devices. The loading head having a 45-mm diameter penetrates the specimens, and the circle ring size has the inner diameter of 75 mm. The first and the third principal stresses (σ_1 and σ_3) in the CS test can be calculated using the following equations [7]:

$$\sigma_1 = 0.092 \times \frac{P}{A} \tag{39}$$

$$\sigma_3 = 1.124 \times \frac{P}{A} \tag{40}$$

Where, P is also the applied load at the P_u and the P_f; and A is the cross-session area of the loading head.

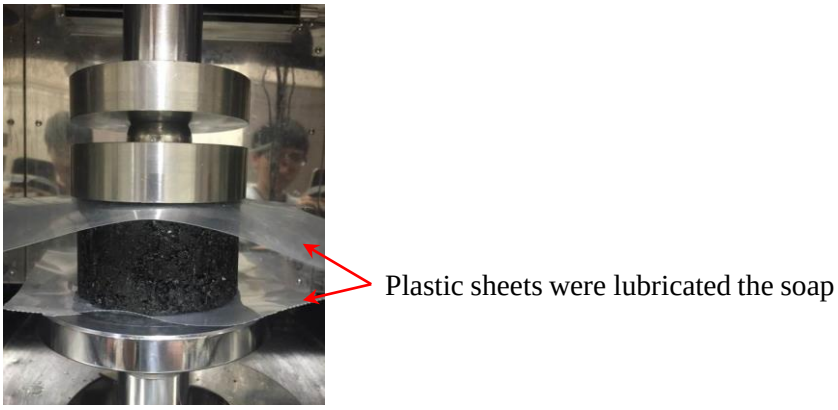

Figure 63. The UC test using the Marshall specimen

The UC test using the Marshall specimen is depicted in Figure 63. As mentioned in section 7.3.3, a height-diameter ratio of 2.0 has been recommended in order to obtain proper strength values [15]. The ratio of height to diameter of the Marshall specimen is 0.62, so the specimen does not meet the suggestion. It has been reported that plastic sheets, which were lubricated with soap, may decrease the discrepancy of the compression strength values when the UC test was conducted using the non-suggestion specimens [1, 15]. Therefore, as shown in Figure 63, we determined to insert two plastic sheets between the specimen sides and loading plates to verify the reliability of this method. The following equation was applied to analyse the compression strength [1]:

$$\sigma_c = \frac{4P}{\pi D^2} \tag{41}$$

Where, D is the diameter of the specimen.

8.3.4. IDT strength test method using the Marshall specimen

The IDT strength test was conducted using cylindrical specimens fabricated in a Marshall mold. Seventy-five blows were applied to each side of the briquettes, which had a standard dimension of 101.7 × 63.5 mm. After the briquettes reached room temperature, the Indonesian specimens were trimmed to a thickness of 25 mm [1]. In order to simplify the testing procedure, two thin disk-shaped Vietnamese specimens were also cut from the middle of the original cylindrical briquette; the average thickness of

these specimens was 30.8 mm. The average diameter-to-thickness ratios were 3.30 and 4.06 for the Vietnamese and Indonesian specimens, respectively. For the purpose of characterizing the shear strength of HMA mixtures using the IDT strength test, the AASHTO T 322-07 standard recommends an acceptable range of 2.82 to 4.18 for the diameter-to-thickness ratio in SGC specimens [16]. Our Marshall specimens complied with this range, which indicates that the IDT strength test has potential applications in the assessment of tensile failure in HMA mixtures.

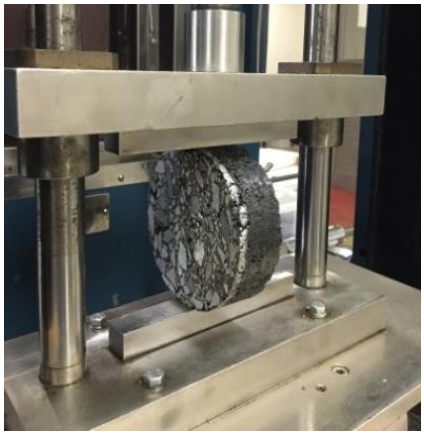

Figure 64. The IDT test using a Marshall specimen

Figure 64 shows the configuration of a mixture specimen and the jig of the IDT strength test. The IDT strength test for the Indonesian specimens was conducted at a temperature of 30 °C and a deformation rate of 2.5 mm/min [1]. The highest average pavement temperature in the southern regions of Vietnam and Indonesia is approximately 50 °C [1, 17]. Ideally, a high temperature in combination with a very high rate of loading is the best condition for the IDT test to evaluate rutting resistance of HMA mixtures [4]. However, previous studies indicated that in the laboratory, the rapid loading rate may be difficult to control, and this can easily lead to transient loads and other dynamic effects [4, 11]. The errors inherent in the dynamic loading are difficult to measure [4, 11]. As a result, the data may be unreliable [11]. Therefore, the IDT test should be conducted at a slower deformation rate and lower temperature to approximately equivalent to the traffic load and temperature conditions that can induce rutting [4]. Therefore, we determined that the appropriate temperature for the IDT strength test for specimens in this study would be 30 °C, as this is 20 °C lower than the highest average pavement temperature. The testing temperature was based on the test protocol proposed by the previous studies [4]. The Vietnamese specimens were tested at a deformation rate of 3.0 mm/min. The higher deformation rate for the Vietnamese specimens was due to their greater thickness. The deformation rates used in this study were lower than those of previous studies because the Marshall specimens were smaller than the SGC

specimens [1]. Before starting the test, the specimens were kept in an environmental chamber at the testing temperature for 15 hours. This curing time should not be less than 12 hours [15].

8.3.5. Wheel tracking test

The WTT was performed to evaluate the resistance of the HMA mixtures to permanent deformation. The sample preparation and testing procedure were previously described in detail in section 4.5.5 and 7.3.4. The results of WTT for seven Vietnamese mixtures were also presented in Table 38.

8.4. Results and discussion

8.4.1. Comparison of shear strength parameters of HMA mixtures under two protocols

Table 42 and Table 43 present the strength values of different tests. The accuracy and repeatability in each test were also evaluated using the coefficient of variation (COV). σ_C and σ_T found from the combination of UC and IDT tests were estimated from four specimens, and σ_1, σ_2, and σ_T found from the combination of UC and CS tests was calculated from three samples. The results indicated that compression and tensile strength obtained the combination of UC and IDT tests tended to exhibit lower COV values than those obtained from the combination of UC and CS tests. Previous research has noted that the COV value of the test for asphalt mixtures should be lower than 15% [18]. Table 42 shows that at both the P_f and P_u, σ_C and σ_T estimated from the combination of UC and IDT tests exhibited low COV values, indicating high accuracy and repeatability of σ_C and σ_T in these tests at both calculations. On the other hands, σ_1, σ_2, and σ_T obtained from the combination of UC and CS tests at the P_f tended to have higher COV values than those at the P_u. Overall, the combination of UC and CS tests presented high accuracy and repeatability of σ_1, σ_2, and σ_T at the P_u only.

Table 44 shows the results of shear strength parameters obtained from the two methods. Figure 65 shows linear relationships of shear strength parameters between the two methods at two stages, i.e., the failure and the ultimate. The correlation coefficients of the *C* between the two methods were high (failure: $R^2 = 0.89$ and ultimate: $R^2 = 0.90$). This means that the *C* obtained from the two protocols may be employed for the same objective, which is used for ranking the cohesion property of HMA mixtures. However, contrary to the authors' expectation, correlation coefficients of ϕ between the two protocols were not high.

Table 42. Strength values of UC and IDT tests at failure load (P_f) and ultimate load (P_u)

Parameter	Mixture	Rep_1	Rep_2	Rep_3	Rep_4	Average (kPa)	COV (%)
σ_C of CU test at P_f	1	830	755	748	722	764	6.1
	2	897	877	857	865	874	2.0
	3	919	1016	944	880	940	6.1
	4	577	610	617	634	610	3.9
	5	749	746	696	686	719	4.6
	6	784	796	770	788	785	1.4
	7	697	696	758	732	721	4.2
σ_C of CU test at P_u	1	1137	1095	1049	1037	1080	4.2
	2	1262	1226	1256	1249	1248	1.3
	3	1330	1477	1363	1312	1371	5.4
	4	804	913	820	836	843	5.7
	5	1014	952	943	920	957	4.2
	6	1047	1040	1035	1031	1038	0.7
	7	955	934	961	946	949	1.2
σ_T of IDT test at P_f	1	110	128	120	120	119	6.0
	2	145	145	138	130	139	5.1
	3	133	187	131	155	151	17.3
	4	87	74	85	86	83	7.6
	5	108	108	113	116	111	3.6
	6	112	121	115	109	114	4.5
	7	94	103	94	94	96	4.8
σ_T of IDT test at P_u	1	161	164	164	166	164	1.3
	2	190	199	189	197	194	2.6
	3	206	221	197	223	212	5.9
	4	115	105	104	110	109	4.6
	5	138	141	135	155	142	6.2
	6	140	149	154	143	147	4.2
	7	123	133	125	127	127	3.4

Table 43. Strength values of UC and IDT tests at failure load (P_f) and ultimate load (P_u)

Test	Mixture	Rep_1	Rep_2	Rep_3	Average (kPa)	COV (%)
σ_c of CU test at P_f (P_u)	1	1710 (2144)	1448 (1876)	1301 (1714)	1486 (1911)	13.9 (11.4)
	2	1484 (1878)	1350 (1774)	1298 (1859)	1378 (1837)	7.0 (3.0)
	3	1630 (2132)	1568 (1995)	1330 (1781)	1509 (1969)	10.5 (9)
	4	962 (1462)	856 (1133)	897 (1263)	905 (1286)	5.9 (12.9)
	5	939 (1294)	911 (1316)	983 (1355)	944 (1322)	3.8 (2.3)
	6	1225 (1472)	1190 (1481)	1417 (1694)	1277 (1549)	9.6 (8.1)
	7	1040 (1270)	1100 (1314)	1029 (1265)	1056 (1283)	3.6 (2.1)
σ_1 of CS test at P_f (P_u)	1	44 (49)	47 (50)	37 (44)	42 (48)	12.3 (6.7)
	2	48 (58)	53 (61)	57 (76)	53 (65)	8.2 (14.8)
	3	56 (70)	62 (82)	85 (99)	67 (84)	22.6 (17.6)
	4	25 (31)	24 (30)	32 (38)	27 (33)	16.9 (13.5)
	5	53 (61)	31 (49)	29 (47)	38 (52)	35.1 (14.7)
	6	33 (38)	25 (31)	33 (36)	30 (35)	14.1 (10.1)
	7	19 (26)	16 (19)	23 (27)	20 (24)	17.3 (19.3)
σ_3 of CS test at P_f (P_u)	1	534 (603)	573 (613)	449 (540)	519 (585)	12.2 (6.7)
	2	590 (706)	649 (743)	696 (926)	645 (792)	8.3 (14.9)
	3	682 (854)	756 (999)	1033 (1214)	824 (1022)	22.5 (17.7)
	4	305 (384)	296 (365)	397 (467)	333 (405)	16.7 (13.4)
	5	648 (743)	375 (594)	358 (571)	460 (636)	35.4 (14.7)
	6	398 (469)	309 (383)	399 (438)	368 (430)	14.1 (10.1)
	7	236 (315)	200 (227)	284 (333)	240 (292)	17.6 (19.3)

Note: Values in parentheses are calculated at the ultimate load (P_u)

Table 44. Shear strength parameters of different protocols

Mixture	UC and IDT tests				UC and CS tests			
	C_f (kPa)	ϕ_f (°)	C_u (kPa)	ϕ_u (°)	C_f (kPa)	ϕ_f (°)	C_u (kPa)	ϕ_u (°)
1	207	33.2	285	34.3	433	29.6	522	32.7
2	241	32.2	337	33.3	463	22.2	593	24.3
3	262	31.8	368	33.5	545	18.3	695	19.6
4	146	38.7	192	41.0	270	28.3	356	32.0
5	193	33.6	247	35.3	323	21.2	450	21.5
6	199	36.2	258	37.2	339	34.1	404	34.9
7	170	39.6	224	39.4	250	39.4	303	39.4

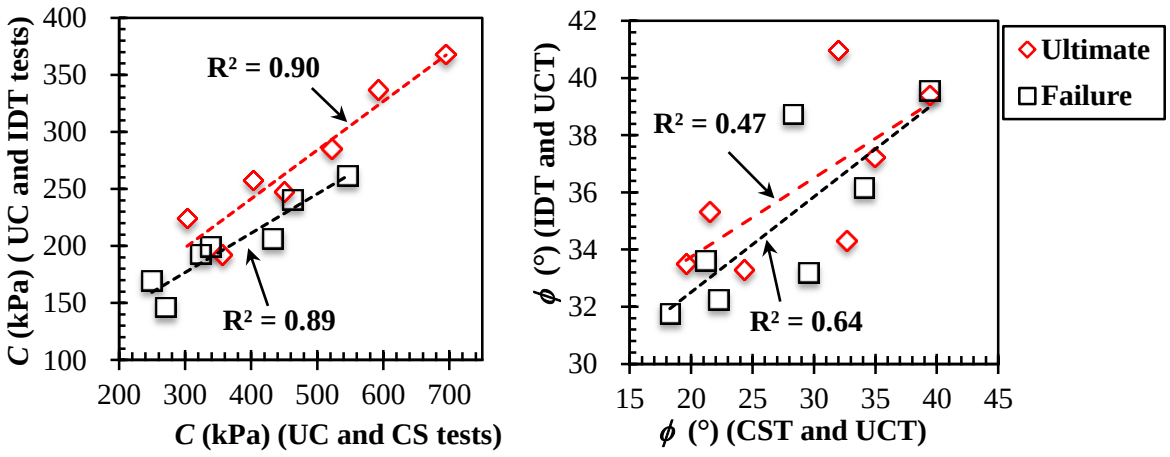

Figure 65. Relationships between C and ϕ values of two protocols

Table 41 and Table 44 indicate that even though the combination of the UC and CS tests was conducted at the higher temperature and lower deformation rate, the C values obtained from this protocol were higher than those obtained from the combination of the UC and IDT tests. The finding is in contradiction with the results reported in a previous study, which showed that there is a decrease in the C with increasing temperatures [10]. The disparity between our findings and those of the previous study may be explained through the compression strength. Generally, the σ_C value decreases with decreasing the deformation rate and increasing the test temperature. However, as shown in Table 42 and Table 43, the σ_C values of the Marshall specimens tended to be higher than those of the prismatic specimens. As a result, the C values obtained from the Marshall specimens were higher than those obtained from the prismatic specimens.

Table 43 shows that the maximum compression strength (σ_{Cu}) values calculated at the ultimate load (P_u) ranged from 1283 to 1969 kPa for the Marshall specimens. A previous study performed the UC test of the Marshall specimens at a deformation rate of 3.75 mm/min and a temperature of 30 °C, and this study reported that the σ_{Cu} values ranged from 2758 to 5370 kPa [1]. The lower deformation rate and the higher temperature may account for the lower σ_{Cu} values of the Marshall specimens obtained in our study relative to those reported in the previous study. However, the σ_C values of the Marshall specimens obtained in the previous study were still higher than those of the prismatic specimens in our study although these tests had the same testing conditions.

In general, the compression stress values of the specimens having a low height-diameter ratio (smaller than 2.0) show higher than those of specimens having the size ratio of 2.0 [15]. As a result, the C values tend to increase when the UC test is performed using the specimens with the low height-diameter ratio. Based on the data in the present study, even though the soap-plastic sheets were used, the UC test

using the Marshall specimens did not produce proper σ_C values. The σ_C of the Marshall specimens in this study was only regarded as an index of σ_C and was not a true value of σ_C.

8.4.2. Evaluation of rutting resistance using the shear strength parameters

Figure 66 and Figure 67 show relationships of shear strength parameters with *DS* for each shear strength method. The results indicated that the *C* had high correlation coefficients with the *DS* for each method and each calculation (ultimate damage and failure damage). The trend lines illustrated that the *DS* values increased with increasing the *C* values.

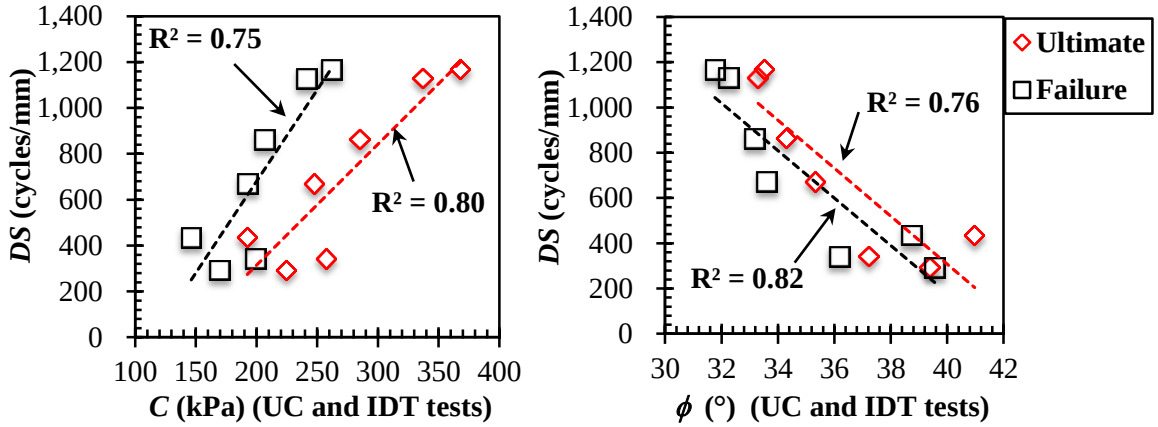

Figure 66. Relationships of *C* and ϕ (UC and IDT tests) with *DS*

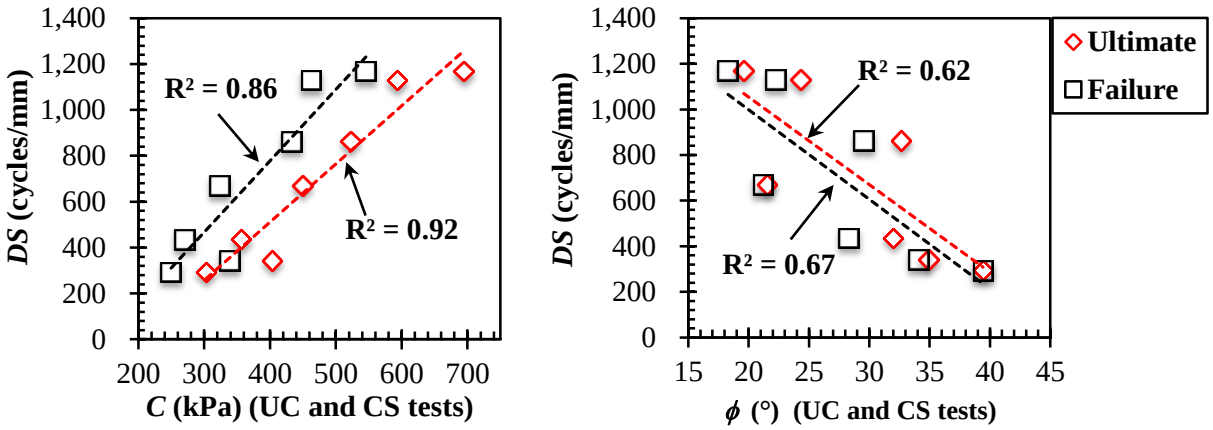

Figure 67. Relationships of *C* and ϕ (UC and CS tests) with *DS*

Contrary to the authors' expectations, the ϕ values had negative coefficients with the *DS* values. The data as shown in Table 44 also indicated that when the ϕ values of mixtures increased, the *C* values decreased. The inverse relationships between the *C* and the ϕ obtained from the UC and the IDT tests also

corroborate those from previous studies [1, 4]. This may account for the negative coefficients between the ϕ and the *DS* obtained in our study. In general, the internal friction of HMA mixtures increases with increasing the content of coarse aggregate [4]. However, the ϕ value obtained from the combination of the UC and the IDT tests was not dependent on the coarse aggregate content as mentioned in section 7.4.5.

The previous study indicated that the ϕ values obtained from the UC test and the CS test increased with the increase in the *C* values [7]. However, the data of the previous study may be insufficient (only three mixtures were investigated) and all the specimens were fabricated by the SGC [7]. In the present study, when the Marshall specimens for the seven mixtures were investigated, the relationships between the ϕ and the *C* were inverse, and the ϕ was not a suitable indicator of rutting resistance.

The results highlighted that the *C* value derived from the combination of UC and CS tests using the Marshall specimens is a potential parameter to evaluate the rutting resistance of HMA mixtures. Therefore, this parameter will help asphalt designers in developing countries during the HMA mixture design process.

8.4.3. Evaluation of rutting resistance using the IDT strength test obtained from the Marshall specimens

Table 45 summaries the IDT strength test (σ_T) results, the *DS*, and *FAA* values for the Vietnamese and Indonesian wearing course mixtures. σ_T values of IDT tests estimated from the Vietnamese Marshall specimens exhibited lower COV values, indicating a high accuracy and repeatability of σ_T in the test. Figure 68 presents the comparison of σ_T and *DS* values between the Vietnamese and Indonesian mixtures. It should be noted that the aggregate gradation in each pair of mixtures presented in these figures has the same aggregate gradation**.** The results indicated that the tensile strength and rutting resistance of Indonesian wearing course mixtures were generally higher than those of Vietnamese wearing course mixtures. This may be explained by the following reasons. Firstly, as shown in Table 45, the *FAA* values of fine aggregate in the Indonesian blends were greater than those in the Vietnamese blends, providing more intimate contact between the backbone aggregate particles for the Indonesian blends. As a result, the Indonesian blends had higher rutting resistance than the Vietnamese blends. Next, as described in section 5.4.5, HMA mixtures that content the granite sand (Blends V4, V6, and V7) had higher the design ACs than HMA mixtures that content the limestone screening (Blends I1, I4, and I6). This may reduce the points of contact among the aggregate particles, and in turn facilitate the movement of the aggregate particles. Consequently, higher AC may result in the lower peak load, σ_T, and rutting resistance of HMA mixtures.

Table 45. σ_T and *DS* values of the thirteen mixtures

Mixture		Rep_1	Rep_2	Rep_3	Rep_4	Average of σ_T (kPa)	COV of σ_T (%)	*DS* (cycles/mm)	*FAA* (%)
Vietnamese	V1	232	227	234	215	227	3.8	863	43.2
	V2	303	291	288	315	299	4.0	1130	43.1
	V3	415	408	373	360	389	6.9	1168	42.9
	V4	**214**	**203**	**210**	**211**	**209**	**2.2**	**435**	**42.9**
	V5	240	240	242	238	240	0.7	670	42.7
	V6	**141**	**159**	**163**	**170**	**158**	**7.8**	**342**	**42.3**
	V7	**183**	**203**	**180**	**194**	**190**	**5.6**	**293**	**43.0**
Indonesian	**I1**	**-**	**-**	**-**	**-**	**251**	**-**	**759**	**45.4**
	I2	-	-	-	-	195	-	505	43.3
	I3	-	-	-	-	317	-	676	45.3
	I4	**-**	**-**	**-**	**-**	**404**	**-**	**993**	**46.0**
	I5	-	-	-	-	357	-	790	39.2
	I6	**-**	**-**	**-**	**-**	**447**	**-**	**1160**	**45.9**

Note: The present study had data of Indonesian mixtures including the average of σ_T and the *DS* only. Identical colors indicate the same aggregate gradations.

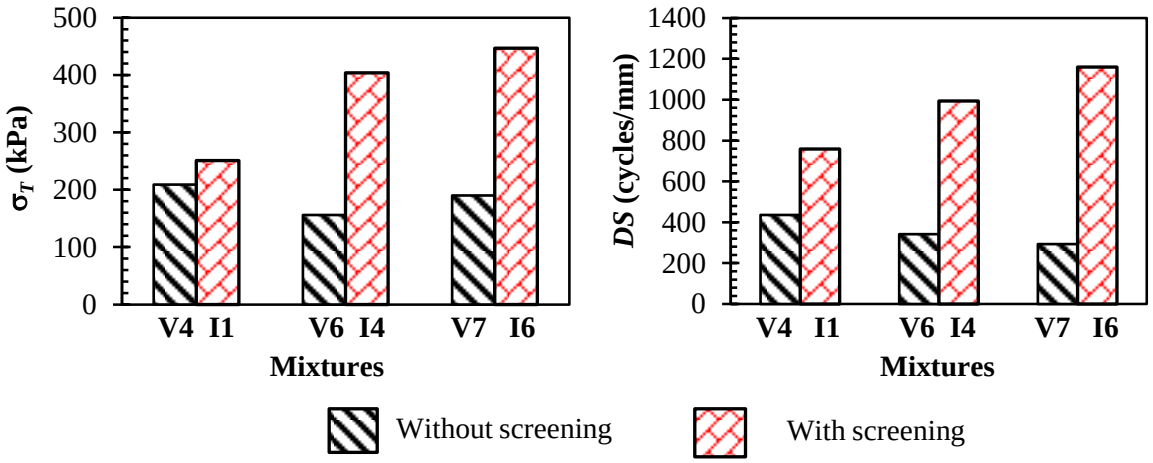

Figure 68. Comparison of σ_T and *DS* values between the Vietnamese and Indonesian mixtures

Figure 69 shows the relationship of the measured *FAA* with *DS* values for the thirteen mixtures. The correlation coefficient between the *FAA* and the *DS* values was low when mixtures with different

aggregate gradations were compared. This indicates that the *FAA* parameter of fine aggregate alone is unable to evaluate the rutting resistance of HMA mixtures with various aggregate gradations.

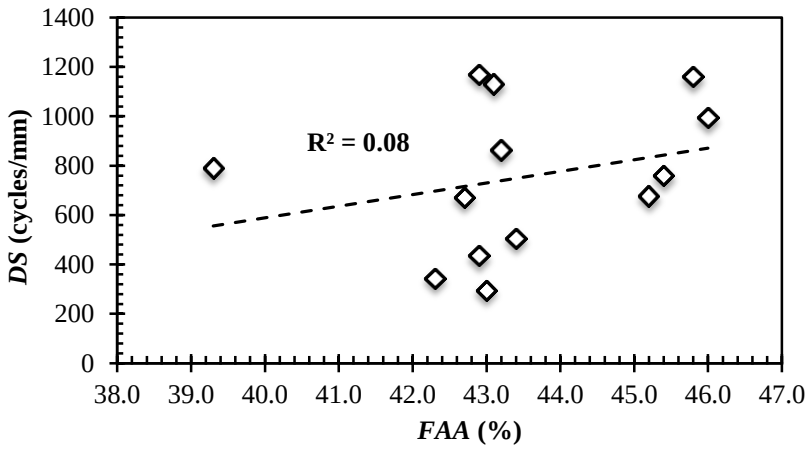

Figure 69. Relationship between *FAA* and *DS*

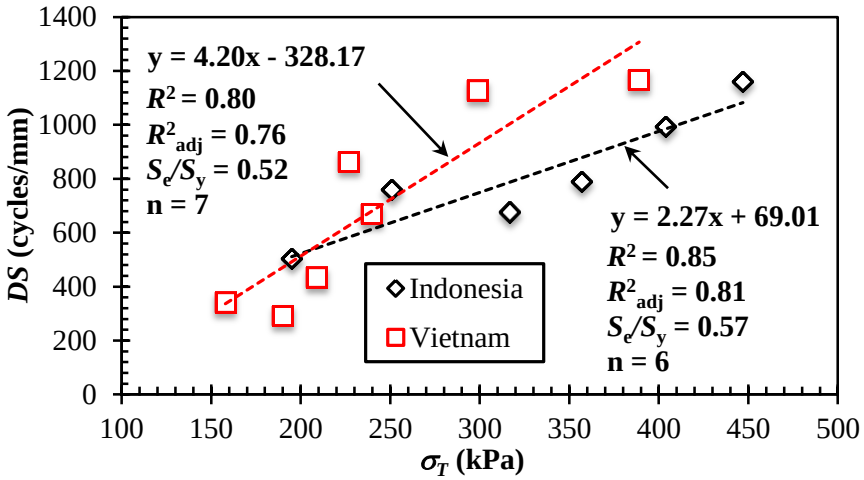

Figure 70. Relationships between σ_T and *DS* for the Vietnamese and Indonesian wearing course mixtures

Figure 70 shows the relationships between the σ_T and *DS* values for the seven Vietnamese and six Indonesian wearing course mixtures. The trend lines showed that the mixtures had good rutting resistance when the σ_T values were high, which corroborates the findings of previous studies [4, 6, 12]. It is worth noting that, as shown in Figure 70, the models demonstrated good R^2 (0.80 and 0.85) and good to fair S_e/S_y (0.52 and 0.57) for both the Vietnamese and Indonesian mixtures, regardless of aggregate source (A model with an R^2 above 0.70 and an S_e/S_y below 0.57 is regarded as having good goodness of fit [19]). In addition, the relationships between the σ_T and *DS* values of both the Vietnamese and Indonesian mixtures (Figure 71) had a reasonably linear correlation coefficient (good R^2: 0.70 and fair S_e/S_y: 0.57). This

finding further supports our postulation that the deformation rate and testing temperature used in this study were suitable for assessing σ_T values from the IDT strength test.

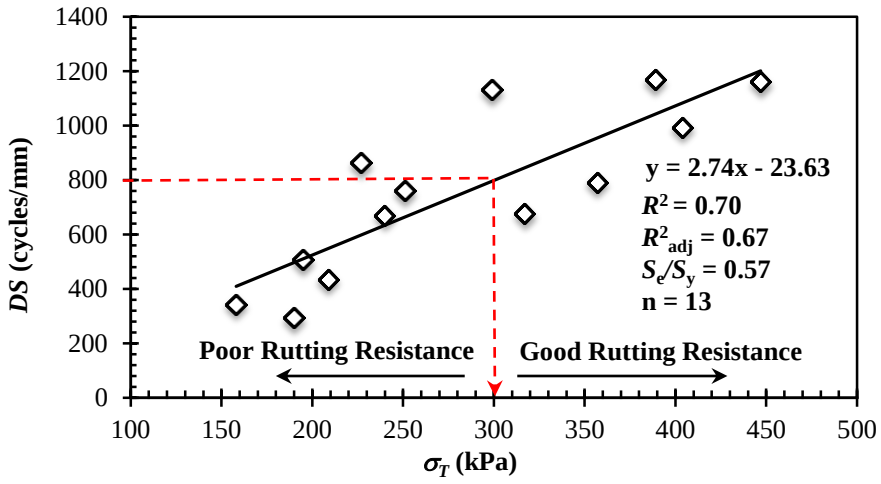

Figure 71. Relationship between σ_T values and *DS* values for the thirteen mixtures

As depicted in Figure 71, the IDT strength test conducted at a relatively slow deformation rate and a moderate temperature has potential applications for assessing the rutting resistance of HMA mixtures. The coefficient of determination (R^2) of the regression was 0.70, which indicates that approximately 70% of the variability in the rutting resistance observed from those thirteen mixtures can be explained by the sole independent variable, the σ_T. It should be noted that other factors (such as characteristics of asphalt binder and aggregate) that influence the rutting resistance were not taken into account. The *DS* values for 12.5-mm NMPS wearing course mixtures that are subject to heavy traffic volume should be a minimum of 800 cycles/mm [1]. This figure also suggests that the σ_T value from conventional Marshall specimens should be higher than 300 kPa in order to provide HMA mixtures with sufficient resistance to permanent deformation. Two previous studies have indicated that the corresponding σ_T values for SGC specimens are 270 kPa and 320 kPa [4, 12]; our recommended σ_T value is therefore approximately equal to the median value of these previously reported values.

8.5. Summary

Based on the experiments presented in the present study, the following conclusions can be drawn:

- The present study compared the shear strength parameters of two distinct methods, i.e., the UC test combined with the IDT test, and the UC test combined with the CS test. The results showed that relationships of the *C* for both protocols were good, whereas the ϕ values of both protocols were not correlated well.

- Even though soap-plastic sheets were applied for the UC test, the σ_C values of the Marshall specimens were higher than those of recommended specimens (the size ratio of 2.0). Therefore, the σ_C values of the Marshall specimens introduced in this study only indicated the index of true σ_C values.
- The high linear relationships between the *C* of the two shear strength methods and rutting resistance of HMA mixtures were obtained. Therefore, not only the combination of UC and IDT tests, but also the combination of UC and CS tests using the Marshall specimens had potential applications for evaluating rutting resistance of HMA mixtures.
- Strong relationships were observed between the tensile strength using the Marshall specimens and rutting resistance of HMA mixtures. IDT strength using the Marshall specimens should exceed 300 kPa to obtain high rutting resistance for 12.5-mm NMPS wearing course mixtures.

References

[1] Haryanto, I., and Takahashi, O. A rutting potential assessment using shear strength properties for Indonesian wearing course asphalt mixtures, International Journal of Pavements 6 (1-2-3), pp. 27-38, 2007.

[2] Kandhal, P., and Allen Cooley, J.R.L. Accelerated laboratory rutting tests: Evaluation of the Asphalt Pavement Analyzer, NCHRP 508, National Research Council, Washington, D.C., 2003.

[3] Tran, N.T., and Takahashi, O. Improvement on aggregate gradation design and evaluation of rutting performance of Vietnamese wearing course mixtures, the 8th international conference on maintenance and rehabilitation of pavements, Singapore, pp. 212-221, 2016.

[4] Christensen, D.W, Bonaquist, R., and Jack, D. P. Evaluation of triaxial strength as a simple test for asphalt concrete rut resistance. FHWAPA-2000-010+97-04(19), Final Report, PTI 2K26, 2000.

[5] Pellinen, T.K., Song, J., and Xiao, S. Characterization of hot mix asphalt with varying air voids content using triaxial shear strength test, Proceeding 8th Conference Asphalt Pavement for Southern Africa, Sun City, South Africa, 2004.

[6] Xiao, S. Investigation of performance parameters for hot-mix asphalt, PhD Thesis, Purdue University, West Lafayette Indiana, 2006.

[7] Zheng, J, Huang. T., and Qian, G.. Investigation into circle shear test method of asphalt mixture. Proceedings of the GeoHunan International Conference II: Emerging Technologies for Design, Construction, Rehabilitation, and Inspection of Transportation Infrastructure, China, pp. 259-266, 2011.

[8] Cai, X., and Wang, D. Evaluation of rutting performance of asphalt mixture based on the granular media theory and aggregate contact characteristics, Road Materials and Pavement Design 14 (2), pp. 325-

340, 2013.

[9] Huang, T., Qian, G., and Zheng, J. Investigation into shear coefficient for circle shear test method of asphalt mixture. Advanced Materials Research 446-449, pp. 2590-2594, 2013.

[10] Wang, H., Liu, X., and Hao, P. Evaluating the shear resistance of hot mix asphalt by the direct shear test, Journal of Testing and Evaluation 36 (6), 485-491, 2008.

[11] Christensen, D.W., et al. Indirect tension strength as a simple performance test, New simple performance tests for asphalt mixes, Report E–C068, Washington DC, pp. 44-57, 2004.

[12] Christensen, D.W., and Bonaquist, R. Using the indirect tension test to evaluate rut resistance in developing hot-mix asphalt mix designs, Practical approaches to hot-mix asphalt mix design and production quality control testing, E-C124, National Research Council, Washington, D.C., pp. 62-77, 2007.

[13] Zaniewski, J.P., and Srinivasan, G. Evaluation of indirect tensile strength to identify asphalt concrete rutting potential, Asphalt Technology Program, Department of Civil and Environmental Engineering, West Virginia University, Washington, 2004.

[14] Japan Road Association, JRA-B003. Method of wheel tracking test, Standard Practice for Asphalt Concrete Mix Design (3), pp. 39-55, 2005.

[15] Erkens, S.M.J.G. Asphalt concrete response (ACRe): Determination, modelling and prediction. PhD thesis, Technical University Delft, Netherlands, 2002.

[16] AASHTO Designation, T 322. Standard method of test for determining the creep compliance and strength of hot-mix asphalt (HMA) using the indirect tensile test device, 2007.

[17] Nguyen, T. N., and Tran, V. T. Temperature distribution in asphalt pavement at the south area of vietnam, Journal of Vietnamese Transportation, 12, 30-31, 2015.

[18] Stewart, C. M., Reyes, J. G., and Garcia, V. M. Comparison of fracture test standards for a Superpave dense-graded hot mix asphalt, Engineering Fracture Mechanics 169, 262-275, 2017.

[19] Witczak, M.W. et al. Simple performance test for Superpave mix design, Report NCHRP 465, Washington, D.C., 2002.

Chapter 9. Conclusion, recommendation, and future research

9.1. Conclusions

The current practices of the Superpave and Marshall standards do not stipulate any evaluation procedures for designing aggregate gradations to ensure proper volumetric parameters and adequate performances. In addition, only the requirements of volumetric parameters in the Superpave and Marshall mix designs are insufficient to achieve a high resistance on rutting and cracking. Furthermore, rutting and cracking testing devices are expensive and have not been widely available in developing countries such as Vietnam and Indonesia. As a result, it is difficult to implement those devices to evaluate a mixture in developing countries. Therefore, this study provided a comprehensive evaluation of the effects of aggregate gradations on the volumetric properties and performances of HMA mixtures. Based on characteristics of aggregate gradations, the present study proposed simple indexes for asphalt designers to obtain a mixture which has high resistance on rutting and cracking.

This study applied the CMD_{area} parameter obtained from the concept of the CMD to evaluate the effects of aggregate gradations on the VMA and rutting resistance of asphalt mixtures. The experiments indicated that the CMD_{area} of aggregate gradation has a strong associated with the VMA of HMA mixtures. Increasing CMD_{area} increases VMA. The results also confirmed that the CMD_{area} is a practical and effective index for evaluating the effect of aggregate gradation on the VMA of asphalt mixtures regardless of aggregate source, mix design, and nominal aggregate particle size. However, the relationship between the CMD_{area} of aggregate gradation and the rutting resistance of HMA mixtures is low, indicating that the use of sole CMD_{area} cannot guarantee a good rutting resistance for HMA mixtures.

Based on the theory of CMD and the DASR model, this study proposed the workability index (*WI*) derived from aggregate gradation and the rutting resistance index (*RRI*) derived from aggregate gradation and asphalt content in order to rank asphalt mixtures with different components and properties. The results indicated that the *WI* and the *RRI* are valuable parameters in ranking and distinguishing the workability and rutting resistance of asphalt mixtures, regardless of compaction energies and compactors. In addition, the $CMD_{area\text{-}stone}$ of aggregate gradations and the workability of HMA mixtures are reasonably correlated. An asphalt mixture having aggregate gradation that has a lower $CMD_{area\text{-}stone}$ value tends to have higher workability.

The present study also introduced two cracking parameters, called the $CMD_{area-DASR}$ of aggregate gradation and the gradation-based cracking resistance index (*GCI*), to evaluate the cracking potential of asphalt mixtures at a high normal temperature (30 °C) in the notched semi-circular bending (SCB) test. These parameters are derived from the characteristics of aggregate gradation. The experiments indicated that both $CMD_{area-DASR}$ and the *GCI* have potential applications for ranking the cracking resistance of HMA mixtures. It was found that the $CMD_{area-DASR}$ had a stronger association with the fracture toughness (σ_f and K_{Ic}) than the J_c. On the other hand, the *GCI* is more strongly associated with the J_c than the fracture toughness (σ_f and K_{Ic}).

Downstream research included cracking tests at a low service temperature (15 °C) to exam the relationships of aggregate gradations and asphalt contents on cracking performance of HMA mixtures. In addition, the present study investigated whether the SCB test can be a good alternative to the three-point bending beam (TPBB) test to assess fracture characteristics of asphalt mixtures. The results indicated that the $CMD_{area-DASR}$ is an effective parameter for evaluating the fracture toughness (σ_f and K_{Ic}) values calculated from the notched SCB and TPBB tests. An asphalt mixture with a higher $CMD_{area-DASR}$ value may have lower fracture toughness (σ_f and K_{Ic}). In addition, it was found that the apparent film thickness (*AFT*) is a potential parameter that provides the effects of the asphalt content on the cracking performance of HMA mixtures. Our work also confirmed that the notched SCB test using the EN 12697-44 standard may provide a good alternative to the TPBB test to evaluate the fracture properties of asphalt mixtures at a low service temperature.

The present study also applied the CMD_{area} and proposed the P_{rms} and CMD_{sand} to examine the effects of aggregate gradation on the shear strength properties (*C*, ϕ, and *K*) of HMA mixtures. Furthermore, the relationships of the shear strength parameters with rutting resistance of HMA mixtures were investigated. The results showed that the CMD_{area} and P_{rms} have potential applications for evaluating both the *C* and ϕ properties of HMA mixtures. In addition, the CMD_{sand} is a practical parameter that can be implemented for evaluating the *K* properties of HMA mixtures. The experiments also indicated that the *AFT* has a strong negative association with the *C* of HMA mixtures. Furthermore, the C obtained from the combination of UC and IDT tests has a potential application for ranking the rutting resistance of wearing course mixtures.

The present study also investigated the tests using the Marshall specimens that have potential applications for evaluating rutting resistance of HMA mixtures. It was found that the *C* parameter found from the combination of UC and CS tests using the Marshall specimens can rank the rutting resistance of different asphalt mixtures. In addition, the results demonstrated a high relationship between the IDT strength using the Marshall specimens and the rutting resistance of HMA mixtures. The minimum value

of the IDT strength using the Marshall specimens should be 300 kPa to guarantee a good rutting resistance for 12.5-mm NMPS wearing course mixtures.

This study also investigated the effects of fine aggregate on rutting and cracking performance of HMA mixtures. Generally, the use of limestone screening instead of natural sands may improve the rutting and cracking resistance of asphalt mixtures when the aggregate gradations were controlled to achieve the same gradations. On the other hand, the fine aggregate angular with different gradations was not strongly associated with the rutting and cracking performance of HMA mixtures.

9.2. Recommendations

The present study discussed various means of evaluating the potential performance of asphalt mixtures. The relationships of mixture compositions with the performance of HMA mixtures are also summarized in Table 46. Aggregate gradation parameters can be estimated at the early stage, resulting in saving the time and effort for mixture designers to select a stable aggregate gradation. In addition, as shown in Table 46, several parameters that do not require any rutting and cracking testing devices have potential applications for ranking cracking and rutting resistance of HMA mixtures. Therefore, these parameters may be practical and cost-effective for mixture designers.

This study showed the high relationship of *GCI* with the J_c when only natural sands were used for all the blends. However, the data obtained from Iman et al.'s research indicated that when asphalt mixtures were fabricated with both different fine aggregate (limestone screenings and natural sands), the low relationship between the *GCI* and the J_c was observed. Moreover, this data showed a negative relationship between J_c and σ_{max}, which was not consistent with the previous studies. With the same aggregate gradation or the same *GCI*, the mixtures using limestone screenings generally had higher J_c values than the mixtures using natural sands. Therefore, downstream research should include extensive tests using a wider range of asphalt binder and aggregate sources to confirm the reliability of the $CMD_{area-DASR}$ and *GCI* parameters in HMA mixture designs.

The future research will include further fatigue testing to confirm the reliability of the J_c properties in HMA mixture designs. The J_c parameter indicates the cracking resistance of HMA mixtures at the cracking initiation stage, which is generally assessed using fatigue testing. Fatigue tests should therefore be conducted to verify whether the J_c index is an eligible parameter of fatigue in HMA mixtures at normal temperatures.

The present study employed the J_c and K_{Ic} of the notched SCB test to evaluate cracking resistance of HMA mixtures at the cracking initiation and propagation stages, respectively. While J_c is used in the ductile fracture or elastic-plastic fracture mechanics analyses, K_{Ic} is used in the brittle fracture or linear-elastic fracture mechanics analyses. There is therefore a need to conduct in-depth investigations that

clarify the application of cracking parameters that should be estimated from the same approach. For example, at normal temperatures, the J_c and *CTOA* of the notched SCB test have potential applications for evaluating the cracking initiation and propagation stages in the ductile fracture.

This study only applied the load-deformation curve instead of the linear variable differential transducers to determine the *CTOA* parameter. Therefore, further research is required to confirm the reliability of *CTOA* when assessing the cracking propagation stage of HMA mixtures. Future work should focus on studying a wider range of asphalt binders, such as virgin asphalt and modified asphalt. In addition, the future work should employ a mixed-level factorial design to understand the effect of variables (mixture components and specimens geometry) on the *CTOA* parameter.

The present study only investigated the relationship of each independent variable with the dependent variable. However, the independent variables may interact with each other, indicating that the interpretation for one independent variable depends on the value of other independent variables. Therefore, there is certainly a need to design an experiment to evaluate both the main and interaction effects of various factors on the performance of asphalt mixtures.

Table 46. Effects of mixture components on performance of asphalt mixtures

Component	Parameter	Volumetric properties	Workability	Rutting resistance	Cracking resistance using the TPBB and the notched SCB tests					Mixture shear strength		
					Low service temperature			High service temperature				
		VMA	*WEI*	*DS*	σ_f and K_{Ic}	ε_f and CTOA	G_f	σ_f and K_{Ic}	J_c	*C*	ϕ	*K*
Fine aggregate	↑*FAA*			↑				↑	↑			
Aggregate gradation	↑CMD_{area}	↑↑↑		↓	↓↓	↑↑	↑↑	↓↓		↓↓↓	↑↑	↓↓
	↑$CMD_{area\text{-}stone}$		↓↓↓									
	↑CMD_{sand}											↓↓↓
	↑$CMD_{area\text{-}DASR}$				↓↓↓	↑	↑	↓↓↓	↓↓↓			
	↑P_{rms}									↓↓↓	↑↑	↓
	↑*DF*		↓↓									
	↑*GCI*							↑↑↑	↑↑↑			
Asphalt content	↑Design AC			↓↓	↓	↑↑	↑↑	↓		↓↓		
	↑V_{be}			↓	↓	↑↑↑	↑↑↑	↓		↓↓		
	↑*AFT*			↓↓	↓↓↓	↑↑↑	↑↑↑	↓↓↓		↓↓↓		
Gradation and asphalt content	↑*WI*		↑↑↑									
	↑*RRI*			↑↑↑								
IDT test	↑σ_T			↑↑↑								
UC and IDT tests	↑*C*			↑↑↑								
	↑ϕ			↓↓↓								
CS and IDT tests	↑*C*			↑↑↑								
	↑ϕ			↓↓↓								

- "↑" indicates increasing parameters;"↑" indicates improved performance; "↓" indicates reduced performance. "↑↑↑" and "↓↓↓": $R^2 \geq 0.7$; "↑↑" and "↓↓": $0.7 > R^2 > 0.4$; "↑" and "↓"$R^2 \leq 0.4$.
- IDT, UC, and CS tests were conducted at relatively low deformation rates and moderate testing temperatures.
- The cracking tests were performed at a low service temperature of 15 °C and a high normal temperature of 30 °C, which are based on the Vietnamese climate.